Characteristics and Petrogenesis of Alaskan-Type Ultramafic-Mafic Intrusions, Southeastern Alaska

By Glen R. Himmelberg *and* Robert A. Loney

U.S. GEOLOGICAL SURVEY PROFESSIONAL PAPER 1564

Field relations, petrography, rock chemistry, mineral chemistry, and interpretation of origin and emplacement of Alaskan-type intrusions

UNITED STATES GOVERNMENT PRINTING OFFICE, WASHINGTON: 1995

U.S. DEPARTMENT OF THE INTERIOR

BRUCE BABBITT, Secretary

U.S. GEOLOGICAL SURVEY

Gordon P. Eaton, Director

For sale by
U.S. Geological Survey, Information Services
Box 25286, Federal Center
Denver, CO 80225

Text and illustrations edited by Mary Lou Callas
Graphics by authors
Layout by Mary Lou Callas

Library of Congress Cataloging-in-Publication Data

Himmelberg, Glen R.
Characteristics and petrogenesis of Alaskan-type ultramafic-mafic intrusions, southeastern Alaska / by Glen R. Himmelberg and Robert A. Loney.
p. cm. — (U.S. Geological Survey professional paper : 1564)
"Field relations, petrography, rock chemistry, mineral chemistry, and interpretation of origin and emplacement of Alaskan-type intrusions."
Includes bibliographical references (p. –).
Supt. of Docs. no.: 119.16:1564
1. Intrusions (Geology)—Alaska. 2. Rocks, Ultrabasic—Alaska. 3. Geochemistry—Alaska. I. Loney, Robert Ahlberg, 1922– . II. Title. III. Series.
QE611.5.U6H56 1995
551.8'8'097982—dc20 95-2236
CIP

CONTENTS

FIGURES

TABLES

Characteristics and Petrogenesis of Alaskan-Type Ultramafic-Mafic Intrusions, Southeastern Alaska

By Glen R. Himmelberg[1] *and* Robert A. Loney[2]

ABSTRACT

Alaskan-type ultramafic-mafic intrusions occur along a belt that extends from Duke Island to Klukwan in southeastern Alaska and fall into two age groups—400 to 440 Ma; and 100 to 118 Ma. Most of the intrusions occur in the Alexander terrane or in the Gravina overlap assemblage, but they are not restricted to these terranes. The Alaskan-type ultramafic bodies range in size from sills only a few meters thick to intrusions about 10 km in maximum exposed dimension. Most of the bodies consist of magnetite-bearing hornblende clinopyroxenite or hornblendite, however many of the larger ones also include dunite, wehrlite, olivine clinopyroxenite, and, in some cases, gabbro. The Blashke Islands and Union Bay bodies are markedly concentrically zoned; dunite in the core is surrounded progressively outward by wehrlite, olivine clinopyroxenite, clinopyroxenite, hornblende clinopyroxenite, and gabbro. In the other large bodies, crude zoning may be present, but individual zones are discontinuous or missing entirely.

Textural, mineralogical, and chemical characteristics of the Alaskan-type ultramafic bodies indicate that they formed from a basaltic magma by crystal fractionation and mineral concentration processes. In general the $Mg/(Mg+Fe^{2+})$ ratio of olivine and clinopyroxene decreases systematically through the series dunite, wehrlite, olivine clinopyroxenite, clinopyroxenite, hornblende clinopyroxenite, and gabbro. The Al_2O_3 content of clinopyroxene, which shows a marked enrichment with differentiation, suggests crystallization from progressively more hydrous melts like those characteristic of arc magmas. The hydrous nature of the magma is also indicated by the common occurrence of phlogopite and hornblende in wehrlite and clinopyroxenite and by hornblendite being part of the differentiation sequence. Clinopyroxene in the later differentiates has a substantial esseneite component that is a result of the hydrous, oxidizing nature of the magma. Rare-earth-element (REE) patterns of the ultramafic rock samples markedly show signatures of cumulus origin involving accumulation of dominantly olivine, clinopyroxene, and hornblende. The absence of a positive Eu anomaly and the relatively flat REE pattern of most gabbro samples suggest that the gabbros are not cumulates but probably represent static crystallization of a differentiated liquid that had undergone substantial removal of olivine, clinopyroxene, and some hornblende. The markedly similar REE abundance levels and patterns for the same rock types in all the bodies studied suggest that all the bodies were derived by differentiation of closely similar parent magmas under near-identical conditions.

The magnesium-rich olivine in Alaskan-type dunite and wehrlite is consistent with crystallization from an unfractionated mantle-derived primary melt. The exact composition of the primary melt is uncertain, but our preferred interpretation is that the parental magma of most Alaskan-type bodies was a subalkaline hydrous basalt. There are striking similarities between the REE abundance levels and patterns of the Alaskan-type clinopyroxenites and gabbros and those of the clinopyroxenite xenoliths and plutonic gabbros associated with Aleutian island-arc volcanism. These similarities suggest that the primary magma was probably a hydrous olivine basalt similar to the primary magma proposed for the Aleutian island-arc lavas. The mineral chemistry and phase equilibria of the ultramafic bodies suggest crystallization in magma chambers at depths of about 3 to 9 km.

The relatively small exposed size and geometry of many of these bodies suggest that they accumulated in subvolcanic feeder conduits, sills, and small magma chambers at shallow levels in the crust. We attribute the concentric zoning of rock types present in some of the bodies to flow differentiation in feeder conduits and sills. Only the Duke Island body shows abundant evidence of stratiform layering and ubiquitous current activity that suggest crystallization and accumulation in a small magma chamber. Although the Red Bluff Bay intrusion on Baranof Island is discussed in this report, evidence suggests that it should not be classified as an Alaskan-type intrusive body.

[1] U.S. Geological Survey and Department of Geology, University of Missouri, Columbia, Mo.

[2] U.S. Geological Survey, Menlo Park, Calif.

Manuscript approved for publication December 5, 1994.

INTRODUCTION

The belt of ultramafic bodies that extends from Klukwan to Duke Island in southeastern Alaska has been known for a long time because of the economic interest in chromium, platinum group elements (PGE), iron, nickel, and copper (Buddington and Chapin, 1929; Kennedy and Walton, 1946; Walton, 1951). Similar bodies and associated ore deposits extend for almost 1,500 km through central British Columbia (Findlay, 1969; Irvine, 1976; Clark, 1980; Nixon and Rublee, 1988; Hammack and others, 1990; Nixon and others, 1990; Nixon and Hammack, 1991), and a third belt about 450 km long occurs in the north-central part of the Ural Mountains of Russia and Kazakhstan (Noble and Taylor, 1960).

In 1960 these bodies were recognized as a separate, distinctive class of intrusions (Noble and Taylor, 1960; Taylor and Noble, 1960). Because of the concentric zoning present in some of the larger bodies they have been referred to as "zoned," "concentrically zoned," or "concentric" ultramafic complexes (Taylor, 1967; Wyllie, 1967; Jackson and Thayer, 1972). The zonal structure is not universal, however, and in those bodies where it is present the zones are generally discontinuous and not symmetrical; only the ultramafic complex at the Blashke Islands (Walton, 1951; Himmelberg and others, 1986b) is symmetrically zoned. Many of the bodies actually consist of only one rock type. For these reasons, Irvine (1974) referred to this class of ultramafic bodies as "Alaskan-type" complexes because that is where the bodies were first recognized as distinctive. This name has been widely adopted and is now applied to similar ultramafic complexes that occur in British Columbia (Findlay, 1969; Clark, 1980; Nixon and Rublee, 1988; Hammack and others, 1990; Nixon and others, 1990), Oregon (Gray and others, 1986), California (James, 1971; Snoke and others, 1981, 1982), Venezuela (Murray, 1972), New South Wales, Australia (Elliott and Martin, 1991), and the Ural Mountains (Taylor, 1967).

The Alaskan-type complexes are characterized as a separate class of intrusions by their tectonic setting, size, composition, internal structure, and mineralization. They form small intrusions in convergent plate-margin settings. The principal minerals in the ultramafic rocks are olivine, clinopyroxene, magnetite, and hornblende; orthopyroxene and plagioclase are extremely rare. Where a complete rock series is present, it includes dunite, wehrlite, olivine clinopyroxenite, clinopyroxenite, hornblende clinopyroxenite, hornblendite, and, in some bodies, gabbro. The clinopyroxenite and hornblende clinopyroxenite are generally rich in magnetite. Some of the larger bodies are crudely concentrically zoned; dunite in the core is successively ringed by wehrlite, olivine clinopyroxenite, and other rocks of the series. Many bodies, however, consist only of hornblende clinopyroxenite or hornblendite. Although all the bodies show evidence of origin by fractional crystallization and crystal concentration, extensive layering is not common. The body on Duke Island is an exception; it shows spectacular layering developed by transportation and deposition of crystals by magmatic convection and density currents (Irvine, 1974). External contacts of all the bodies with their country rocks are sharp, steep, and generally marked by thermal aureoles. Mineralization, where present, is dominantly titanium-vanadium magnetite and platinum-group minerals (PGM).

Most of the ultramafic rocks in southeastern Alaska are included in the Alaskan-type group. Exceptions are the basal ultramafic rocks of the tholeiitic, informally named La Perouse layered gabbro (Himmelberg and Loney, 1981; Loney and Himmelberg, 1983) in the Fairweather Range, the ultramafic rocks associated with the norite, diorite, granodiorite complex on Yakobi Island and at Mirror Harbor on northern Chichagof Island (Himmelberg and others, 1987), and the residual mantle harzburgite exposed in the Atlin quadrangle southeast of Skagway (Himmelberg and others, 1986a). Serpentinites near Point Marsden and north of Greens Creek on northern Admiralty Island, and in the Coast Mountains south of the Taku River retain no primary mineralogy or primary structures to indicate their origin. The complete serpentinization, however, does indicate that they were rich in olivine. We do discuss the ultramafic complex at Red Bluff Bay (Loney and others, 1975) here with the Alaskan-type bodies; however, as pointed out below, inclusion of it as an Alaskan-type complex remains questionable.

This study describes and interprets the rock and mineral chemistry of most of the large bodies and several smaller ones that previous workers included as Alaskan-type complexes in southeastern Alaska. As evidenced by the characteristics of the Alaskan-type complexes listed above, recognition of these bodies as a unique group is based largely on field relations and petrographic characteristics. With the exception of the complexes at Union Bay (Ruckmick and Noble, 1959), Duke Island (Irvine, 1974), and the Blashke Islands (Himmelberg and others, 1986b), little information has been available on the rock and mineral chemistry of these bodies. As discussed below, some of these bodies are of different ages, and few have the full range of field and petrographic characteristics of the classic concentrically zoned bodies. However, all are remarkably similar in rock and mineral chemical characteristics which, along with their field and petrographic characteristics, clearly establish these bodies as a separate class of ultramafic-mafic intrusions. All together, these features suggest remarkably similar petrogenetic histories for each of these bodies. We summarize the field relations and other features of these bodies to provide a framework for the discussion of the chemistry of these rocks. Thus, this report provides a current and comprehensive description of the Alaskan-type ultramafic bodies. We utilize the combined field, petrographic, structural, and chemical data to (1) constrain the conditions of crystallization and accumulation of the ultramafic bodies, (2) evaluate the nature of the parental magma composition, and (3) propose an intrusive mechanism to explain the distribution of rock types and concentric structure. The results of this study provide insight into the

complex structural and petrological processes operating at high crustal levels in arc environments. We believe that this type of understanding is crucial to development of valid petrogenetic models of arc-eruptive magmas.

REGIONAL SETTING AND AGE

The regional geologic framework of southeastern Alaska includes six main geologic features (fig. 1). (1) The Chugach terrane is composed of mostly flysch; the remainder is melange that consists of Cretaceous metaflysch and mafic metavolcanic rocks. (2) The Wrangellia terrane is composed of Permian and Triassic graywacke, limestone, and mafic metavolcanic rocks. (3) The Alexander terrane is composed of coherent, barely metamorphosed Ordovician through Triassic graywacke turbidites, limestone, and volcanic rocks. (4) The Gravina overlap assemblage depositionally overlies the eastern margin of the Alexander terrane and consists of variably metamorphosed and deformed Upper Jurassic to mid-Cretaceous flysch and intermediate to mafic volcanic rocks. (5) The Yukon Prong terrane consists of metapelite, metabasalt, marble, and quartzite; it has possible ancient crustal affinities. (6) The Stikine terrane is composed of upper Precambrian basement rocks, some Devonian strata and Mississippian and Permian volcaniclastic rocks, mafic to felsic volcanic rocks, and carbonate rocks that were locally deformed and intruded in before Late Triassic time. The informally named Coast plutonic-metamorphic complex (Brew and Ford, 1984) has been superimposed on the Yukon Prong and adjacent terranes as a result of tectonic overlap and (or) compressional thickening of crustal rocks during collision of the Alexander and Wrangellia terranes with the Stikine terrane, the intervening Gravina overlap assemblage, and the Yukon Prong rocks (Monger and others, 1982; Brew and others, 1989).

The Alaskan-type ultramafic bodies are not restricted to any one terrane (fig. 1). Most were intruded into the Alexander terrane or into the Gravina overlap assemblage. The Red Bluff Bay body, however, occurs west of the main belt of Alaskan-type bodies on the east side of Baranof Island in what is generally interpreted to be the Chugach terrane, and the Port Snettisham, Windham Bay, and Alava Bay bodies occur in rocks that are probably part of the Yukon Prong terrane.

The ultramafic bodies fall into two age groups. Lanphere and Eberlein (1966) reported K-Ar ages that range from 100 to 110 Ma for 10 of the bodies. For the Duke Island body, Saleeby (1991) reported concordant U-Pb zircon ages of 108 to 111 Ma, and Meen and others (1991) reported the $^{40}Ar/^{39}Ar$ age for hornblendes of 118.5 Ma. On the basis of U-Pb zircon ages for gabbro pods in hornblendite at Union Bay, Rubin and Saleeby (1992) interpret that body to have an approximate age of 102 Ma. Loney and others (1987) reported data that suggest a much older age of about 429.1 Ma for the Salt Chuck body. Similar ages were obtained by M.A. Lanphere (written commun., 1989) for ultramafic bodies on Dall Island (400.1 Ma) and Sukkwan Island (440.5 Ma).

The older group of Alaskan-type complexes was intruded into the Alexander terrane prior to collision with the Stikine and Yukon Prong terranes. The distribution of the younger group of Alaskan-type complexes in the Alexander terrane, the Gravina overlap assemblage, and the Yukon Prong terrane, however, is consistent with the interpretation that the Alexander terrane was adjacent to the western margin of North America prior to their intrusion (Rubin and Saleeby, 1992). The distribution and age span of the Alaskan-type complexes indicates long-lived arc-basaltic magmatism associated with the Alexander terrane. Because the older group of intrusions occur outboard of the younger group, an eastward migration of the basaltic magmatism with time is suggested. The arc-basaltic magmatism was part of a complex, ongoing, long-lived, magmatic, metamorphic, and tectonic evolution of the convergent continental margin of western Canada and southeastern Alaska (Brew and Ford, 1985; Brew and others, 1989; Rubin and Saleeby, 1992).

FIELD RELATIONS AND PETROGRAPHY

Taylor and Noble (1960) reported the occurrence of 39 ultramafic bodies that they considered to be of the Alaskan-type in southeastern Alaska. Subsequently several other small bodies have been discovered. Most of the Alaskan-type intrusions occur in a belt referred to by Brew and Morrell (1983) as the Klukwan-Duke mafic-ultramafic belt. Detailed maps and descriptions have been published for the bodies at Union Bay (Ruckmick and Noble, 1959), the Blashke Islands (Walton, 1951; Himmelberg and others, 1986b), Duke Island (Irvine, 1974), Red Bluff Bay (Guild and Balsley, 1942; Loney and others, 1975), and Salt Chuck (Loney and Himmelberg, 1992). Summaries of the major features of the Alaskan-type bodies have been given by Taylor and Noble (1960) and Taylor (1967).

This study is based on field, petrographic, and rock and mineral chemistry investigations of the Alaskan-type complexes at Klukwan, Haines, Douglas Island, Port Snettisham, Kane Peak, Blashke Islands, Union Bay, Salt Chuck, Alava Bay, Sukkwan Island, Dall Island, Long Island, and Red Bluff Bay. Although our studies of Blashke Islands (Himmelberg and others, 1986b) and Salt Chuck (Loney and Himmelberg, 1992) were published separately, we include some of the data in this report in order to provide a single comprehensive database. Geologic maps of the Union Bay, Kane Peak, Blashke Islands, and Red Bluff Bay areas show the major rock types and characteristics of each of the bodies studied and the locations of analyzed samples (figs. 2, 3, 7, 10). Several of the larger bodies not included in this report are listed in table 1. Rock names have been changed from those in earlier publications to conform to the classification recommended by the

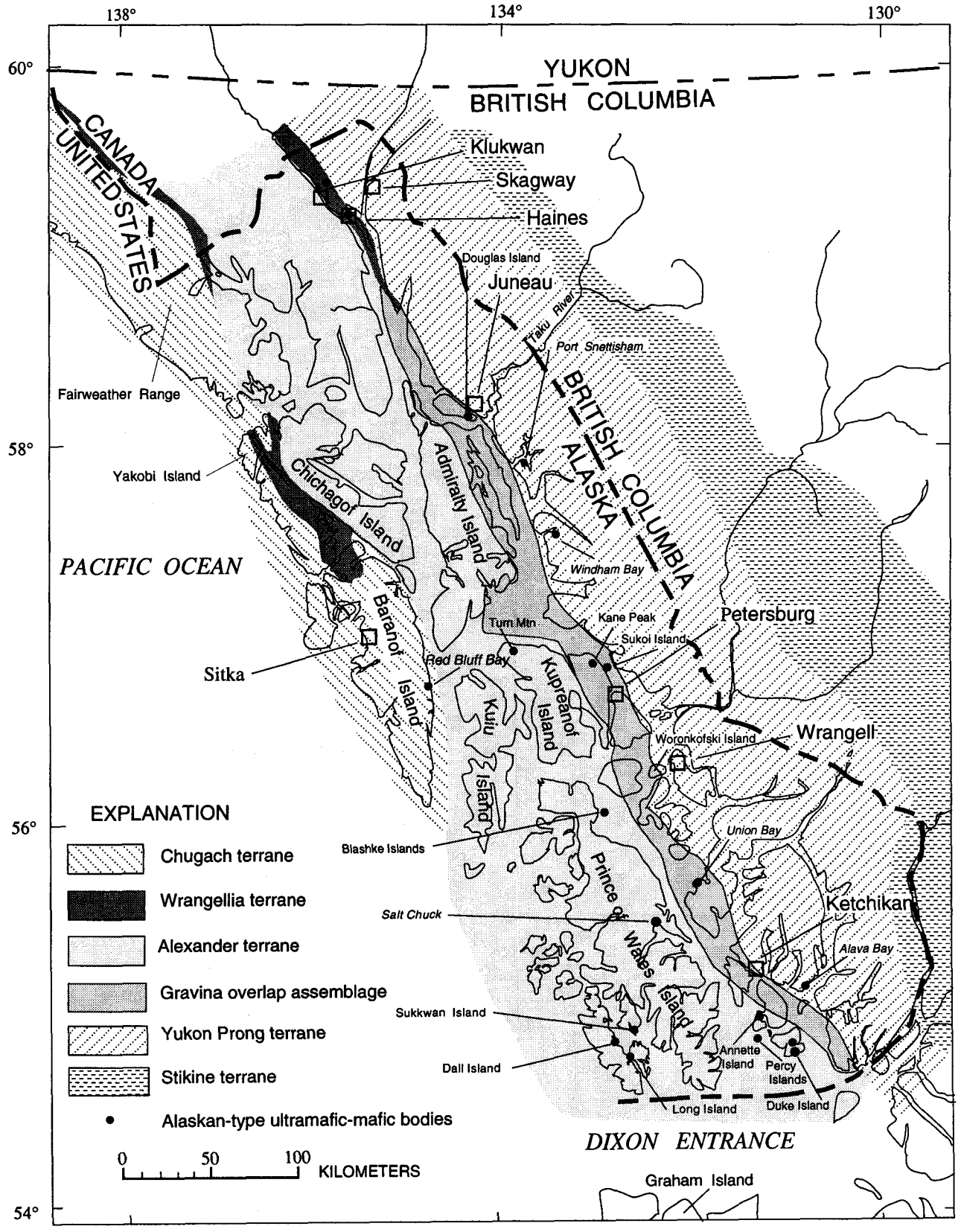

Figure 1. Map of southeastern Alaska showing locations of Alaskan-type ultramafic-mafic intrusions and major tectonostratigraphic units. Map compiled from Berg and others (1978), Monger and others (1982), Brew and Ford (1984), Samson and others (1989), Brew (1990), Gehrels and others (1990), Karl and others (1990), Brew and others (1991), and Ford and Brew (1993).

IUGS Subcommission on the Systematics of Igneous Rocks (1974). Owing to the excellent studies by Irvine (1967a, 1974), the Duke Island ultramafic body is not included in this study, but its major features are referred to in this report. Other small Alaskan-type intrusive bodies in southeastern Alaska not discussed here or shown on figure 1 include those at Hasselborg Lake, Admiralty Island (D.A. Brew, oral commun., 1991); Mole Harbor, Admiralty Island (Lathram and others, 1965); Woronkofski Island (Taylor, 1967; Brew and others, 1984); and Sukoi Island (Taylor, 1967).

As mentioned above, it is uncertain if the Red Bluff Bay body should be included as an Alaskan-type intrusion. We therefore exclude Red Bluff Bay from the general description that follows and instead discuss its characteristics separately at the end of this section.

Most of the Alaskan-type ultramafic bodies are roughly circular to elliptical in plan with relatively steep contacts. They range in size from only a few meters to about 10 km in maximum exposed dimension (Union Bay, fig. 3). The larger bodies include those at Klukwan, Haines, Port Snettisham, Kane Peak, Red Bluff Bay, Blashke Islands, Union Bay, Salt Chuck, Annette Island, and Duke Island (fig. 1). Those at Blashke Islands, Kane Peak, Union Bay, and Duke Island contain essentially all the components of the classic concentrically zoned ultramafic complexes (figs. 3, 7, 10; table 1). Each has a dunite core; wehrlite, olivine clinopyroxenite, and clinopyroxenite, which in some cases is rich in magnetite and hornblende, occur progressively outward. Only at the Blashke Islands, however, is the zoning symmetrical and continuous (fig. 10). Hornblendite occurs in the outer zones of Union Bay (fig. 3), Kane Peak (fig. 7), and Duke Island, and gabbro forms the outermost zones of the Union Bay (fig. 3) and Blashke Islands (fig. 10) bodies. The Annette Island body consists of dunite only, and the one at Salt Chuck consists primarily of magnetite clinopyroxenite and magnetite gabbro that are irregularly gradational. Essentially all the other ultramafic bodies, including the larger ones at Klukwan, Haines, and Port Snettisham, consist dominantly of magnetite-bearing hornblende clinopyroxenite and hornblendite (table 1).

The ultramafic rocks have cumulus textures that reflect their origin and concentration by crystal fractionation processes[3]. Most of the ultramafic rocks are medium- to coarse-grained adcumulates. Textures are generally subhedral to anhedral granular with mutually interfering, gently curved grain boundary segments. Dunite and wehrlite consist of adcumulus olivine and interstitial postcumulus clinopyroxene, which is poikilitic in some wehrlite samples. Chromian spinel is an accessory mineral in dunite and wehrlite. At Kane Peak an olivine-rich peridotite with interstitial orthopyroxene, hornblende, and biotite grades into dunite and wehrlite. Orthopyroxene-bearing peridotite has not been observed in any of the other ultramafic bodies. In olivine clinopyroxenite and clinopyroxenite, olivine and clinopyroxene are generally both cumulus, chromian spinel is generally absent, but magnetite is usually present; hornblende where present is generally postcumulus in olivine clinopyroxenite but cumulus in clinopyroxenite. In the Salt Chuck clinopyroxenite, plagioclase is commonly present as a postcumulus or minor cumulus phase. Hornblende clinopyroxenite consists of cumulus clinopyroxene, magnetite, and hornblende. Magnetite is particularly abundant in clinopyroxenite and hornblende clinopyroxenite at Klukwan, Port Snettisham, Union Bay, and, to a lesser extent, at Salt Chuck. The Blashke Islands and Kane Peak bodies generally contain magnetite only as an accessory phase and hornblende is not abundant. Clinopyroxenite, hornblende clinopyroxenite, and hornblendite in most of the intrusions also contain as much as nearly 10 percent biotite. At Kane Peak and Dall Island, biotite (phlogopite) is also present as an accessory phase in some samples of dunite and wehrlite.

Contacts between major rock units within any given complex range from gradational to sharp. Veins and dikes of clinopyroxenite and olivine clinopyroxenite are common in dunite and wehrlite. Individual rock units range from massive to internally layered. The layering is generally isomodal with mineral-ratio contacts and originated by gravity-settling or flow-differentiation processes (see: "Intrusive mechanism and zonal structure" discussion). In most bodies the layering is on the scale of centimeters in thickness and extends laterally only a few meters. At Union Bay, however, centimeter- to meter-scale thick layering is common in wehrlite and olivine clinopyroxenite and extends laterally for tens to hundreds of meters. Spectacular examples of cross bedding, graded bedding, and other complex layering features occur at Duke Island (Irvine, 1974). Similar layering features are reported on the Percy Islands (Taylor, 1967) but have not been observed in the other Alaskan-type ultramafic bodies.

Of the Alaskan-type bodies studied for this report, gabbro occurs only at Union Bay (fig. 3), the Blashke Islands (fig. 10), and Salt Chuck (Loney and Himmelberg, 1992; fig. 1). Gabbro also occurs at Duke Island, but it has been determined to be older than the ultramafic rocks (Irvine, 1974; Gehrels and others, 1987). At the Blashke Islands and Union Bay the gabbro forms a discontinuous outermost zone with sharp contacts against the adjacent ultramafic rocks. At Salt Chuck the clinopyroxenite and gabbro grade irregularly into one another by a gradual increase in postcumulus plagioclase in the magnetite clinopyroxenite prior to appearance of cumulus plagioclase in gabbro. Specific rock types of the gabbro unit on the Blashke Islands range gradationally and irregularly from olivine-bearing hornblende-pyroxene gabbro and gabbro-norite, near the contact with olivine clinopyroxenite, to hornblende gabbro toward the outer contact with the country rock. At Union Bay the gabbro unit is a relatively homogeneous gabbronorite having as much as nearly 5 percent each biotite and magnetite; near the margins, however, the mafic unit is commonly a hornblende

[3] The cumulus terminology is that proposed by Wager and others (1960) as redefined by Irvine (1982). Although many cumulates show evidence of originating by crystal settling, an origin is not specified in the definition of cumulate.

gabbro or diorite. Orthopyroxene is absent in the gabbros at Salt Chuck, but magnetite and biotite (as much as 10 percent) are common. All the gabbros are subhedral granular with a grain size of about 1 to 4 mm. At the Blashke Islands much of the gabbro is characterized by a centimeter-scale flow banding that is manifested by variable concentrations of plagioclase and mafic minerals. The gabbros at Salt Chuck and Union Bay, however, are generally massive with only local development of plagioclase lamination or centimeter-scale layering.

The enclosing country rocks of the larger ultramafic bodies have undergone intense contact metamorphism. Aureole widths are generally related to the size of the intrusion and range from less than 100 m to about 300 m. Maximum grade of metamorphism is generally hornblende-hornfels facies. The Kane Peak, Alava Bay, and Red Bluff Bay bodies have been affected by intrusion of younger granitic plutons (Loney and others, 1975; Brew and others, 1984; Loney and Brew, 1987). The Kane Peak and Alava Bay ultramafic bodies are only locally recrystallized.

The Red Bluff Bay intrusion (figs. 1, 2) is the largest body in a discontinuous, ill-defined, northwest-trending belt of ultramafic rocks on Baranof Island (Guild and Balsley, 1942; Loney and others, 1975). The belt extends for about 70

Table 1. Major rock types and characteristics of Alaskan-type ultramafic-mafic bodies, southeastern Alaska.

	Rock types	Features	References
Alava Bay	Biotite-bearing hornblendite	Elliptical shape; maximum dimension 2 km; locally recrystallized by granite.	This report.
Blashke Islands	Dunite; wehrlite; olivine clinopyroxenite; gabbronorite; olivine hornblende gabbro; hornblende pyroxene gabbro; hornblende gabbro.	Circular shape; 3.5-km diameter; concentrically zoned	Walton (1951); Himmelberg and others (1986b); this report.
Dall Island	Biotite wehrlite; biotite hornblende clinopyroxenite; clinopyroxenite; hornblende clinopyroxenite; biotite hornblendite.	Circular shape? 0.5 to 1 km diameter; meter-scale layering of rock types.	This report.
Douglas Island	Clinopyroxenite; hornblende clinopyroxenite; plagioclase clinopyroxenite.	Sills several meters wide	Brew and others (1987); this report.
Haines	Hornblende olivine clinopyroxenite; hornblende clinopyroxenite; biotite magnetite clinopyroxenite.	Elliptical shape?; maximum dimension 8 to 10 km	This report.
Kane Peak	Hornblende biotite peridotite; dunite; wehrlite; olivine clinopyroxenite; clinopyroxenite; hornblendite.	Roughly circular shape; 3- to 3.5-km diameter; crudely zoned; locally recrystallized by monzodiorite.	Walton (1951); this report.
Klukwan	Magnetite clinopyroxenite; hornblende magnetite clinopyroxenite.	Eliptical shape; maximum dimension 5 km	Taylor and Noble (1960); this report.
Long Island	Plagioclase-bearing hornblendite	Sill 6 m thick	This report.
Port Snettisham	Hornblende magnetite clinopyroxenite; biotite magnetite clinopyroxenite; hornblende biotite magnetite clinopyroxenite.	Elliptical shape; 3.5-km maximum dimension	Thorne and Wells (1956); this report.
Red Bluff Bay	Dunite; wehrlite; clinopyroxenite	Elliptical shape; 7-km maximum diamension. Recrystallized by granitic pluton. Classification as Alaskan-type uncertain.	Guild and Balsley (1942); Loney and others (1975); this report.
Salt Chuck	Clinopyroxenite; magnetite clinopyroxenite; biotite magnetite clinopyroxenite; magnetite melagabbro; magnetite gabbro; gabbro.	Tadpole shape; 7.3 by 1.6 km. Clinopyroxenite and gabbro irregularly gradational.	Loney and Himmelberg (1992); Watkinson and Melling (1992); this report.
Sukkwan Island	Hornblende clinopyroxenite; hornblendite	Tapered tabular shape; 1.5 km long	This report.
Union Bay	Dunite; wehrlite; olivine clinopyroxenite; clinopyroxenite; magnetite clinopyroxenite; hornblende clinopyroxenite; hornblendite; gabbro; gabbronorite.	Elliptical shape; 11.5 by 8 km; concentrically zoned	Ruckmick and Noble (1959); this report.
Annette Island	Dunite	Elliptical shape; 1.5-km maximum dimension; two exposures of hornblende clinopyroxenite 1 to 3 m wide on periphery of dunite.	Taylor and Noble (1960).
Duke Island	Dunite; wehrlite; olivine clinopyroxenite; hornblende magnetite clinopyroxenite; hornblendite.	Two separate bodies exposed; 5.5 by 3.2 km and 4 by 3.2 km, probably connected at depth; crudely zoned; spectacular layering developed by crystal transport and deposition by magmatic convection and density currents.	Irvine (1974).
Percy Islands	Olivine clinopyroxenite; hornblende magnetite clinopyroxenite.	Circular shape; 5.5-km diameter; layering features similar to those on Duke Island.	Stebbins (1957); Taylor (1967).
Turn Mountain	Hornblendite	Circular shape; 5-km diameter	Brew and others (1984).
Windham Bay	Clinopyroxenite; hornblende clinopyroxenite	Roughly circular shape; 3-km diameter	Brew and Grybeck (1984).

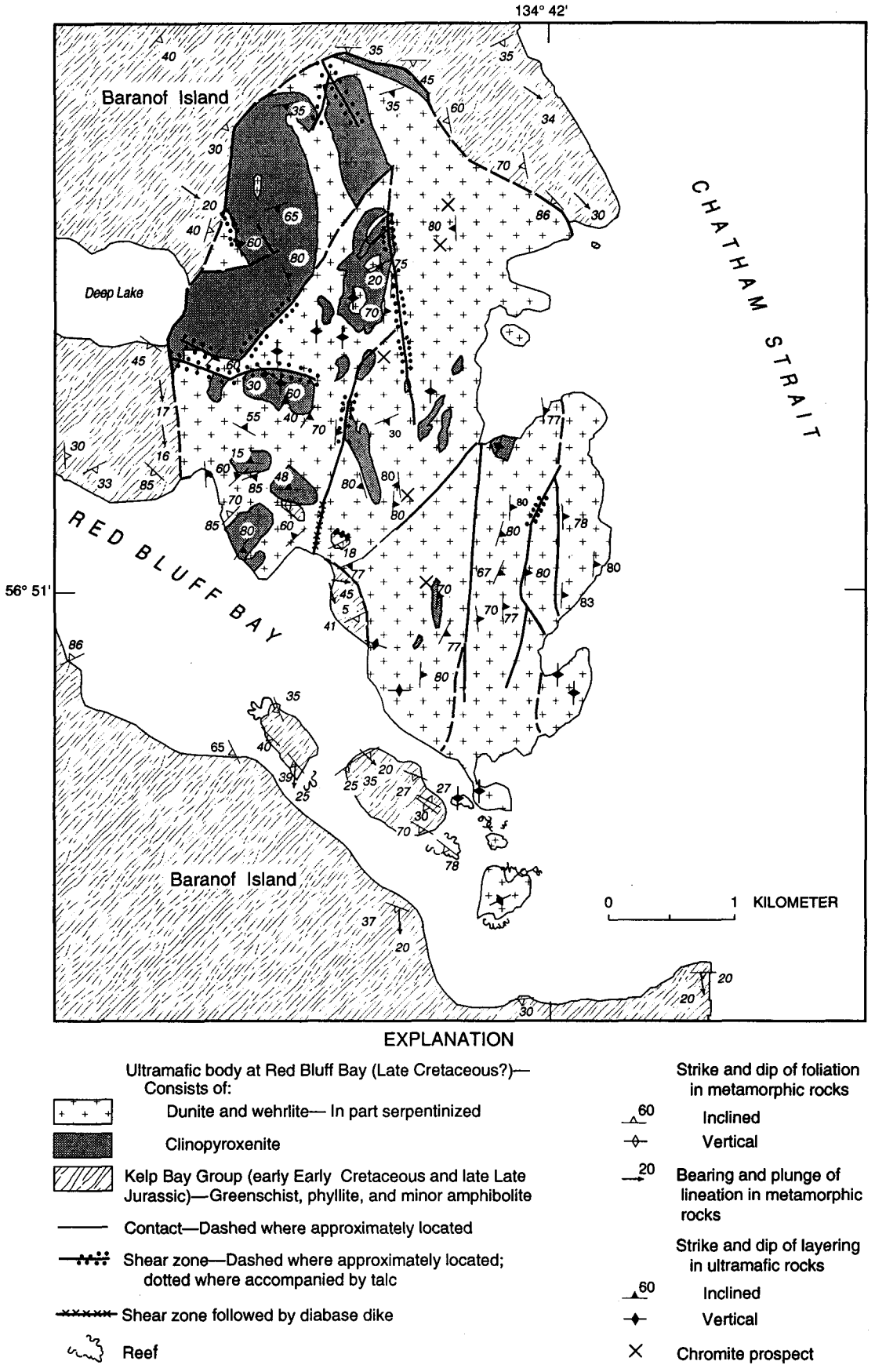

Figure 2. Geologic map of ultramafic complex at Red Bluff Bay, Baranof Island, southeastern Alaska. Map modified from Guild and Balsley (1942) and Loney and others (1975).

km, and, except for the Red Bluff Bay body, the ultramafic rocks occur as small scattered outcrops of sheared serpentinite. The Red Bluff Bay body consists of dunite, wehrlite, and clinopyroxenite, but there is no regular zoning pattern (fig. 2). The dunite and wehrlite are gradational and have no distinct contacts or regular distribution; because the relative amounts of the two rock types are unknown, we include both of them in a single dunite and wehrlite unit. In contrast, the clinopyroxenite unit as mapped contains virtually no olivine and has sharp contacts with the olivine-bearing rocks. The clinopyroxenite occurs in the body as irregular masses, cumulus layers (2–50 cm thick), and crosscutting veins. The Red Bluff Bay body differs from the typical Alaskan-type intrusions in that it contains chromian spinel layers and lenses in concentrations great enough to have encouraged development of chromite prospects (Guild and Balsley, 1942; Loney and others, 1975). Likewise, in contrast to the typical Alaskan-type body, the Red Bluff Bay body contains virtually no hornblende, and magnetite occurs only as a secondary mineral resulting from serpentinization and recrystallization. Cumulus textures are preserved even though the body has been extensively recrystallized (see below).

Limited data suggest that the small, serpentinized bodies northwest of Red Bluff Bay were derived from ultramafic bodies similar to the Red Bluff Bay body. These bodies are mostly serpentinite with very sparse clinopyroxene grains and local concentrations of thin chromitite layers. The sparsity of clinopyroxene is partly a result of the contact metamorphism caused by Eocene plutons, which converted most of the clinopyroxene to fibrous amphibole. The chromian spinel largely survived metamorphism, although it is commonly rimmed by magnetite (Loney and others, 1975; Loney and Brew, 1987). As neither orthopyroxene nor serpentine pseudomorphs after orthopyroxene (bastites) have been reported in them, these complexes suggest that they may have been derived from clinopyroxene-bearing olivine-rich bodies such as the Red Bluff Bay ultramafic body.

The ultramafic complex at Red Bluff Bay is in contact with greenschist, phyllite, and minor amphibolite of the Kelp Bay Group (late Late Jurassic (Tithonian) and early Early Cretaceous (Berriasian)), but there is no evidence of contact metamorphism by the ultramafic body. The contact relations are obscured by shear zones along the contacts and by the fact that the ultramafic body lies in the upper albite-epidote hornfels facies part of the contact aureole of the middle Eocene (44.3-Ma) Baranof Lake (tonalite) pluton (Loney and others, 1975). In the Red Bluff Bay body, the serpentine that has been recrystallized to antigorite and the olivine and clinopyroxene that have commonly reequilibrated to more magnesium-rich compositions indicate that they too recrystallized in response to the intrusion of the Baranof Lake pluton. On the Basis of these relations, the age of the Red Bluff Bay body, and the belt of serpentinites as well, lies between about 44 Ma and 138 Ma (Berriasian).

The dunite-wehrlite-clinopyroxenite association in the Red Bluff Bay body and the limits on the age of the body are characteristics that are similar to those of the Alaskan-type group of intrusions. However, the occurrence of chromitite lenses and layers and the virtual absence of primary magnetite and hornblende are atypical of Alaskan-type intrusions. The rock association, textures, and structures of the Red Bluff Bay body are equally compatible with an origin as crustal cumulates within an ophiolite complex (Coleman, 1977; Himmelberg and Loney, 1980; Pallister and Hopson, 1981; Elthon and others, 1982; Loney and Himmelberg, 1989). However, the absence of any orthopyroxene-bearing residual harzburgite in this belt of ultramafic rocks argues against these rocks representing a part of a dismembered ophiolite.

RELATION OF ALASKAN-TYPE ULTRAMAFIC INTRUSIONS TO REGIONAL STRUCTURE AND METAMORPHISM

GENERAL STATEMENT

Intrusion of the younger Alaskan-type ultramafic bodies throughout the extensive Klukwan-Duke mafic-ultramafic belt (Brew and Morrell, 1983) during a relatively short interval of time, 100 to 118 Ma (Lanphere and Eberlein, 1966; Lanphere, written communication, 1989; Saleeby, 1991; Meen and others, 1991; Rubin and Saleeby, 1992), provides a regionally identifiable time datum. Therefore, the relation of the intrusions to major regional events, such as deformation and metamorphism, is critical to the study of the tectonic history of southeastern Alaska. Of the complexes studied, only those at Union Bay, Kane Peak, and the Blashke Islands show the critical relations of deformation and metamorphism in both the intrusion and the country rocks.

According to Lanphere and Eberlein (1966) and Lanphere (1968), the Alaskan-type ultramafic complexes of southeastern Alaska were intruded after folding and low-grade regional metamorphism of Paleozoic and lower Mesozoic stratified rocks of the western metamorphic belt (D_1 and M_1 of Brew and others, 1989) in Late Cretaceous time, prior to intrusion of plutonic rocks of the Late Cretaceous and early Tertiary Coast plutonic-metamorphic complex. However, evidence from this study of Union Bay and Kane Peak (fig. 1) and from Duke Island (Irvine, 1974) shows that these bodies intruded the western metamorphic belt during the late stages of the regional D_1 deformation and M_1 metamorphism and were affected by these events to some extent. In the Blashke Islands (fig. 1), however, the ultramafic intrusion and the surrounding sedimentary rocks are beyond the western limits of the western metamorphic belt (Brew and others, 1992) and were not noticeably affected by the regional metamorphism.

The following discussion relies heavily on olivine microfabrics. Olivine microfabrics and structural states have proved to be important tools in the study of ultramafic rocks because definitive structural data are commonly difficult to obtain in outcrop. The optical preferred orientation of olivine in mafic igneous rocks may have been produced by synigneous mechanisms, largely laminar igneous flow and gravity settling in magma, or by postigneous tectonic deformation (Den Tex, 1969). Obviously the latter may be superposed upon the former. Orientations due to igneous processes are dependent on the shape of the olivine crystals, whereas tectonically produced fabrics are independent of the crystal shape (Avé Lallemant, 1975; Nicolas, 1992). We have used these and other criteria to distinguish between these processes in the Union Bay, Kane Peak, and Blashke Islands bodies. Because olivine is an orthorhombic mineral, the X, Y, and Z axes will have the following definitions in petrofabric discussions: X = fast ray = b = ⊥(010)=[010]; Y = intermediate ray = c = ⊥(001)=[001]; Z = slow ray = a = ⊥(100)=[100].

UNION BAY COMPLEX

The zoned ultramafic complex at Union Bay is about 11.5 km long and about 8 km wide (figs 3, 4). As mapped by Ruckmick and Noble (1959), and confirmed by our work, the intrusive body is composed of a discontinuous outer gabbro unit around an irregular, central ultramafic mass. Locally, such as at Union Bay itself and near Vixen Inlet, the ultramafic rocks (magnetite clinopyroxenite, unit Kupx, fig. 3) are in contact with the country rocks, which are composed of the Upper Jurassic and Lower Cretaceous Gravina sequence of Rubin and Saleeby (1991). As interpreted by Ruckmick and Noble (1959), the intrusive consists of a western, subhorizontal lopolithic part, about 8 km long and 4.8 km wide, composed dominantly of clinopyroxenite, and a smaller eastern vertical pipe or cylinder about 1.6 km in diameter, composed dominantly of dunite (figs. 3, 4). In their view, the lopolith is a tongue-like or nappe-like body, closed on the west but open on the east, and was fed from a conduit now represented by the pipe. Beyond the contact zone, the country rocks are dominantly greenschist facies phyllite, also derived from the Gravina sequence (fig. 3). The contact zone is about 300 m wide. Country rock in the outer part is recrystallized to quartz-oligoclase-biotite-almandine schist. Schist grain size gradually increases toward the contact with the ultramafic rock and becomes noticeably coarser and more gneissic within about 150 m of the contact.

Our mineral fabric and field structural-geometric studies indicate that the intrusion of the ultramafic complex at Union Bay was contemporaneous with at least the last stages of folding of the country rocks. During the folding, both the igneous rocks of the complex and the metamorphic country rocks were plastically deformed about similarly oriented axial planes. The metasedimentary rocks were tightly folded about northwest-trending axes and subvertical axial planes during the regional M_1 metamorphism of the western metamorphic belt (late Early Cretaceous and (or) early Late Cretaceous; Brew and others, 1992.) The best example of this folding is in the northwest part of the area, in the vicinity of Vixen Inlet (fig. 3), where the rocks are little disturbed by the intrusion. The poles-to-bedding plots (+) in this area yield a π_1 axis that trends 303° and plunges 10° (fig. 5*A*). In the contact zone, however, poles-to-bedding and poles-to-foliation plots (Δ), combined, yield a π_2 axis plunging steeply to the northeast. This latter π orientation appears to reflect the bending of the earlier folds around the solid, hot ultramafic body. A similar relation was observed in the Kane Peak area.

The in-dipping attitudes in the cumulus layering in the ultramafic rocks immediately west of Mount Burnett (figs. 3, 5*B*) define the hinge of an open, southeast-plunging synform in the complex sandwich of layers that forms the lopolith. Other similarly oriented but generally smaller folds occur in the intrusive body, and some of them extend into and involve the metasedimentary country rock (fig. 3). On the basis of π-axis analysis (fig. 5*B*), the synclinal axis in the igneous layering plunges about 26° to the southeast (126°). The north limb has an average strike of 067° and a dip of 35° south, and the southwest limb has an average strike of 350° and a dip of 35° northeast. The axial plane strikes 300° and dips 85° southwest, similar in orientation to the regional trend (fig. 5*A*) in the metamorphic rocks. The synform dies out abruptly at the western margin of the pipe, where a moderately to steeply dipping, more or less domal (quaquaversal) structure prevails.

The tectonic stresses that produced regional folding of the country rocks and of the layers in the Union Bay intrusion also affected the optical preferred orientation of olivine in the intrusion. The olivine microfabric was investigated in two areas in the Union Bay intrusion: (1) The eastern domal domain, consisting mostly of a dunite mass at the center of the pipe (fig. 3); and (2) the western synformal domain, centered around the south side of Mount Burnett, consisting mostly of interlayered dunite and clinopyroxenite in the hinge of the major synform in the lopolith (figs. 3, 5*B*). Both fabrics have a similar symmetry, but the microfabric of the domal domain has a more pronounced preferred orientation (figs. 6*A*, *B*). As is common in olivine tectonites, both fabrics have a pronounced X maximum normal to the plane containing maxima and partial girdles of Y and Z, the greatest maxima of which tend to be 90° apart. In this plane, Y lies near the center of the diagram (subvertical), and Z usually plunges gently to the northwest; weaker concentrations of Z axes form a girdle that ranges through horizontal to gentle southeast plunges. The X maximum is about normal to the axial plane of the synform, and accordingly the Y-Z plane lies near the axial plane (fig. 6*B*) and not near the plane of the cumulate layering. The orientation of the layering at or near the specimen locality is shown by great circles (S) in figs. 6*A*, *B*. The fact that the olivine microfabric is best developed in the domal domain is evidence that the metamorphism was regional and

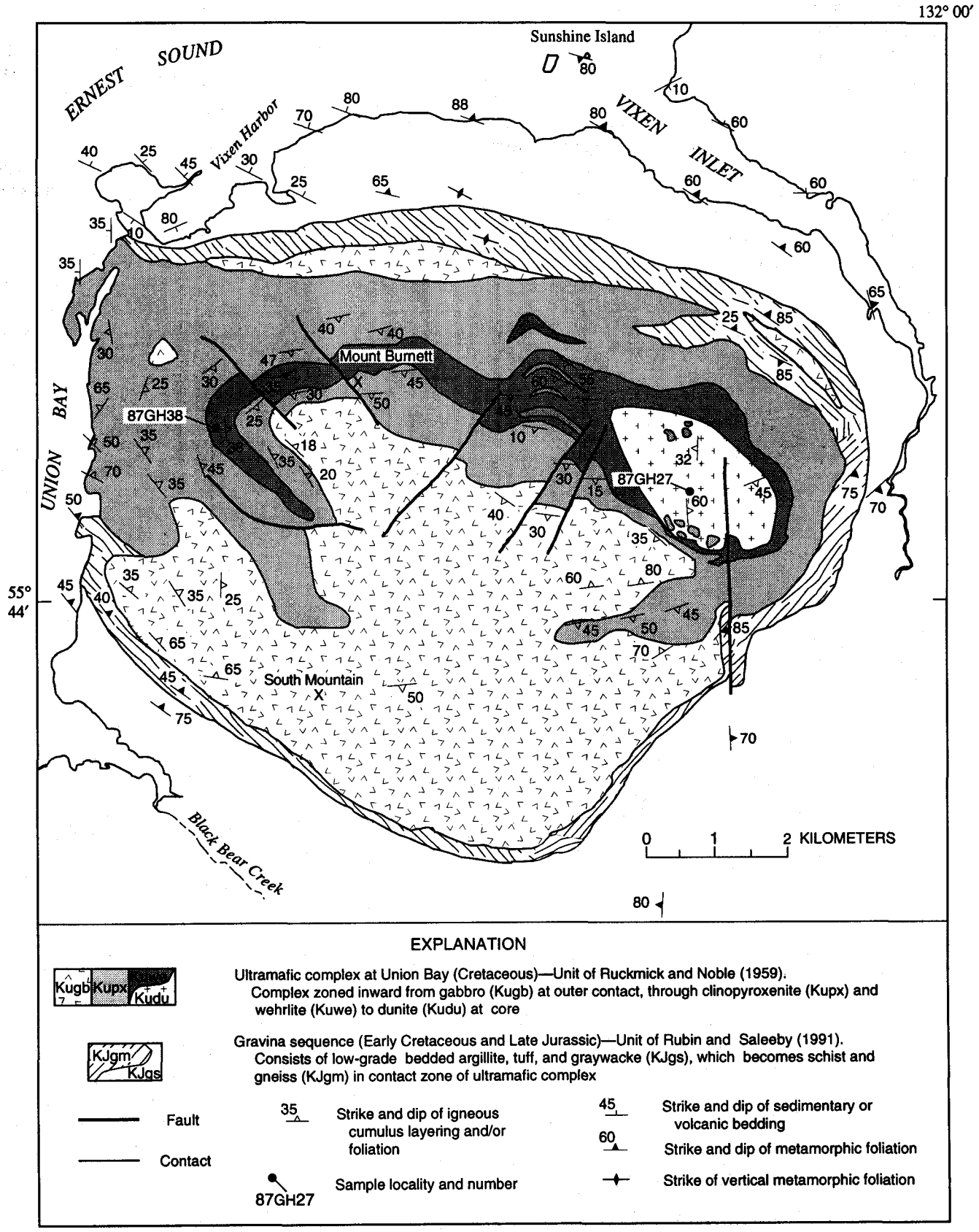

Figure 3. Geologic map of ultramafic complex at Union Bay, southeastern Alaska, showing locations of oriented samples used for microfabric analyses. See figure 4 for hypothetical cross section. Map modified from Ruckmick and Noble (1959).

not related to local conditions. The syncline and other folds are manifestations of regional metamorphism accompanied by penetrative deformation.

The symmetrical geometry of the major units of the Union Bay body strongly suggests flow differentiation during emplacement (fig. 4). However, the existing olivine microfabric seems to be controlled by the regional deformation rather than by an original igneous processes. The regional metamorphism (M_1) and deformation seem to have occurred when the body was hot enough to permit the plastic deformation of olivine, which obscured the original igneous orientation. According to Carter and Avé Lallemant (1970), at pressures less than 5 kb, significant plastic deformation of olivine may occur at temperatures of from 300 to 400°C; this is consistent with the probable conditions of the low-grade M_1 metamorphism.

KANE PEAK COMPLEX

The Alaskan-type ultramafic complex in the Kane Peak area crops out on the northeast coast of Kupreanof Island about 20 km northwest of Petersburg (fig. 1). It forms a 6-km^2 outcrop area that is slightly elongate in a northeastward direction. Projection of the converging contacts suggests that the complex extends northeastward as much as 1.5 km beneath Frederick Sound (fig. 7). The Kane Peak complex intruded mainly metamorphic pelites and semipelites of the Seymour Canal Formation of Late Jurassic and Early Cretaceous age (fig. 7) (Brew and others, 1984). It has produced a vaguely defined contact aureole of uncertain thickness that is represented in places by coarser grained, more intensely foliated rocks. Along the northwest and southwest contacts the aureole is unclear because the complex is in contact with a migmatite unit (fig. 7) of regional extent that was also probably derived from the Seymour Canal Formation by metamorphism related to the younger 90-Ma quartz monzodiorite pluton (fig. 7) (Brew and others, 1984; Douglass and Brew, 1985), which also intrudes the ultramafic complex on the west (Burrell, 1984; Brew and others, 1984). The pluton has recrystallized the ultramafic rocks along the mutual contact, as indicated by the fine polygonal crystallization of olivine and abundant serpentine veining in the ultramafic rocks of the border zone.

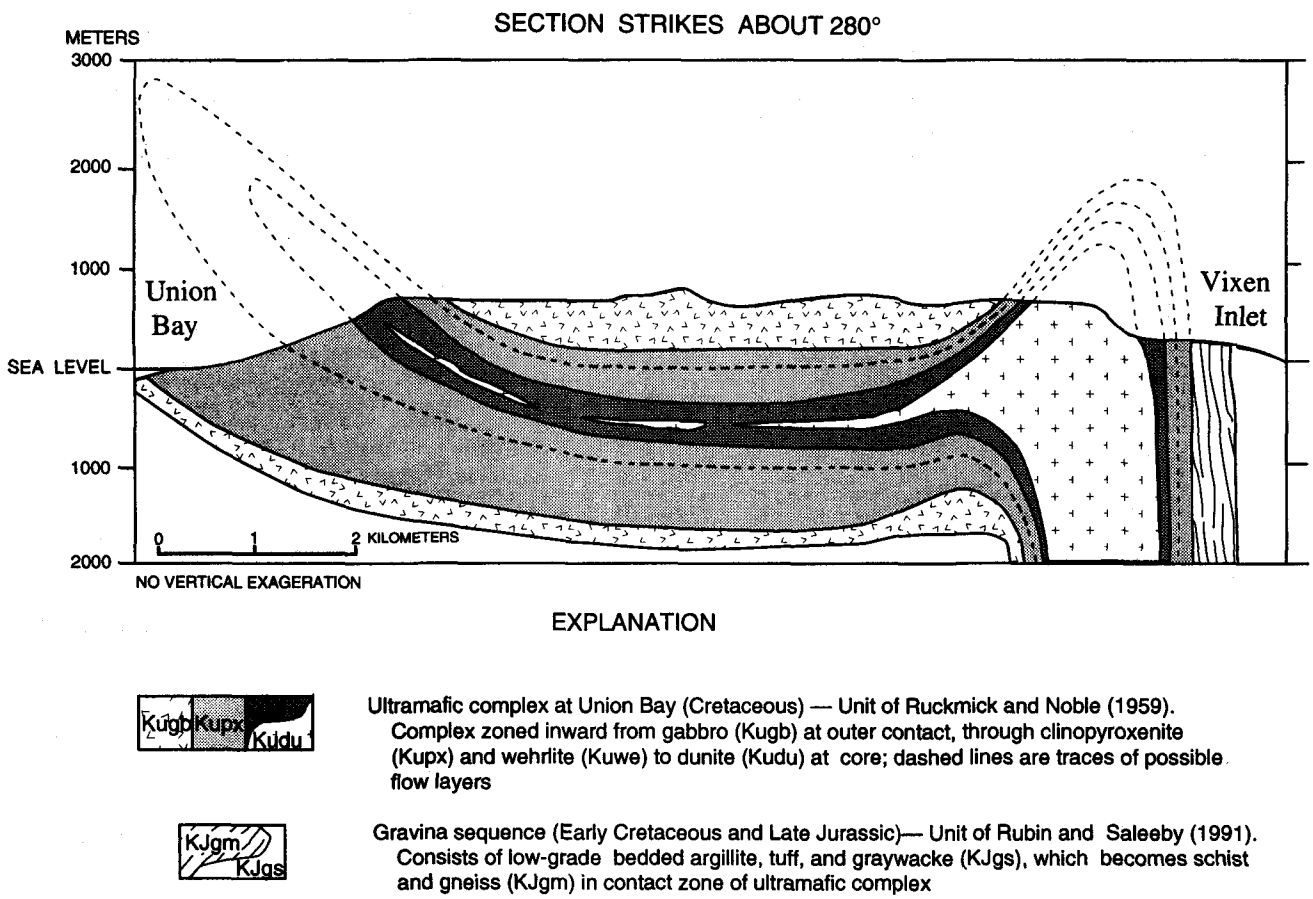

Figure 4. Hypothetical cross section through ultramafic complex at Union Bay, southeastern Alaska, modified from Ruckmick and Noble (1959, pl. 4).

The Kane Peak ultramafic complex contains hornblendite border zones, averaging about 100 m wide, along the northwest and southeast contacts. On the northeast, the complex is covered by Frederick Sound, and on the southwest the border zone seems to be absent, probably cut out by the younger (90-Ma) quartz monzodioritic intrusion. About 80 percent of the poorly exposed interior of the body is composed of dunite and wehrlite that grade into one another by variation in clinopyroxene content. Small-scale cumulus layers occur locally, but, because of the poor exposures and the massive nature of the dominant rock, little is known about the layering. Texturally it could have formed either by static gravity settling or flow differentiation processes (see "Intrusive mechanism and zonal structure").

The general trend of the country rock structure on northeast Kupreanof Island is northwestward, typical of that in the Gravina overlap assemblage. Important elements making up the structural fabric are steeply eastward-dipping limbs of gently northwest-plunging isoclinal folds. The structural domain of the metasedimentary country rocks (fig. 7) north of the ultramafic complex in the Kane Peak area, and in the migmatite belt, is typical of this trend (fig. 8*A*). Poles-to-bedding plots define a π axis that plunges gently to the northwest, subparallel to the field-measured, gently plunging fold axes and steeply dipping axial plane. South of the ultramafic body, this pattern is modified; the poles-to-bedding plots define a π axis that plunges steeply east (fig. 8*B*). This general attitude is shared by a steeply plunging northeastward-striking fold axis and an eastward-striking, moderately north-dipping axial plane. Lineations, crenulations, mineral streaks, and elongations throughout this domain also have this preferred orientation, the mean lineation vector (MLV) of which is shown (fig. 8*B*, *C*). These data suggest that the regional deformation was deflected around either a preexisting ultramafic body or one that was intruded during the deformation.

Figure 6. Equal-area, lower hemisphere plots of olivine X, Y, and Z axes in ultramafic complex at Union Bay, southeastern Alaska. Contours show concentrations of percentages (1, 2, 3, 4, 5, and 6 percent) per 1 percent of area. ■, pole of X-maximum circle; S, layering (see text). *A*, Specimen 87GH27 from domain 1 (pipe, 98 axes). *B*, Specimen 87GH38 from domain 2 (synform, 100 axes).

However, unlike Union Bay, there is no clear evidence of tectonic influence on the olivine microfabric; instead, the fabric appears clearly related to cumulus layering. The fabric was determined for two localities: One a dunite at the northeast end of the body (fig. 9*A*), and the other a wehrlite at the southwest end near Kane Peak (fig. 9*B*). Layering was visible only in the wehrlite (great circle S in fig. 9*B*), which also has a much stronger olivine preferred orientation for the X axis (>11 percent) than does the dunite (5 to 6 percent, fig. 9*A*). Although the field-measured layering orientation is slightly different from that of the plane normal to the main X maxima, it is close enough to show the relation of the olivine axes to the layering: namely, X normal to the layering, and Y and Z near the plane of the layering. This fabric suggests that olivine, having pronounced (010) faces, either (1) settled in a

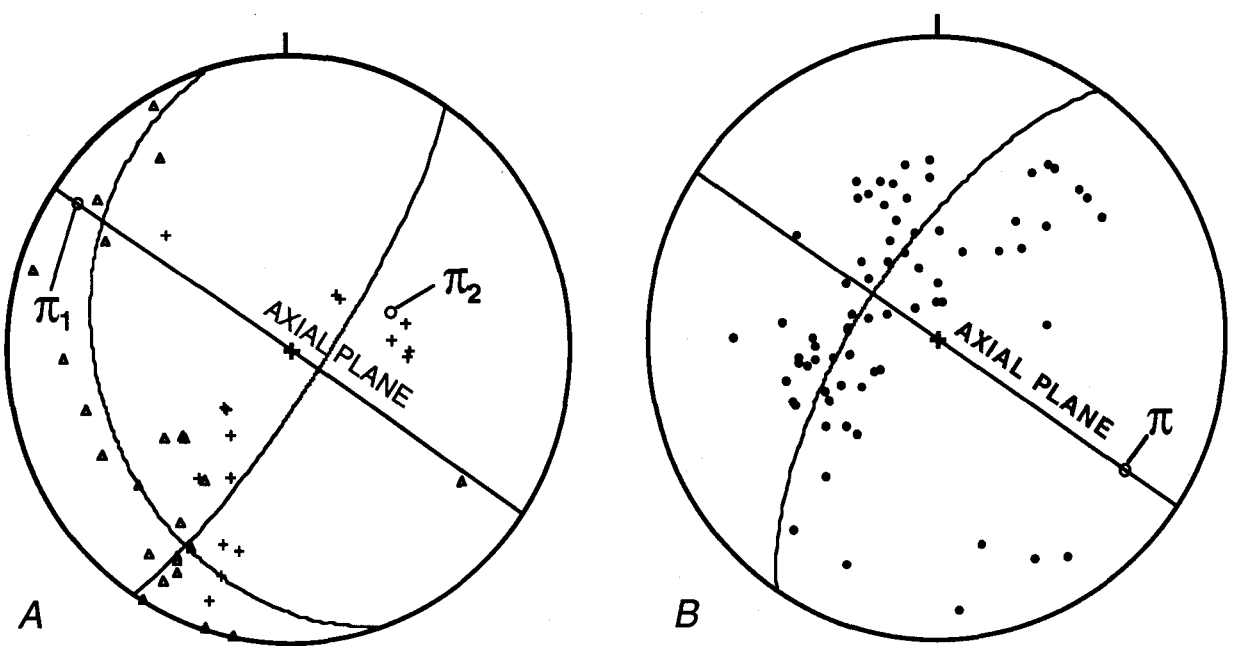

Figure 5. Equal-area, lower hemisphere plots of structural data in Union Bay area, southeastern Alaska. *A*, Poles to bedding (+, 15 poles) in country rock in the Vixen Inlet area (fig. 3) and to foliation (Δ, 22 poles) in metamorphic contact zone of intrusion. π_1 is for bedding, π_2 is for foliation. *B*, Poles to cumulus layering and igneous lamination in Union Bay ultramafic intrusion (70 poles).

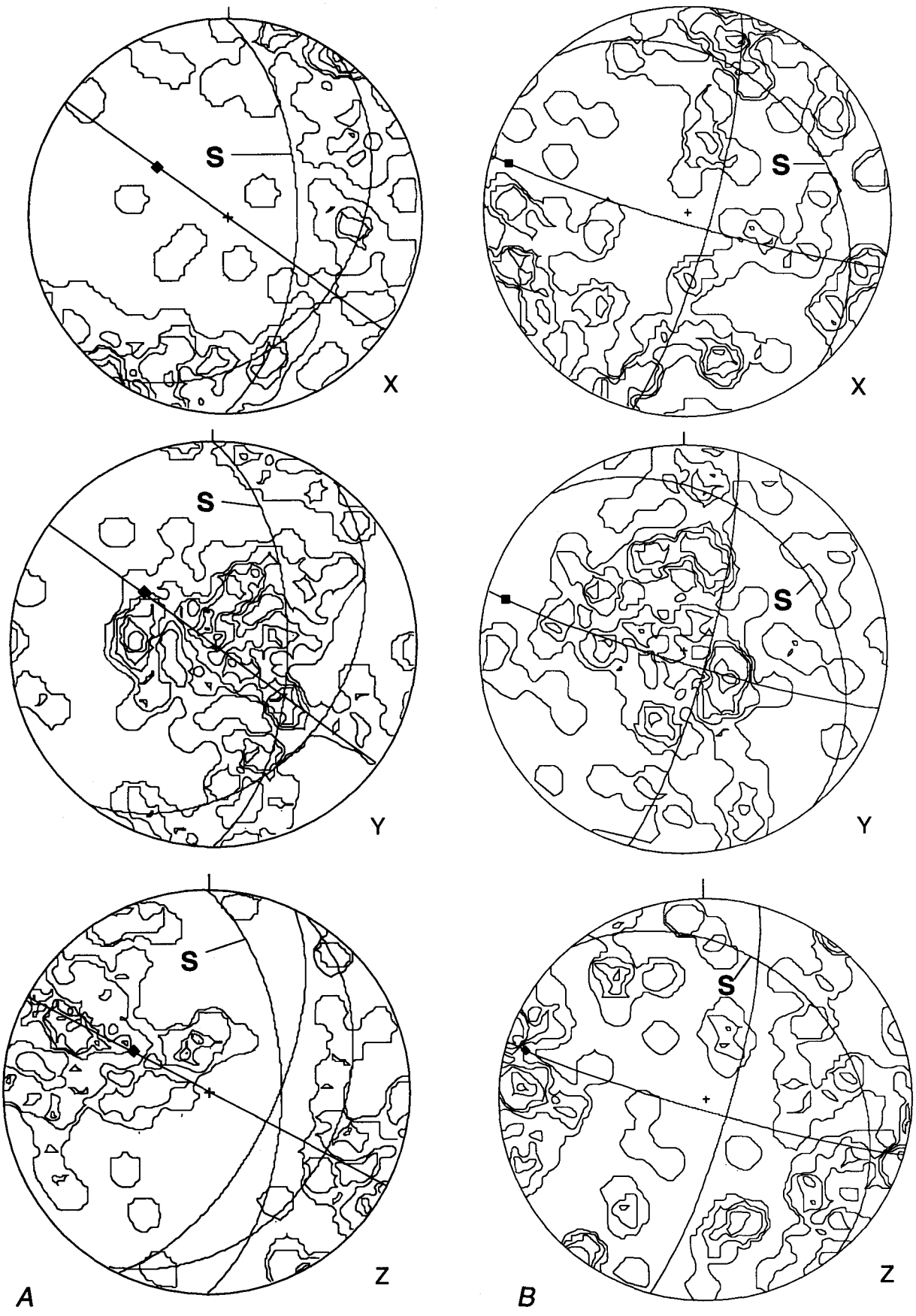
S
X
S
X
S
Y
S
Y
S
Z
S
Z
A
B

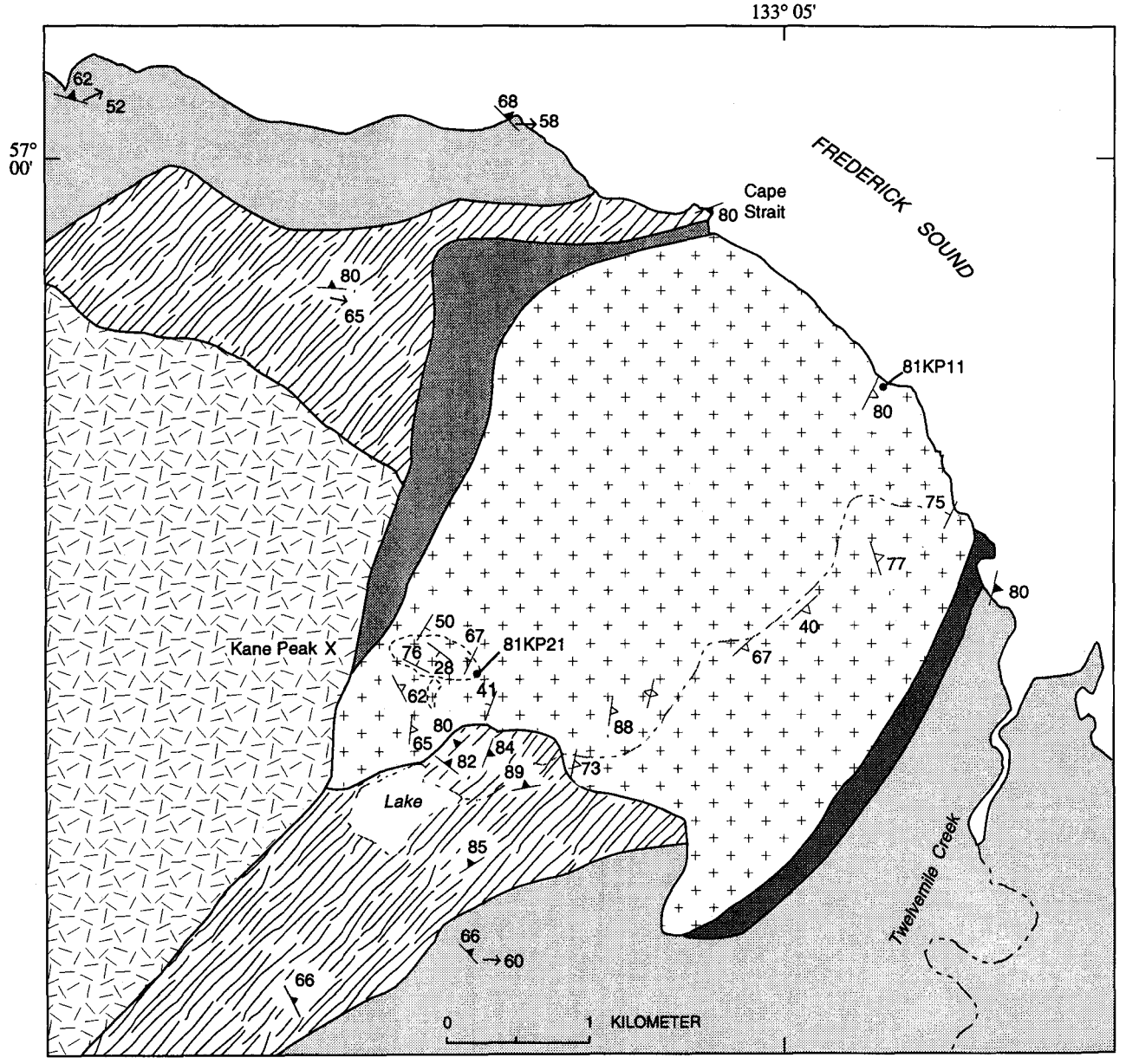

Figure 7. Geologic map of ultramafic complex in Kane Peak area, Kupreanof Island, southeastern Alaska, showing locations of oriented samples used for microfabric analyses. Map modified by us from Walton (1951) with assistance of S.M. Karl and A.B. Ford on basis of fieldwork done in 1980.

magma and came to rest with the X axis (⊥(010)) normal to the layering (Den Tex, 1969) or (2) obtained this orientation during magmatic laminar flow. If the crystals are elongate parallel to the c-crystallographic axis (= Y), then accordingly the Y axes would tend to be aligned parallel to the current direction (Brothers, 1959,1964; Nicolas, 1992). Similar flow-related fabrics have been described by Wilson (1992) from the Great Dyke of Zimbabwe in which orthopyroxene crystals show a strong (8.8 percent) preferred orientation of (010) face parallel to layering and equally strong preferred orientation of the c axes (= Z) in the plane of the layering.

Data on the layering is very limited but do show a dominantly subvertical attitude (fig. 7). Furthermore, plots of the olivine Y axes (= c) of the Kane Peak ultramafic body (fig. 9) show a dominantly subvertical orientation that is close to that of the layering and is compatible with subvertical magmatic flow of crystals described above. This fabric could be produced by subvertical magmatic flow in a feeder conduit, such as proposed for flow differentiation (see "Intrusive mechanism and zonal structure"; also Nicolas, 1992). The subvertical internal orientation, coupled with the probable subvertical contacts, is more compatible with flow differentiation in a subvertical conduit than with gravity settling on a subhorizontal surface, which would require a rotation of approximately 90° to obtain its present orientation. Presumably such rotation would be unnecessary in diapiric intrusion (Irvine, 1974), but supporting evidence for this is unclear or absent.

BLASHKE ISLANDS COMPLEX

The massive dunite core, which forms the bulk of the ultramafic complex on the Blashke Islands (figs. 1, 10), gives little indication of fine-scale layering, lamination, or other small scale primary igneous features. However, the general symmetrical configuration of rock types suggests a steeply dipping to subvertical cylinder. The country rocks in the Blashke Islands area are dominantly argillite and graywacke of the Descon Formation of Early Ordovician through Early Silurian age and are part of the Alexander terrane. Away from the high-grade hornfels of the contact zone, these rocks, although folded, show little indication of regional penetrative deformation and metamorphism of an intensity and grade that

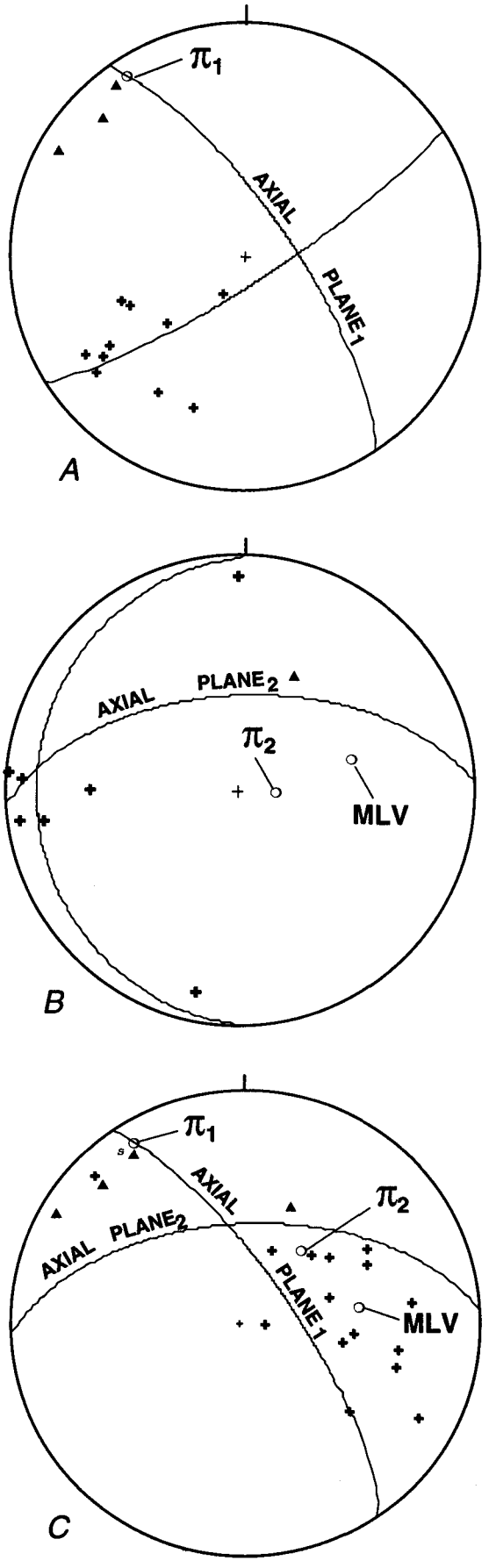

Figure 8. Equal-area, lower hemisphere plots of structural data in metaturbidites in Kane Peak area (fig. 7), southeastern Alaska. ▲, fold axes; MLV, mean linear vector of small structural features; mesoscopic axial plane. *A*, Poles to bedding in metaturbidites north of migmatite belt along north border of ultramafic complex. π_1, pole to best-fit great circle; +, poles to bedding. *B*, Poles to bedding in metaturbidites south of ultramafic complex. π_2, pole to best-fit great circle; +, poles to bedding. *C*, Fold axes (▲) and lineations (+) for metaturbidites in areas of plots *A* and *B* combined. Great circles represent axial-plane orientations in both areas; π_1, pole to best fit in plot *A*; π_2 derived from combined bedding.

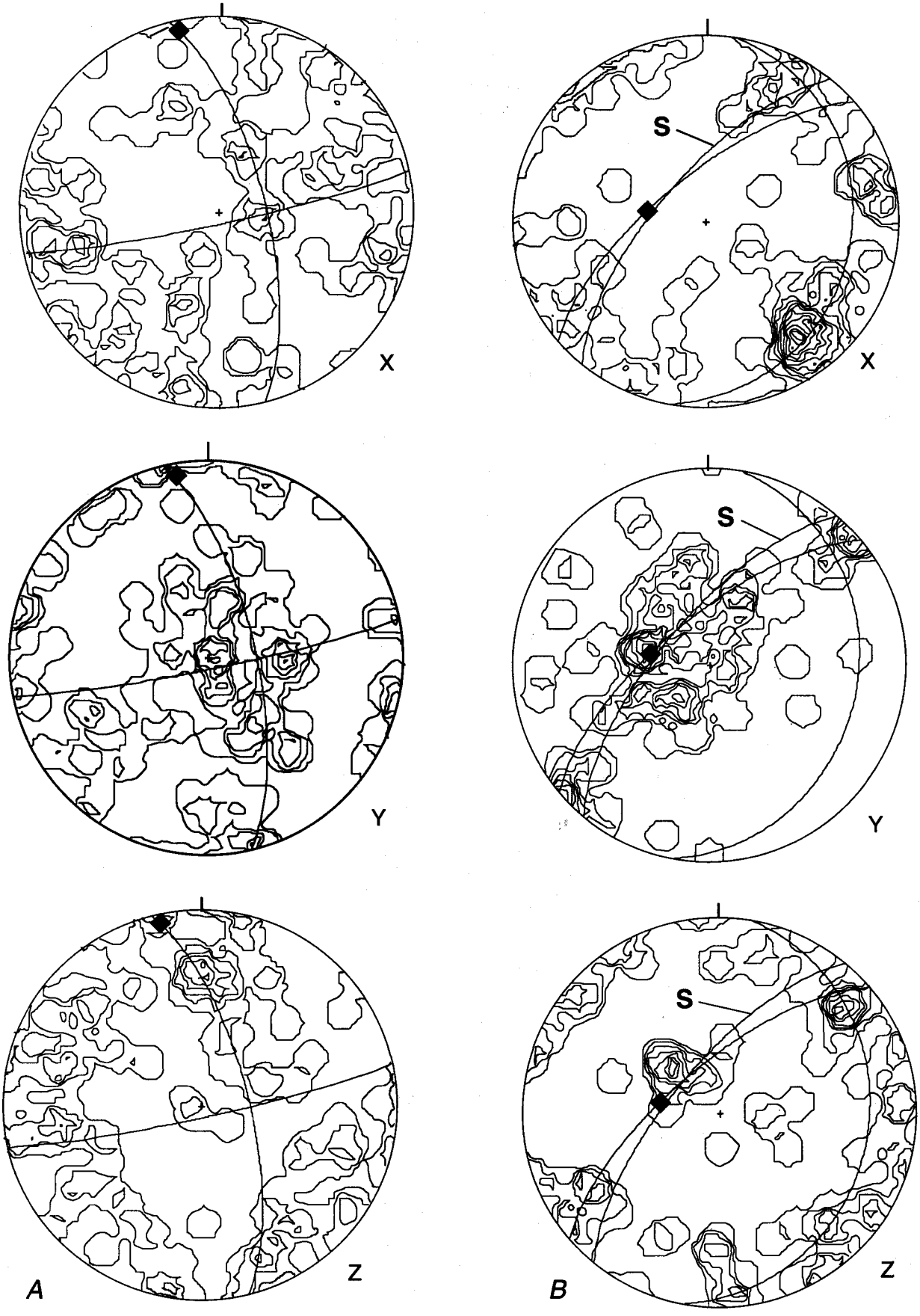
X
S
X
Y
S
Y
A
Z
S
B
Z

would produce a syntectonic recystallization of olivine in the ultramafic body, such as that at Duke Island (Irvine, 1974) and Union Bay. Brew and others (1992) consider the Blashke Islands area to be outside the metamorphic and deformational belt that affected the Union Bay and Kane Peak bodies. In contrast to that at Union Bay, the Blashke Islands contact zone reflects this lack of tectonic influence; it is a 100-m-wide zone of massive fine-grained hornfels with a well-developed granoblastic polygonal texture. The maximum-phase metamorphic mineral association is plagioclase-hornblende-orthopyroxene-clinopyroxene-biotite-iron oxide, indicative of the pyroxene-hornfels facies.

The apparent absence of a tectonic signature on the olivine microfabric of the dunite of the Blashke Islands body is compatible with paleomagnetic studies by Sherman C. Grommé (oral commun., 1989) that indicate the absence of tectonic deformation of the Blashke Islands complex. His data indicate tectonic folding of the Duke Island ultramafic complex and reinforce the conclusions of Irvine (1974). It appears, therefore, that Alaskan-type complexes in the southern part of the belt, at Union Bay and Duke Island, were intruded during or before the regional M_1 metamorphism and deformation (Brew and others, 1989), whereas regional metamorphism died out to the north-northwest before it reached the Blashke Islands.

As in the Kane Peak complex, the olivine microfabric in the dunite consists of a pronounced subvertical Y (= ⊥(010)) maximum and distinct subhorizontal X and Z maxima (fig. 11). Also as before, this fabric is compatible with olivine crystals that have well-developed (010) faces and a pronounced elongation parallel to c, either by gravity settling in a magma or by movement during subvertical magmatic flow differentiation. In the latter process, olivine crystals having well-developed (010) faces and elongation parallel to c are brought parallel to the magmatic flow direction (Nicolas, 1992; see "Intrusive mechanism and zonal structure"). In the former process, according to Den Tex (1969), large crystal faces of mineral grains settling under gravity in a mafic magma tend to come to rest parallel to the surface of accumulation, and the crystals become aligned parallel to long dimensions only if a current is present. As at Kane Peak, the subvertical internal orientation and large-scale subvertical cylindrical geometry of the intrusion is more compatible with flow differentiation in a subvertical conduit than with gravity settling on a subhorizontal surface, which would require considerable rotation to its present orientation.

◀ **Figure 9.** Equal-area, lower hemisphere plots of olivine X, Y, and Z axes in ultramafic complex in Kane Peak area, southeastern Alaska. ■, pole of X-maximum circle. *A*, Dunite specimen 81KP21; contours show concentrations of percentages (1, 2, 3, 4, 5, 6, 7, and 8 (Z), 9 (Y), 10, 11, and 12 (X) percent) per 1 percent of area (97 axes). *B*, Wehrlite specimen 81KP11; contours show concentrations of percentages (1, 2, 3, 4, and 5 (X), 6 (Y and Z) percent) per 1 percent of area (100 axes), S, layering.

In summary, structural and olivine microfabric studies of the ultramafic bodies at Union Bay, Kane Peak, and the Blashke Islands show different but possibly regional progressive relations relative to regional deformation and metamorphism. The Union Bay body was folded along with the country rocks during the earliest deformation and metamorphic event in the M_1 western metamorphic belt; the olivine microfabric indicates tectonic recystallization during this event. Data suggest that the Kane Peak body was possibly intruded during that regional deformation event, but the olivine microfabric retains an igneous signature. The ultramafic body at the Blashke Islands shows no evidence of being involved in the deformation of the western metamorphic belt. Both the Kane Peak and Blashke Islands intrusions appear to be subvertical, cylindrical structures that contain subvertical olivine microfabrics suggestive of subvertical magmatic flow. The absence of penetrative deformational structures in the country rocks surrounding the Blashke Islands body suggests that this area of the Alexander terrane lies outside the western limit of the western metamorphic belt.

ROCK CHEMISTRY

MAJOR ELEMENTS

The chemical composition and Mg # [$Mg/(Mg+Fe^{2+})$] of CIPW normative silicates for rocks of Alaskan-type intrusions are given in table 2. The analyses were obtained by using X-ray fluorescence spectroscopy. FeO, Fe_2O_3, and H_2O were determined by independent methods. Dunite, wehrlite, and olivine-rich clinopyroxenite are partly serpentinized. In addition to serpentine minerals, brucite and magnetite are the main products of serpentinization. Coleman and Keith (1971) showed that, with the exception of the addition of fluids, the relative amounts of the major oxides do not change during serpentinization, and we presume that this is the case for the Alaskan-type ultramafic rocks. The relatively high H_2O contents, the Fe_2O_3 contents, and the normative magnetite reported in table 2 for dunite and wehrlite reflect the degree of serpentinization.

Because the rocks of the Alaskan-type intrusions are cumulates with variable proportions of silicates and magnetite, the relation of rock chemistry to chemical trends due to fractionation is best indicated by the Mg # of the normative silicates. In the larger bodies that have a range of rock types, the Mg # of the normative silicates shows a substantial range that is generally consistent with a normal fractional crystallization trend. Slight variations from a normal trend can be attributed to (1) serpentinization that increases the normative silicate Mg #, (2) variable proportions of modal olivine, clinopyroxene, and hornblende each of which have different Mg #s, and (3) magnetite clinopyroxenite samples that have clinopyroxene with a high esseneite component that results in a Mg # which may be higher than the Mg # of rocks that crystallized earlier in the fractionation sequence.

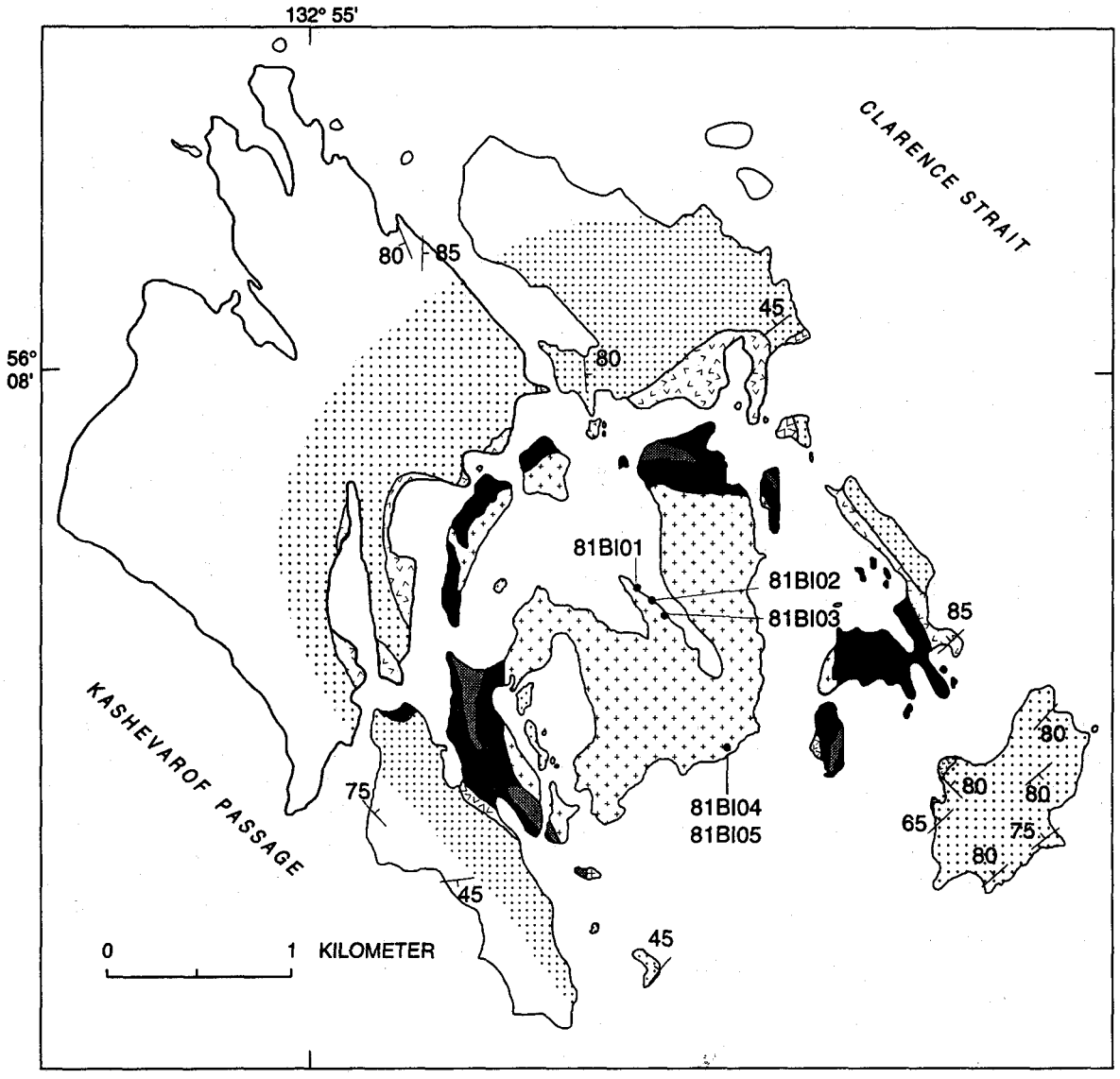

EXPLANATION

Ultramafic complex at Blashke Islands (Early Cretaceous) — Consists of:

Dunite —Olivine and less than 2 percent chromite. Contains as much as 5 percent clinopyroxene near contact with wehrlite or olivine clinopyroxenite

Wehrlite — Olivine, clinopyroxene, and chromite. Mineral ratios are extremely variable

Olivine clinopyroxenite — Clinopyroxene and olivine. Locally may contain hornblende

Gabbro — Transitional from clinopyroxene gabbro at ultramafic contact to hornblende gabbro at country-rock contact

Descon Formation (Early Silurian and Ordovician) — Graywacke, conglomerate, limestone, shale, volcanic rocks. Contact-metamorphosed part (mostly hornfels) stippled

Contact

65 Strike and dip of bedding in country rock

81B101 Oriented sample locality and number

◀ **Figure 10.** Geologic map of ultramafic complex at Blashke Islands, southeastern Alaska, showing locations of oriented samples used for microfabric analyses. Map modified from Walton (1951) and Himmelberg and others (1986b).

TRACE ELEMENTS

Concentrations of trace elements are summarized in table 3, and those of the rare earth elements (REE) are presented graphically in figure 12. On the basis of studies of REE abundances in other ultramafic rocks that have been serpentinized and metamorphosed (Pallister and Knight, 1981; Harnois and Morency, 1989; Harnois and others, 1990), we presume that the REE of the Alaskan-type complexes were relatively immobile during serpentinization and metamorphism and are representative of the primary rock. The chondrite-normalized REE plots were made using the computer program and average chondrite values supplied by Wheatley and Rock (1988). The REE patterns clearly distinguish the different units of the Alaskan-type ultramafic-mafic complexes, and the ultramafic rocks markedly show their signature of cumulus origin involving dominantly olivine, clinopyroxene, and hornblende accumulation. The dunites are dominated by olivine accumulation (>90 percent) and thus have very low REE concentrations (0.03–0.9 x chondrite) (fig. 12*A*). The dunite REE patterns are generally flat and do not display the U- or V-shaped pattern characteristic of dunite and olivine-rich peridotite of residual origin (Pallister and Knight, 1981; Prinzhofer and Allègre, 1985; McDonough and Frey, 1989; Harnois and others, 1990). The wehrlite samples show REE patterns similar to the dunites, but their higher REE concentration is due to cumulus clinopyroxene (fig. 12*B*). The cause of the high Ce value for the one sample of the Kane Peak complex (81KP17A, table 3) is unknown, but it might be related to a local weathering process (Floss and Crozaz, 1991) or to an undetected analytical problem. Kane Peak phlogopite peridotite samples (81KP2A and 81KP5A, table 3) show a small light REE (LREE) enrichment compared to dunite and wehrlite samples (fig. 12*C*). These samples of olivine cumulates have significant amounts of interstitial hornblende and lesser amounts of interstitial phlogopite and plagioclase. The LREE may be concentrated in these interstitial minerals and reflect a slightly LREE-enriched intercumulus melt. Olivine clinopyroxenites and clinopyroxenites have RE concentrations that range from

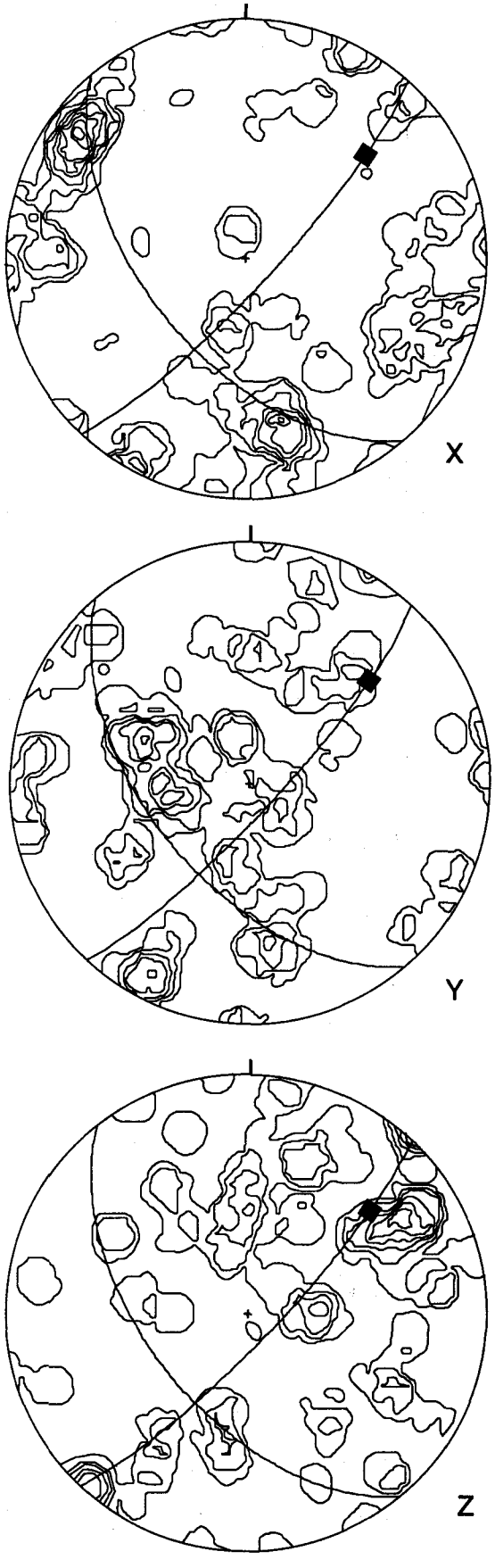

► **Figure 11.** Equal-area, lower hemisphere plots of olivine X, Y, and Z axes in ultramafic complex at Blashke Islands (fig. 10), southeastern Alaska. Dunite specimen 81BI01; contours show concentrations of percentages (1, 2, 3, 4, 5, and 6 (Y), 7 (Z), 8 and 9 (X) percent) per 1 percent of area. ■, pole of X-maximum circle.

Table 2. Chemical compositions (in weight percent) of Alaskan-type ultramafic and mafic rocks, southeastern Alaska.

[X-ray fluorescence spectroscopy analyses by A. Bartel, N. Elsheimer, K. Lewis, D. Siems, J. Taggart. Rock name abbreviations: Du, dunite; Whr, wherlite; Hbl, hornblende; Mag, magnetite; Ol, olivine; Phl, phlogopite; Px, pyroxene. $Mg/(Mg+Fe^{2+})$, atomic ratio of normative silicates.]

	Blashke Islands										
Sample No.----	80BI37	80BI44	80BI48	80BI10	80BI14	80BI28	80BI17	80BI15	80BI49	80BI29	80BI19
Rock type ----	Du	Whr	Ol Cpxite	Du	Ol Cpxite	Ol Hbl Gbn	Hbl Gb	Hbl Px Gb	Gbn	Hbl Px Gb	Hbl Gb
SiO_2	35.60	37.30	50.80	38.50	48.60	46.90	45.50	42.40	45.00	43.20	46.70
TiO_2	.00	.00	.14	.00	.31	.85	1.10	1.20	1.06	1.18	1.34
Al_2O_3	.31	.41	1.75	.35	3.66	16.80	19.40	19.80	17.40	20.00	19.30
Fe_2O_3	4.56	5.19	1.82	3.12	2.57	3.15	5.53	6.25	6.02	6.48	2.41
FeO	4.84	5.04	2.96	6.82	5.25	8.23	6.09	6.16	6.73	6.13	7.55
MnO	.17	.19	.10	.19	.14	.21	.21	.20	.21	.21	.22
MgO	43.20	38.50	19.80	43.20	18.00	7.64	5.61	6.53	7.28	5.67	4.91
CaO	.23	2.81	20.70	1.75	20.10	13.10	12.50	14.00	14.00	13.50	9.70
Na_2O	.00	.00	.15	.00	.22	2.20	2.39	1.80	1.75	2.19	3.44
K_2O	.00	.00	.00	.00	.00	.19	.48	.14	.10	.20	.88
P_2O_5	.00	.00	.00	.00	.00	.16	.20	.00	.11	.27	.44
H_2O	9.26	9.54	1.67	5.28	.85	.37	.60	.80	.26	.37	2.05
Total	98.17	98.98	99.89	99.21	99.70	99.80	99.61	99.28	99.92	99.40	98.94
$\frac{Mg}{(Mg+Fe^{2+})}$	.96	.96	.94	.93	.89	.69	.78	.82	.80	.81	.61

	Kane Peak—Continued			Port Snettisham		Salt Chuck			
Sample No.----	81KP14A	81KP1B	81KP1C	87GH19A	87GH17A	86GH23A	86GH20A	86GH25A	86GH9B
Rock type-----	Cpxite	Diorite	Hblite	Cpxite	Cpxite	Mag Cpxite	Mag Cpxite	Mag Cpxite	Mag Gb
SiO_2	50.70	51.10	40.40	36.80	38.00	40.40	41.40	41.30	40.40
TiO_2	.64	1.60	1.92	2.43	2.50	.92	.83	.90	.92
Al_2O_3	4.70	13.80	12.80	6.55	6.43	5.67	4.72	5.54	15.40
Fe_2O_3	2.65	1.04	2.49	14.39	13.40	13.89	12.56	12.89	8.58
FeO	6.17	8.33	13.42	9.81	10.25	8.00	7.49	6.57	5.68
MnO	.17	.17	.24	.18	.27	.21	.20	.18	.22
MgO	14.70	7.10	10.00	11.60	10.20	12.00	12.40	12.10	8.00
CaO	18.70	9.46	11.90	16.50	18.10	17.70	19.10	19.60	16.80
Na_2O	.65	2.40	1.70	.40	.60	.00	.23	.25	.65
K_2O	.74	1.88	1.08	.73	.27	.28	.00	.06	.76
P_2O_5	.00	1.88	.94	.19	.25	.02	.00	.00	.09
H_2O	.25	.75	.75	.09	.00	.63	1.05	.49	2.09
Total	100.07	99.51	97.64	99.67	100.27	99.72	99.98	99.88	99.59
$\frac{Mg}{(Mg+Fe^{2+})}$	.85	.66	.62	.94	.89	.95	.94	.99	.92

	Union Bay —Continued						
Sample No.-----	87GH35A	87GH41A	87GH36A	87GH29A	87GH40A	87GH37A	87GH28A
Rock type-------	Ol Cpxite	Mag Cpxite	Ol Cpxite	Mag Cpxite	Mag Hblite	Gb	Gbn
SiO_2	49.40	31.30	50.10	39.60	36.70	49.80	50.70
TiO_2	.25	2.22	.32	1.19	1.98	.72	.70
Al_2O_3	1.86	5.61	2.37	6.63	12.60	18.60	16.90
Fe_2O_3	2.52	21.67	3.14	13.03	10.91	4.65	2.83
FeO	5.61	12.61	6.17	9.14	10.78	5.44	7.26
MnO	.15	.98	.23	.21	.19	.23	.20
MgO	20.00	10.50	17.10	12.90	10.70	4.48	7.24
CaO	19.80	13.50	20.30	16.50	11.50	9.96	11.00
Na_2O	.26	.00	.35	.46	1.75	3.43	2.58
K_2O	.00	.04	.00	.11	1.04	1.08	.55
P_2O_5	.00	.00	.00	.00	.09	.60	.18
H_2O	.39	.98	.64	.68	.84	.84	.32
Total	100.24	99.41	100.72	100.45	99.08	99.83	100.46
$\frac{Mg}{(Mg+Fe^{2+})}$	.89	.91	.87	.90	.82	.73	.70

Pd, peridotite; Cpxite, clinopyroxenite; Hblite, hornblendite; Gb, gabbro; Gbn, gabbronorite. Mineral abbreviations (recommended by Kretz, 1983): Bt, biotite;

	Kane Peak										
Sample No.----	81SK48A	81KP7A	81SK45A	81KP2A	81SK46A	81KP5A	81KP20A	81KP15A	81KP17A	81KP22A	81KP23A
Rock type-----	Du	Du	Du	Hbl Phl Pd	Whr	Hbl Phl Pd	Cpxite	Cpxite	Whr	Cpxite	Ol Cpxite
SiO_2----------	40.10	40.10	39.60	40.70	42.10	38.50	51.70	51.90	42.70	50.50	42.60
TiO_2----------	.04	.04	.04	.16	.08	.08	.18	.24	.08	.18	.08
Al_2O_3---------	.00	.00	.00	1.91	.39	.81	1.13	1.58	.48	1.16	.39
Fe_2O_3---------	2.09	1.66	2.45	4.31	2.47	3.46	1.06	1.44	2.09	1.20	1.69
FeO----------	6.62	7.95	8.14	6.56	7.76	6.60	4.13	4.62	9.46	5.22	10.00
MnO----------	.14	.17	.18	.19	.17	.16	.11	.13	.20	.16	.20
MgO----------	46.80	45.70	44.30	37.30	39.80	42.20	21.50	18.70	36.30	23.70	37.70
CaO----------	.26	1.10	1.28	1.90	4.72	.66	19.80	20.90	6.54	17.30	5.82
Na_2O---------	.00	.00	.00	.30	.00	.00	.00	.00	.00	.00	.00
K_2O----------	.00	.00	.00	.26	.00	.06	.00	.00	.00	.00	.00
P_2O_5---------	.00	.02	.00	.10	.02	.04	.00	.00	.00	.00	.00
H_2O----------	2.87	2.37	2.88	5.01	1.88	6.74	.25	.25	1.50	.50	.62
Total--------	98.92	99.11	98.87	98.70	99.39	99.31	99.86	99.76	99.35	99.92	99.10
$\frac{Mg}{(Mg+Fe^{2+})}$	.94	.92	.92	.93	.91	.94	.91	.90	.88	.90	.88

	Salt Chuck—Continued						Union Bay			
Sample No.---	86GH8A	86GH11A	86GH7A	86GH1A	86GH27A	86GH3B	87GH27B	87GH34A	87GH33A	87GH27A
Rock type----	Bt Mag Cpxite	Mag Cpxite	Gb	Mag Gb	Mag Gb	Gb	Du	Whr	Ol Cpxite	Du
SiO_2----------	36.00	41.10	40.70	40.50	43.30	47.20	38.20	39.00	51.60	38.30
TiO_2----------	1.31	1.02	.94	.74	.84	.61	.00	.00	.12	.04
Al_2O_3---------	12.70	7.35	16.10	18.50	17.00	19.70	0.00	.16	1.38	.39
Fe_2O_3---------	10.16	11.33	6.70	7.54	6.79	4.26	3.63	4.84	1.18	3.77
FeO----------	9.11	7.16	6.65	4.91	5.40	3.62	6.90	6.17	3.24	11.00
MnO----------	.26	.23	.34	.21	.23	.24	.19	.20	.10	.26
MgO----------	8.13	11.40	7.03	6.30	6.44	3.67	45.80	41.70	20.20	44.60
CaO----------	15.00	17.80	13.70	17.00	14.50	10.40	0.25	2.34	21.70	.24
Na_2O---------	.40	.45	1.25	.65	1.62	1.73	0.21	.18	.21	.19
K_2O----------	1.56	.41	1.48	.96	.98	4.83	.00	.00	.00	.00
P_2O_5---------	1.12	.10	.81	.06	.40	.51	.00	.00	.00	.00
H_2O----------	1.40	1.21	2.85	2.25	1.86	2.47	4.93	5.37	.35	.00
Total--------	97.15	99.56	98.55	99.62	99.36	99.24	100.11	99.96	100.08	98.79
$\frac{Mg}{(Mg+Fe^{2+})}$	.80	.94	.80	.91	.86	.82	.93	.95	.93	.89

about 5 to 20 x chondrites and have open convex-upward patterns (figs. 12*D, E, F*). On the basis of mineral-melt distribution coefficients (Hanson, 1980), the ranges in concentration can be attributed largely to modal proportions of olivine and clinopyroxene. The RE concentrations of gabbros (5–60 x chondrite) are generally higher than for clinopyroxenite (figs. 12*G, H*). The REE pattern for gabbro samples ranges from about flat to having a very slight heavy REE (HREE) depletion. Only two gabbro samples from the Union Bay complex show a small positive Eu anomaly suggesting plagioclase accumulation. The absence of a positive Eu anomaly and the relatively flat REE pattern of the other gabbro samples suggest that most of the gabbros are not cumulates but may represent static crystallization of a differentiated liquid that has undergone substantial removal of olivine, clinopyroxene, and some hornblende. The highest RE concentrations (20–90 x chondrite) are in two samples of hornblendite from the Kane Peak body (fig. 12*I*).

A striking aspect of the REE is that, except for that on the Blashke Islands, all the complexes studied show markedly similar REE abundance levels and patterns for the various rock units. REE patterns of rocks on the Blashke Islands show a relative depletion in LREE compared to those of other bodies, thus yielding steeper slopes and crossing patterns. Nevertheless the overall similarity in REE patterns leads to the qualitative conclusion that all the complexes were derived by differentiation of closely similar parent magmas under near-identical conditions. A striking similarity between the REE abundance levels and patterns of the Alaskan-type clinopyroxenites and gabbros and those of the clinopyroxenite

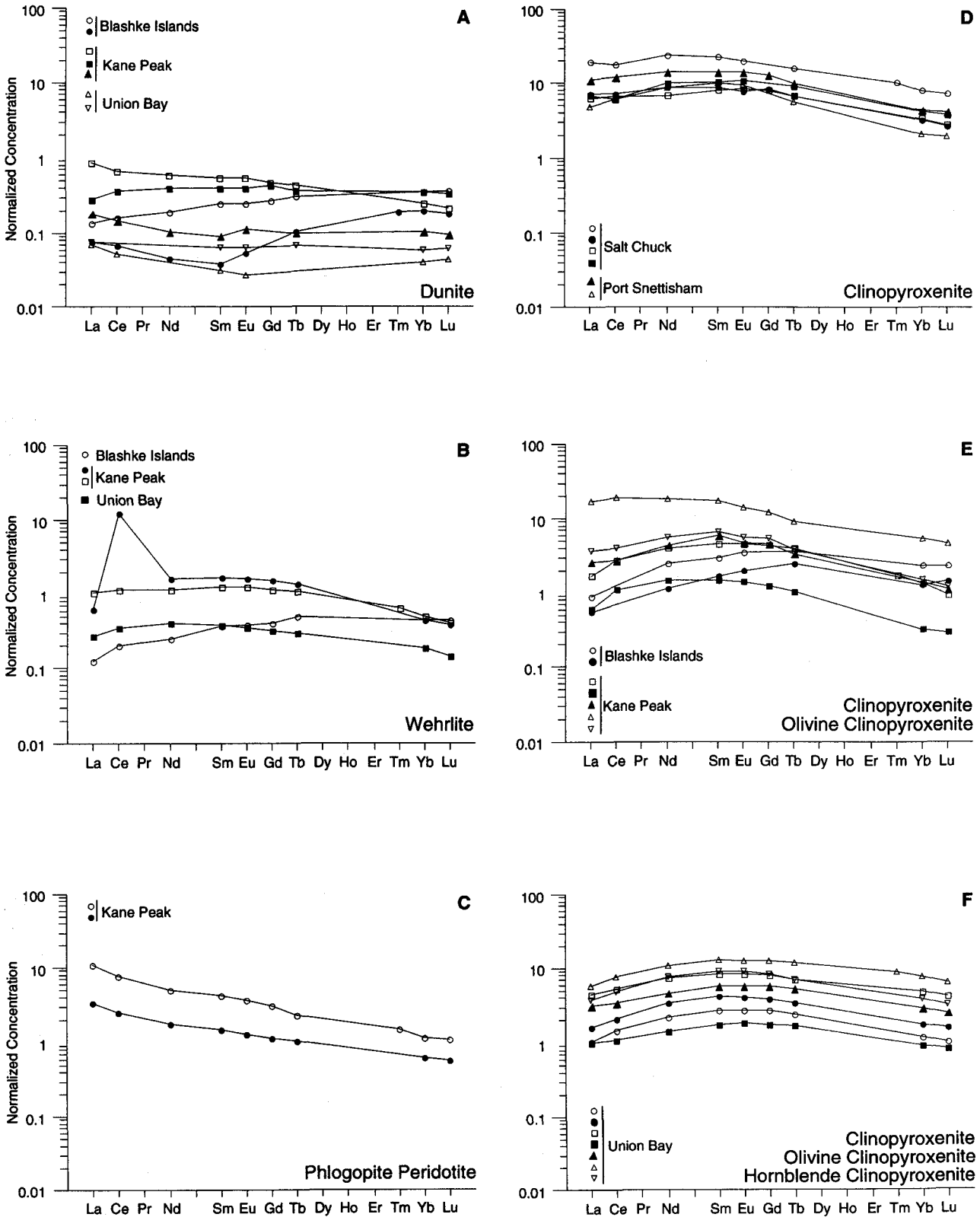

Figure 12. REE patterns of ultramafic and mafic rocks of Alaskan-type intrusions at Blashke Islands, Kane Peak, Union Bay, Salt Chuck, and Port Snettisham, southeastern Alaska. RE concentrations are normalized to chondrite values given by Wheatley and Rock (1988). *A*, Dunite. *B*, Wehrlite. *C*, Phlogopite peridotite. *D*, *E*, and *F*, Clinopyroxenite, olivine clinopyroxenite, and hornblende clinopyroxenite.

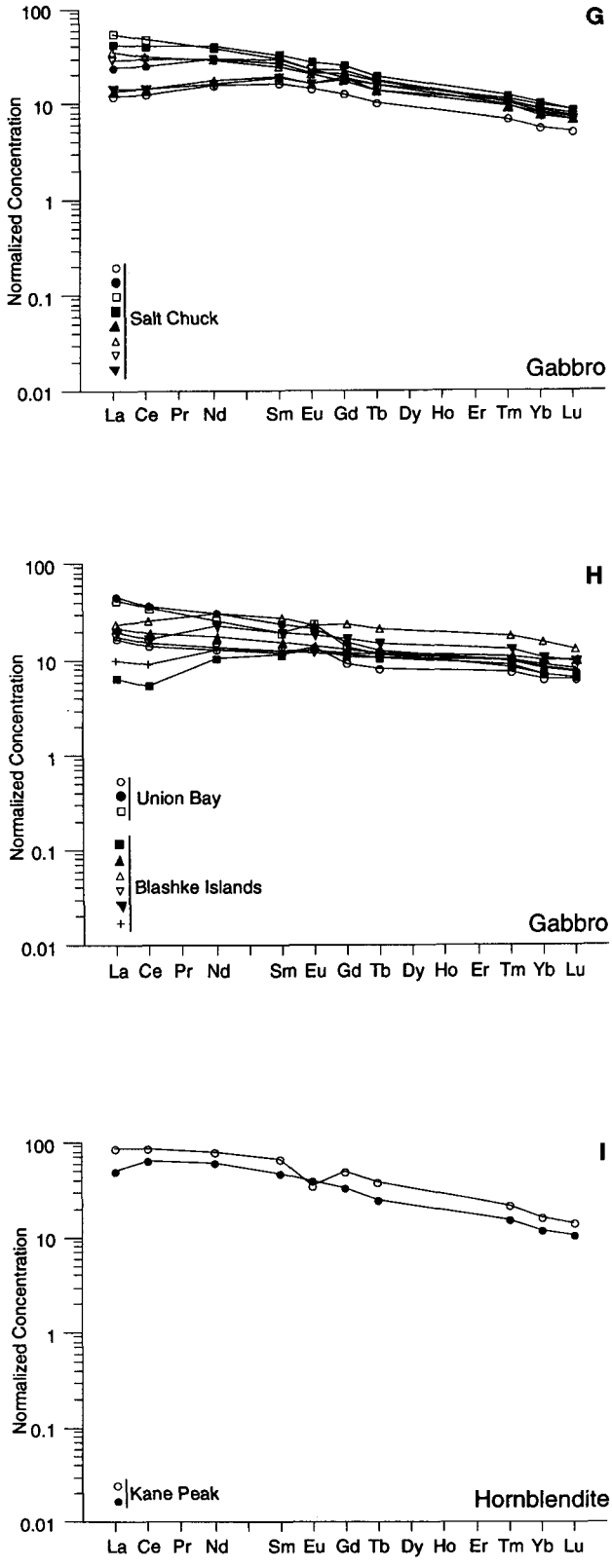

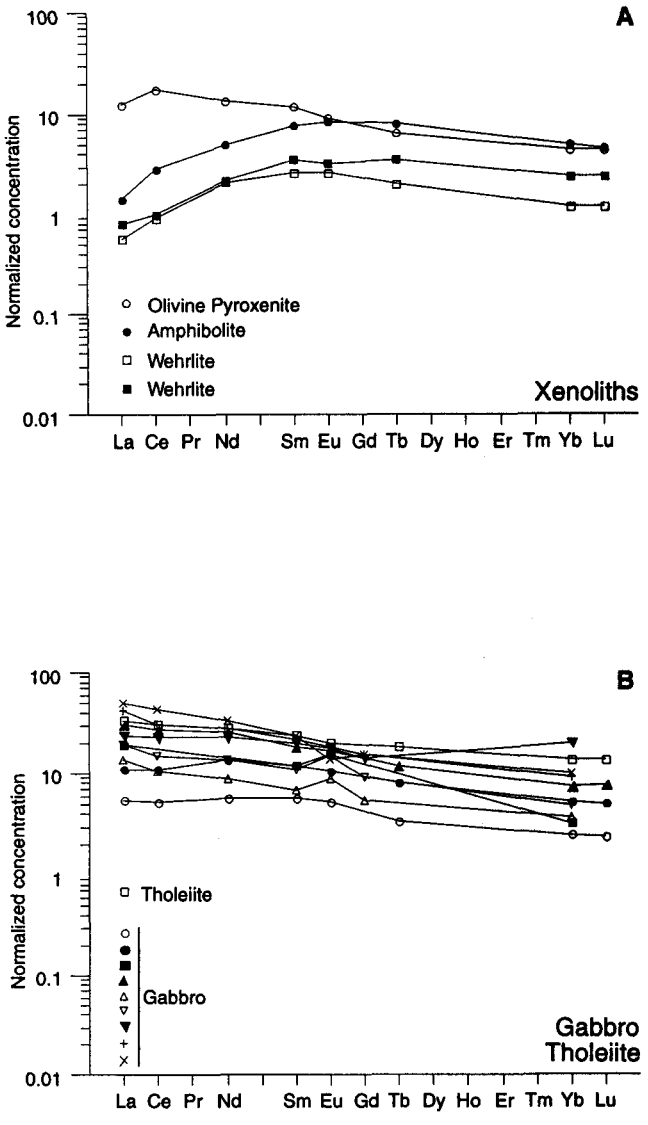

Figure 13. REE patterns of ultramafic xenoliths (*A*), plutonic gabbros (*B*), and a tholeiite flow (*B*) associated with Aleutian island-arc volcanism, Alaska. RE concentrations are from Perfit and others (1980), Kay and others (1983), and DeBari and others (1987) and are normalized to chondrite values given by Wheatley and Rock (1988).

Figure 12. Continued. *G* and *H*, Gabbro. *I*, Hornblendite.

Table 3. Trace–element contents (in parts per million) of Alaskan-type ultramafic and mafic rocks, southeastern Alaska.

[Instrumental neutron activation analyses by J.R. Budahn, R.J. Knight, D.M. McKown. -, not detected. Mineral abbreviations: Bt, biotite; Hbl, hornblende;

Sample No., Rock type	Ba	Sr	Co	Ni	Cr	Cs	Hf	Rb	Sb	Ta	Th	U
Blashke												
80BI10, Dunite	13.10	<2.0	131	855	2190	0.085	0.115	3.2	0.045	0.0342	0.010	0.0239
80BI37, Dunite	5.08	<2.0	131	1050	5870	.013	.0738	1.7	-	.0161	.0184	.0060
80BI44, Wehrlite	13.4	<4.0	119	720	1640	.11	.0583	3.9	.088	.0499	.027	.0221
80BI14, Ol Clinopyroxenite	47.5	<30	57.9	113	1230	.15	.135	3.9	.31	.025	<.050	<.050
80BI48, Ol Clinopyroxenite	19.2	<30	42.7	162	1520	.14	.135	3.9	-	.025	<.050	.013
80BI15, Hbl Px Gabbro	70.5	787	39.1	52.5	61.3	.11	.618	<1.0	<.062	.069	<.050	.30
80BI17, Hbl Gabbro	163	669	30.4	-	26.3	.196	1.10	<1.0	<.075	.128	.590	.297
80BI19, Hbl Gabbro	235	855	34.9	-	8.57	.183	1.20	16.8	.187	.225	.435	.223
80BI28, Ol Hbl Gabbronorite	89.5	623	39.7	-	118	-	.805	3.1	.14	.0942	<.050	<.050
80BI29, Hbl Px Gabbro	106	892	30.6	20	14.9	.11	.933	<1.0	.095	.133	.0952	.051
80BI49, Gabbronorite	102	654	38.8	33	80.7	-	.557	6.1	.091	.0453	<.050	.074
Kane												
81KP7A, Dunite	11	12	127	1750	2460	0.016	0.168	0.63	-	0.0067	0.0605	0.0415
81SK045A, Dunite	12.5	<10	136	1340	3090	.066	.067	<.37	0.091	.0084	<.0085	.0065
81SK048A, Dunite	5.6	<10	128	2110	3590	.036	.053	<.32	-	.0083	.0087	.011
81KP2A, Hbl Phl Peridotite	90.7	110	116	1310	2870	.302	.419	3.16	.14	.0752	.661	.304
81KP5A, Hbl Phl Peridotite	31.5	19	126	1630	3220	.065	.166	1.4	-	.0211	.179	.114
81KP17A, Wehrlite	9.6	14	123	825	920	.023	.0433	.63	-	.0039	.017	.0063
81KP20A, Clinopyroxenite	4.2	24	44.8	316	2480	.034	.0518	<.55	.26	.0096	.035	.016
81SK046A, Wehrlite	30.6	<10	127	1120	1530	.032	.12	<.44	.080	.0159	.029	.0365
81KP23A, Ol Clinopyroxenite	8.1	11	119	865	1410	.092	.028	.62	-	.0199	.025	.015
81KP14A, Clinopyroxenite	247	89.7	50.3	98.4	213	.398	1.62	29.6	.20	.102	.244	.124
81KP15A, Clinopyroxenite	28.4	125	51.6	203	1360	.054	.268	3.6	.12	.0565	<.050	.03
81KP22A, Clinopyroxenite	35	66.2	56.8	291	2130	.12	.228	4.39	.154	.0279	.0574	.017
81KP1B, Diorite	213	415	29.7	95.1	253	.559	2.21	15.4	.36	.403	1.69	1.14
81KP1C, Hornblendite	177	281	54.5	46.4	84.3	.154	2.30	11.5	.14	.262	.368	.193
Salt												
86GH8A, Bt Mag Clinopyroxenite	659	1100	71.1	46.2	5.56	0.479	1.11	39.2	0.073	0.0372	0.453	0.184
86GH11A, Mag Clinopyroxenite	126	331	61.9	51	14.0	-	1.64	9.96	.30	.016	.606	.24
86GH20A, Mag Clinopyroxenite	70	<310.	65.7	28.7	12.3	.24	.671	<1.0	.765	-	.242	.072
86GH23A, Mag Clinopyroxenite	104	87.2	64.8	40.2	18.3	.123	.578	7.44	.18	.116	.104	.014
86GH25A, Mag Clinopyroxenite	52.6	85	63.5	45	26.9	-	.657	6.8	-	-	.10	<.050
87GH42A, Bt Mag Clinopyroxenite	749	1160	68.5	39.4	8.46	.465	1.03	40.4	.114	.057	.464	.108
87GH43A, Bt Mag Clinopyroxenite	70.8	391	67.6	48.2	5.86	.043	1.43	9.6	1.19	.069	.433	.126
86GH1A, Mag Gabbro	241	1480	41.2	19.7	8.81	.351	1.02	25.5	.196	.0318	.278	.123
86GH3B, Gabbro	687	1860	24.8	6.7	1.90	.332	1.27	130	.124	.0426	2.19	1.04
86GH7A, Gabbro	480	1530	42.5	24	2.3	.340	1.04	37.2	.22	.023	.850	.305
86GH9B, Mag Gabbro	172	1240	49.6	38	5.57	.19	1.14	19.9	.137	.0161	.281	.120
86GH27A, Mag Gabbro	360	1480	39.8	22.3	5.06	.322	.952	24.6	-	.020	.309	.0793
Port												
87GH17A, Clinopyroxenite	64	120	63.3	-	14.2	0.31	1.35	<1.0	0.20	0.108	0.160	0.058
87GH19A, Clinopyroxenite	150	170	76.4	51.7	25.6	0.21	0.804	13.4	.14	.039	.11	<.050
Union												
87GH27A, Dunite	<2.7	<10	153	1380	11800	-	0.040	<0.34	-	0.0221	<0.0044	<0.0030
87GH27B, Dunite	4.2	<10	125	873	2930	.013	.026	<.48	-	.0041	<.0086	<.0008
87GH34A, Wehrlite	8.9	<10	121	777	2660	.021	.026	<.61	.16	.0051	<.014	<.0031
87GH33A, Ol Clinopyroxenite	35.9	<30	38.6	186	3690	-	.098	2.7	.11	.063	.0339	.0224
87GH35A, Ol Clinopyroxenite	26.4	32	60.3	184	1720	.14	.18	1.8	-	.058	.032	.0363
87GH36A, Ol Clinopyroxenite	13	<30	57.9	162	762	.29	.583	3.5	.41	.043	<.050	.028
87GH49A, Ol Clinopyroxenite	19.4	80	43.3	320	3360	-	.136	4.6	.096	.049	<.050	.0216
87GH41A, Mag Clinopyroxenite	29.1	33	107	84.6	52.3	-	.438	4.3	.30	.221	.22	.0335
87GH47A, Clinopyroxenite	19	89	52.3	76.1	550	.021	.691	1.62	.552	.0075	.176	.0477
87GH29A, Mag Clinopyroxenite	46	35.0	79.4	79.4	26.8	.053	.416	2.4	.494	.112	.0366	.051
87GH40A, Mag Hornblendite	161	440	87.9	29	5.76	.13	1.14	7.5	.235	.0762	.849	.219
87GH28A, Gabbronorite	210	917	34.6	79.0	300	-	.553	3.9	.082	.0460	.13	.044
87GH37A, Gabbro	533	1120	27.5	11.7	10.3	.160	.493	8.51	.051	.0418	.372	.12
87GH44A, Gabbro	473	1320	29.1	17	3.37	-	.537	5.0		.0400	.237	<.050

Mag, magnetite; Ol, olivine; Phl, phlogopite; Px pyroxene.]

Zn	Zr	Sc	La	Ce	Nd	Sm	Eu	Gd	Tb	Tm	Yb	Lu	Sample No., Rock type
Islands													
74.4	-	12.4	0.0450	0.140	0.12	0.0503	0.0191	0.074	0.0149	-	0.0782	0.0124	80BI10, Dunite.
67.2	23	5.32	.0254	.058	.029	.0079	.0042	-	.0050	0.0059	.0444	.0063	80BI37, Dunite.
72.7	-	16.3	.0414	.17	.16	.0740	.0290	.11	.0241	-	.0946	.0147	80BI44, Wehrlite.
-	41	109	.295	-	1.54	.600	.273	-	.180	-	.524	.0802	80BI14, Ol Clinopyroxenite.
-	-	89.7	.179	-	.72	.348	.151	-	.121	-	.28	.0492	80BI48, Ol Clinopyroxenite.
80.2	31	40.7	2.10	4.80	6.71	2.30	.980	3.01	.505	.278	1.58	.219	80BI15, Hbl Px Gabbro.
87.5	52	33.3	7.27	16.3	11.1	3.10	1.09	3.57	.559	.345	2.19	.338	80BI17, Hbl Gabbro.
62.9	86.8	36.8	7.77	22.7	19.1	5.49	1.73	6.62	1.02	.549	3.35	.441	80BI19, Hbl Gabbro.
92.1	36	46.2	5.69	13.4	8.72	2.57	.931	3.10	.492	.310	1.96	.275	80BI28, Ol Hbl Gabbronorite.
100	41	34.2	6.60	14.8	14.1	3.90	1.39	4.62	.701	.405	2.31	.319	80BI29, Hbl Px Gabbro.
89.9	37.5	51.9	3.22	7.84	8.02	2.53	.958	3.26	.556	.308	1.82	.257	80BI49, Gabbronorite.
Peak													
59.2	<1.9	5.74	0.286	0.593	0.37	0.112	0.0414	0.13	0.021	-	0.0543	0.0074	81KP7A, Dunite.
60.2	11	6.18	.0929	.32	.25	.0829	.0315	.12	.018	-	.0769	.0117	81SK045A, Dunite.
55.5	3.2	3.38	.0597	.13	.065	.0188	.0089	-	.0047	-	.023	.0033	81SK048A, Dunite.
80.7	13	6.33	3.54	6.71	3.21	.857	.280	.843	.109	0.045	.255	.0367	81KP2A, Hbl Phl Peridotite.
63.0	5.0	3.96	1.09	2.18	1.09	.298	.102	.32	.0505	-	.136	.0196	81KP5A, Hbl Phl Peridotite.
65.5	21	19.8	.207	10.6	1.00	.337	.126	.43	.0663	-	.0976	.0130	81KP17A, Wehrlite.
53.1	25	52.2	.565	2.4	2.56	.92	.346	1.22	.189	.055	.292	.0330	81KP20A, Clinopyroxenite.
55.5	16	13.5	.341	.982	.71	.249	.0954	.32	.0525	.02	.109	.0137	81SK046A, Wehrlite.
72.2	11	17.6	.194	.931	.921	.304	.110	.34	.0512	-	.0702	.01	81KP23A, Ol Clinopyroxenite.
114	61.5	75.1	5.65	16.6	11.6	3.58	1.08	3.47	.445	-	1.18	.164	81KP14A, Clinopyroxenite.
58.5	12	59.9	1.19	3.43	3.55	1.37	.443	1.53	.185	-	.341	.0428	81KP15A, Clinopyroxenite.
53.9	23	43.9	.845	2.34	2.81	1.19	.363	1.25	.165	-	.313	.0390	81KP22A, Clinopyroxenite.
116	127	50.9	29.0	77.0	51.0	13.7	2.75	13.9	1.82	.685	3.60	.478	81KP1B, Diorite.
148	111	53.0	16.1	55.2	39.6	9.71	3.08	9.27	1.20	.485	2.67	.360	81KP1C, Hornblendite.
Chuck													
124	-	33.0	7.83	21.2	18.7	5.37	1.63	5.57	0.808	0.312	1.77	0.244	86GH8A, Bt Mag Clinopyroxenite.
94.1	96.8	81.5	6.24	15.2	15.3	4.55	1.52	-	.765	.329	1.78	.247	86GH11A, Mag Clinopyroxenite.
-	-	107	2.35	6.24	5.64	1.76	.596	2.3	.328	-	.709	.0927	86GH20A, Mag Clinopyroxenite.
93.2	31	103	2.03	5.61	4.30	1.66	.656	2.25	.32	-	.736	.0982	86GH23A, Mag Clinopyroxenite.
117	-	98.1	2.22	5.06	6.26	2.16	.833	-	.449	-	.935	.132	86GH25A, Mag Clinopyroxenite.
134	148	32.2	9.33	25.1	18.9	5.77	1.79	6.11	.852	.325	1.84	.251	87GH42A, Bt Mag Clinopyroxenite.
106	500	75.9	4.60	12.0	10.0	3.70	1.25	4.84	.744	.291	1.60	.229	87GH43A, Bt Mag Clinopyroxenite.
80.1	52.8	37.3	3.97	10.6	9.54	3.32	1.07	3.49	.486	.211	1.2	.168	86GH1A, Mag Gabbro.
87.7	42	13.5	18.1	40.9	24.4	5.93	1.75	5.10	.743	.339	2.15	.291	86GH3B, Gabbro.
130	-	27.4	14.0	34.4	25.8	6.67	2.05	6.73	.902	.373	2.20	.291	86GH7A, Gabbro.
81.1	54.0	41.0	4.37	12.2	11.2	3.98	1.26	4.98	.657	.289	1.70	.230	86GH9B, Mag Gabbro.
85.9	29	35.0	11.5	26.8	17.7	4.81	1.56	4.68	.641	.330	1.90	.259	86GH27A, Mag Gabbro.
Snettisham													
159	103	74.1	3.60	10.1	8.86	2.88	1.07	3.55	0.481	-	0.962	0.145	87GH17A, Clinopyroxenite.
111		79.7	1.59	5.17	5.50	1.99	.741	-	.275	-	.462	.0689	87GH19A, Clinopyroxenite.
Bay													
3	6.7	4.46	0.0233	0.045	<0.024	0.0062	0.0021	-	<0.0015	-	0.0088	0.0015	87GH27A, Dunite.
4	17	3.98	.0257	<.054	.037	.0133	.0049	-	.0033	-	.013	.0021	87GH27B, Dunite.
62.5	14	8.44	.091	.31	.25	.0769	.0270	0.090	.014	-	.040	.0049	87GH34A, Wehrlite.
78.1	19	64.1	.340	1.27	1.39	.549	.209	.740	.112	-	.266	.0360	87GH33A, Ol Clinopyroxenite.
73.7	38	73.2	.524	1.82	2.09	.846	.315	1.08	.16	-	.395	.0546	87GH35A, Ol Clinopyroxenite.
176	53.1	93.8	1.45	4.55	4.74	1.74	.642	2.20	.339	-	1.05	.145	87GH36A, Ol Clinopyroxenite.
11	25	46.5	.326	.947	.875	.363	.143	.492	.0819	-	.198	.0281	87GH49A, Ol Clinopyroxenite.
128	39	84.2	1.04	2.93	2.90	1.14	.441	1.57	.255	-	.635	.0835	87GH41A, Mag Clinopyroxenite.
98.6	9.4	75.3	1.87	6.77	6.96	2.61	.977	3.45	.569	0.272	1.66	.220	87GH47A, Clinopyroxenite.
123	33	79.9	1.20	4.06	4.78	1.89	.696	2.29	.345	-	.850	.111	87GH29A, Mag Clinopyroxenite.
98.0	-	66.7	2.82	6.88	8.21	3.14	1.25	-	.588	-	1.15	.147	87GH40A, Mag Hornblendite.
91.5	45	34.9	5.58	12.0	8.17	2.44	1.05	2.51	.388	.228	1.39	.209	87GH28A, Gabbronorite.
106	-	21.6	15.0	31.9	19.4	4.74	1.62	4.29	.601	.300	1.80	.251	87GH37A, Gabbro.
91.3	38.3	20.7	13.7	29.9	16.3	3.97	1.84	3.74	.543	.264	1.56	.224	87GH44A, Gabbro.

xenoliths and plutonic gabbros associated with Aleutian island-arc volcanism (fig. 13) (Perfit and others, 1980; Kay and others, 1983; DeBari and others, 1987) allows the Aleutian volcanic rocks to serve as models for constraining the parental magma composition of the Alaskan-type complexes.

MINERAL CHEMISTRY

Mineral chemistry and trends in mineral chemistry are among the best indicators of chemical fractionation trends of magmas which, in turn, reflect the composition of the parent magma(s) and the physical conditions of crystallization. Chemical compositions and structural formulas of olivine, orthopyroxene, clinopyroxene, hornblende, biotite, chromian spinel, and plagioclase are arranged in tables 4 through 10, respectively, by location and decreasing Mg # [Mg/(Mg+Fe^{2+})] for Fe-Mg silicates, Cr # [Cr/(Cr+Al)] for chromian spinel, and anorthite (An) content for plagioclase. All minerals were analyzed with a JEOL model 733 Superprobe at Washington University, St. Louis, Missouri. Matrix corrections were made by the method proposed by Bence and Albee (1968) using the correction factors of Albee and Ray (1970). Because of the high oxygen fugacity of the magma, at least by the time of crystallization of abundant magnetite, structural formulas for pyroxene, hornblende, and chromian spinel were calculated by normalizing to a fixed number of cations, and Fe^{3+} and Fe^{2+} were calculated from charge balance. Calculation of Fe^{3+} and Fe^{2+} by this procedure is subject to bias resulting from errors in the analysis, particularly for Si, and the procedure might yield Mg #s that are erroneously high for low-iron minerals. Nevertheless, Loney and Himmelberg (1992) showed the method to be effective for clinopyroxene in the Salt Chuck intrusion. Olivine structural formulas were normalized to 4 oxygens, and biotite formulas were calculated by normalizing to 11 oxygens with all iron as FeO, which obviously introduces some error.

In general the Mg # of olivine and clinopyroxene decreases systematically through the series dunite, wehrlite, olivine clinopyroxenite, clinopyroxenite, hornblende clinopyroxenite, and gabbro. At Red Bluff Bay the olivine Mg # ranges from 0.949 in dunite to 0.897 in clinopyroxenite. These values are substantially higher than those for corresponding rock types in the other bodies, and we interpret them to reflect reequilibration during regional thermal metamorphism imposed by the Tertiary intrusions. The clinopyroxene Mg # at Red Bluff Bay, however, ranges from 0.974 in wehrlite to 0.934 in clinopyroxenite and is comparable to values for similar rock types at Kane Peak and some at Union Bay, although those at Union Bay have higher esseneite components.

Excluding the Red Bluff Bay intrusive, the Mg # of olivine varies as follows: In dunite 0.912 to 0.863, with most values between 0.902 and 0.891 (table 4); in wehrlite 0.901 to 0.846; and in olivine clinopyroxenite-clinopyroxenite from about 0.882 to 0.804, although one sample of clinopyroxenite from Union Bay has a value of 0.744, which is about the same as for olivine in a Blashke Islands gabbro sample (0.766). On the basis of the most Mg-rich, nonmetamorphic olivine composition and simple olivine-melt equilibria at 1-bar pressure (Roeder and Emslie, 1970), a minimum Mg # of about 0.75 is indicated for the dunite parent magma; the value would be higher for higher pressures (Ulmer, 1989).

The major chemical variations in pyroxene are illustrated in figures 14 and 15. Orthopyroxene is rare in the ultramafic rocks and was observed as a common constituent only in olivine-rich peridotite at Kane Peak, where it has a Mg # of 0.89 (table 5) and coexists with olivine of about the same Mg #. On the other hand, orthopyroxene is common in the gabbroic rocks at Union Bay and the Blashke Islands. Many of the samples are gabbronorite, and the Mg # ranges from 0.748 to 0.532

According to the calculation and classification scheme of the International Mineralogical Association (IMA; Morimoto and others, 1988) all clinopyroxene in the ultramafic rocks and most clinopyroxene in the gabbros would be classified as diopside. However, Loney and Himmelberg (1992) showed that clinopyroxenes in magnetite clinopyroxenite and gabbro of the Salt Chuck intrusion have a substantial Fe^{3+} content, most of which is in the esseneite component and thus not accounted for in the IMA calculation procedure. Thus we adopted the approach used by Loney and Himmelberg (1992) and have calculated the Wo, En, and Fs components of the clinopyroxenes (table 6) using the calculation scheme of Lindsley and Andersen (1983). When projected onto the pyroxene quadrilateral (fig. 14), most of the clinopyroxenes plot as Mg-rich augite.

The Al_2O_3 content of clinopyroxene shows a marked enrichment with differentiation, as indicated by cumulus assemblages and Mg # of the clinopyroxene (fig. 15). The trend is similar to that shown by clinopyroxene in arc cumulates (Conrad and Kay, 1984; DeBari and others, 1987; DeBari and Coleman, 1989; Loucks, 1990) and contrasts with the trend typically observed in low-pressure anorogenic igneous provinces such as midocean ridges or back-arc basins (Himmelberg and Loney, 1980; Pallister and Hopson, 1981; Elthon and others, 1982; Komor and others, 1985; Loney and Himmelberg, 1989; Loucks, 1990). Using data from three Alaskan-type ultramafic bodies (Duke Island and Union Bay Alaska, and Tulameen, British Columbia) as well as from other arc-cumulate suites, Loucks (1990) demonstrated that the trend of the Al^{iv}/TiO_2 ratio in clinopyroxene in arc cumulates is distinct from that trend in rift-related tholeiites; the differences in the trends and the usefulness of this discrimination diagram is further substantiated by the data presented here (fig. 16).

The increase with differentiation of Al_2O_3 in clinopyroxene has been used to support the hypothesis that after fractionation of ultramafic cumulates, the residual magma, parental to arc crust, is a high-alumina basalt (Murray, 1972; Conrad and Kay, 1984; Kay and Kay, 1985a, b). The trend of alumina enrichment with differentiation also has been thought to reflect crystallization of clinopyroxene

Table 4. Analyses of olivine in Alaskan-type ultramafic and mafic rocks, southeastern Alaska.

[Electron microprobe analyses (in weight percent) by G.R. Himmelberg. Blashke Islands analyses from Himmelberg and others (1986b). Abbreviations given in table 2. Mg/(Mg+Fe+Mn), atomic ratio of normative silicates. -, not detected; n.d., not determined.]

	Blashke Islands											Dall Island
Sample No.---	80BI37	80BI5	80BI6	80BI10	80BI43	80BI12	80BI44	80BI13	80BI47	80BI14	80BI15	90GH6A
Rock type----	Du	Du	Du	Du	Du	Du	Whr	Ol Cpxite	Whr	Ol Cpxite	Gabbro	Phl Whr
SiO_2	42.00	41.10	41.40	41.10	40.80	41.10	41.40	41.40	40.30	38.70	39.00	40.89
FeO*	9.51	10.50	10.50	10.60	10.40	11.90	11.90	12.00	12.40	17.90	20.90	11.01
MnO	-	.02	.02	.03	-	.07	.07	.02	.03	.28	.77	.16
MgO	49.40	48.10	48.20	48.60	47.90	47.20	47.20	47.40	47.50	41.90	39.80	49.05
CaO	.17	.26	.21	.05	.18	.08	.08	.07	.09	.37	.17	.03
NiO	.10	.09	.09	.10	.07	.04	.11	.04	.04	n.d.	.08	.31
Total	101.18	100.07	100.42	100.48	99.35	100.39	100.76	100.93	100.36	99.15	100.72	101.46
Cations per 4 oxygens												
Si	1.013	1.008	1.011	1.005	1.008	1.011	1.014	1.012	0.996	0.996	1.002	0.994
Fe	.192	0.215	.215	.217	.215	.245	.244	.245	.256	.385	.449	.224
Mn	-	.000	.000	.001	-	.001	.001	.000	.001	.006	.017	.003
Mg	1.776	1.759	1.755	1.770	1.763	1.730	1.723	1.727	1.749	1.607	1.524	1.778
Ca	.004	.007	.005	.001	.005	.002	.002	.002	.002	.010	.005	.001
Ni	.002	.002	.002	.002	.001	.001	.002	.001	.001	.000	.002	.006
Mg/(Mg+Fe+Mn)	.903	.891	.891	.891	.891	.875	.875	.875	.872	.804	.766	.887

	Kane Peak											
Sample No.---	81SK48A	81KP7A	81KP17A	81SK45A	81SK43A	81KP2A	81SK46A	81KP5A	81KP23A	81KP20A	81KP22A	81KP15A
Rock type----	Du	Du	Whr	Du	Whr	Hbl Phl Pd	Whr	Hbl Phl Pd	Ol Cpxite	Whr	Cpxite	Cpxite
SiO_2	40.44	40.06	40.14	40.01	39.92	39.36	39.65	39.77	39.40	39.27	39.06	38.66
FeO*	8.53	9.44	9.47	10.94	11.59	12.18	12.48	12.52	14.61	14.47	14.87	17.61
MnO	.13	.17	.16	.20	.19	.20	.20	.25	.25	.21	.21	.24
MgO	50.38	49.55	49.39	48.39	48.40	47.26	47.52	47.43	46.08	45.11	45.42	43.12
CaO	.14	.01	.02	.06	.03	.00	.04	.00	.02	.00	.02	.02
NiO	.27	.24	.27	.20	.14	.24	.21	.24	.14	.16	.16	.10
Total	99.87	99.46	99.44	99.79	100.25	99.23	100.09	100.20	100.49	99.21	99.72	99.74
Cations per 4 oxygens												
Si	0.989	0.988	0.990	0.990	0.986	0.986	0.986	0.987	0.985	0.993	0.985	0.987
Fe	.174	.195	.195	.226	.239	.255	.259	.260	.305	.306	.314	.376
Mn	.003	.003	.003	.004	.004	.004	.004	.005	.005	.004	.004	.005
Mg	1.836	1.821	1.815	1.784	1.782	1.764	1.760	1.755	1.717	1.700	1.708	1.642
Ca	.004	.000	.001	.002	.001	.000	.001	.000	.001	.000	.000	.000
Ni	.005	.005	.005	.004	.003	.005	.004	.005	.003	.003	.003	.002
Mg/(Mg+Fe+Mn)	.912	.902	.901	.886	.880	.872	.870	.869	.847	.846	.843	.812

	Red Bluff Bay					Union Bay						
Sample No.---	90GH16A	90GH11A	90GH18A	90GH15A	90GH15B	87GH27B	87GH49A	87GH34A	87GH33A	87GH27A	87GH35A	87GH36A
Rock type----	Du	Du	Whr	Whr	Cpxite	Du	Ol Cpxite	Whr	Cpxite	Du	Cpxite	Ol Cpxite
SiO_2	41.69	41.57	41.17	41.02	40.52	40.19	39.52	39.93	39.23	39.60	38.65	37.45
FeO*	5.02	6.23	7.51	9.12	9.91	10.21	11.19	11.60	12.87	12.89	18.18	23.35
MnO	.06	.17	.19	.15	.18	.19	.18	.21	.23	.24	.28	.34
MgO	52.97	52.03	51.09	49.98	49.29	48.69	47.86	48.12	46.62	46.44	42.67	38.60
CaO	.01	.01	.01	.00	.00	.17	.00	.08	.01	.22	.03	.02
NiO	.20	.45	.33	.39	.35	.12	.17	.11	.11	.19	.12	.05
Total	99.95	100.45	100.30	100.66	100.24	99.56	98.91	100.04	99.06	99.57	99.93	99.79
Cations per 4 oxygens												
Si	1.000	0.999	0.997	0.997	0.993	0.993	0.988	0.988	0.987	0.991	0.988	0.984
Fe	.101	.125	.152	.185	.203	.211	.234	.240	.271	.270	.389	.513
Mn	.001	.003	.004	.003	.004	.004	.004	.004	.005	.005	.006	.007
Mg	1.894	1.864	1.844	1.810	1.800	1.793	1.783	1.775	1.748	1.733	1.626	1.511
Ca	.000	.000	.000	.000	.000	.004	.000	.002	.000	.006	.001	.001
Ni	.004	.009	.006	.008	.007	.002	.003	.002	.002	.004	.002	.001
Mg/(Mg+Fe+Mn)	.949	.935	.922	.906	.897	.893	.882	.879	.864	.863	.805	.744

* Total iron as FeO.

Table 5. Analyses of orthopyroxene in Alaskan-type ultramafic and mafic rocks, southeastern Alaska.

[Electron microprobe analyses (in weight percent) by G.R. Himmelberg. Blashke Islands analyses from Himmelberg and others (1986b). Abbreviations given in table 2. Mg/(Mg+Fe^{2+}), atomic ratio of normative silicates. n.d., not determined.]

	Blashke Islands			Kane Peak		Union Bay	
Sample No.- -	80BI15	80BI49	80BI28	81KP5A	81KP2A	87GH28A	87GH50A
Rock type- -	Gb	Gbn	Ol Hbl Gbn	Hbl Phl Pd	Hbl Phl Pd	Gbn	Bt Gbn
SiO_2	54.10	54.10	52.90	54.90	55.29	51.03	50.51
TiO_2	.21	.20	.13	.05	.13	.29	.16
Al_2O_3	2.08	1.66	1.25	2.06	2.09	1.90	1.51
Cr_2O_3	n.d.	n.d.	n.d.	.47	.43	.03	.00
FeO*	16.20	16.60	23.70	8.05	8.02	22.03	27.52
MnO	.90	.77	.83	.23	.21	.55	1.00
MgO	25.90	25.90	20.60	32.25	32.31	21.83	17.07
CaO	1.55	1.34	1.47	.79	.90	1.07	1.66
Na_2O	.04	.04	.05	.02	.01	.01	.03
Total	100.98	100.61	100.93	98.79	99.39	98.73	99.46
	Formula per 4 cations						
Si	1.942	1.951	1.970	1.932	1.936	1.923	1.951
Al^{IV}	.058	.049	.030	.068	.064	.077	.049
Al^{VI}	.031	.022	.025	.018	.022	.008	.019
Ti	.006	.005	.004	.001	.003	.008	.005
Cr	.000	.000	.000	.013	.012	.001	.000
Fe^{3+}	.018	.019	.001	.036	.024	.053	.023
Fe^{2+}	.468	.482	.737	.201	.211	.642	.867
Mn	.027	.024	.026	.007	.006	.017	.033
Mg	1.387	1.393	1.144	1.693	1.687	1.227	.983
Ca	.060	.052	.059	.030	.034	.043	.069
Na	.003	.003	.004	.001	.001	.001	.002
$\frac{Mg}{(Mg+Fe^{2+})}$	.748	.743	.608	.894	.889	.657	.532
Wo†	.032	.028	.031	.016	.018	.023	.037
En	.724	.722	.590	.879	.873	.641	.512
Fs	.244	.250	.380	.105	.109	.335	.451

* Total iron as FeO; Fe^{3+} and Fe^{2+} in mineral formula caluclated from charge balance.
† Pyroxene components calculated according to the procedures of Lindsley and Andersen (1983).

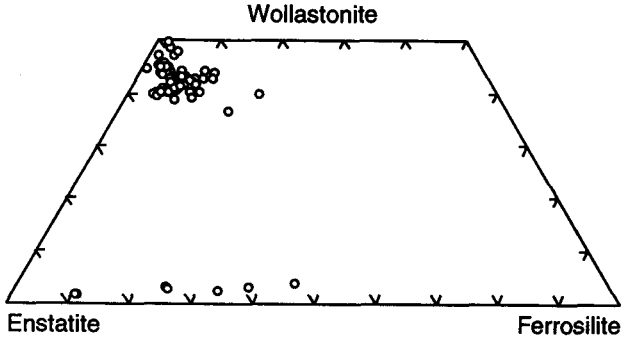

Figure 14. Plot of compositions of clinopyroxene and orthopyroxene (circles) in ultramafic rocks and gabbro of Alaskan-type intrusions, southeastern Alaska.

from progressively more hydrous melts characteristic of arc magmas (Murray, 1972; Conrad and Kay, 1984; Loucks, 1990). The theory that the hydrous nature of the magma gave rise to the Alaskan-type ultramafic cumulates is supported by the common occurrence of phlogopite and hornblende in wehrlite and clinopyroxenite, and by hornblendite as part of the differentiation sequence. In contrast, hydrous minerals are not common in ultramafic cumulates of ophiolite sequences or other rift-related differentiation products (Himmelberg and Loney, 1980; Pallister and Hopson, 1981; Elthon and others, 1982; Komor and others, 1985; Loney and Himmelberg, 1989). The alumina content of orthopyroxene in the ultramafic rocks is not unusual (≤2.09 weight percent); however, orthopyroxene is rare in the ultramafic rocks and is restricted to the earliest differentiates.

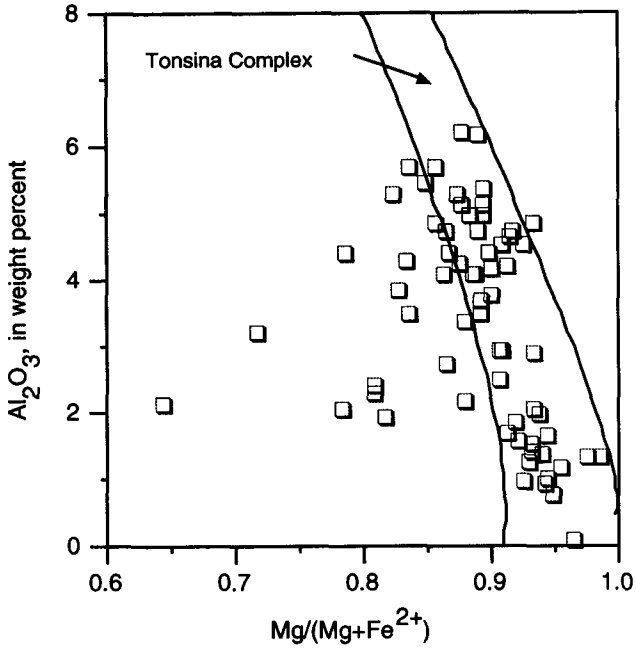

Figure 15. Plot of weight percent Al_2O_3 against Mg # [Mg/(Mg+Fe^{2+})] of clinopyroxene (open squares) in ultramafic rocks and gabbro of Alaskan-type intrusions, southeastern Alaska. Field of Tonsina Complex of Burns (1985), from DeBari and Coleman (1989).

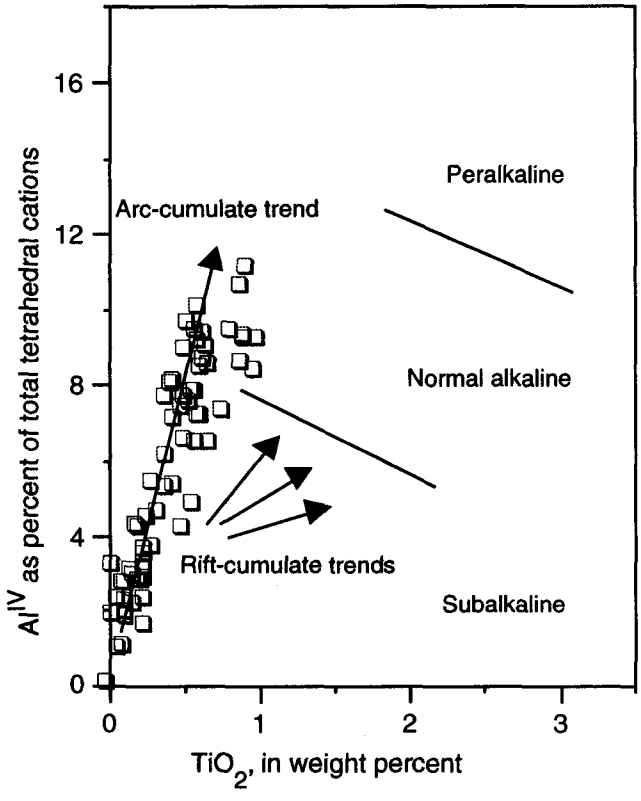

Figure 16. Plot of Al^{IV} content, expressed as a percentage of total tetrahedral Al, against TiO_2 for clinopyroxene in clinopyroxenite and gabbro of Alaskan-type intrusions, southeastern Alaska. Field boundaries from LeBas (1962); trend arrows from Loucks (1990).

The esseneite component ($CaFe^{3+}AlSiO_6$) of clinopyroxene generally increases with the differentiation sequence of rocks. Clinopyroxene with substantial Fe^{3+} and esseneite component occurs in hornblende clinopyroxenite and magnetite clinopyroxenite at Douglas Island, Haines, Klukwan, Port Snettisham, and Union Bay (table 6). Experimental studies of Holloway and Burnham (1972) and arguments by Loucks (1990) demonstrate that when Fe_2O_3/FeO is buffered in the melt, increasing P_{H_2O} causes crystallization of increasingly Fe^{3+}-rich and Al-rich clinopyroxenes (as esseneite and possibly Ca-tschermakite components). The elevated P_{H_2O} promotes oxidation of iron which enhances crystallization of Fe^{3+}-rich esseneitic clinopyroxene. The occurrence of clinopyroxene that has the higher esseneite component in hornblende- and magnetite-rich clinopyroxenites is consistent with these arguments and suggests that the magmas that crystallized the Alaskan-type ultramafic rocks generally became more hydrous as fractionation proceeded. The absence of abundant magnetite and hornblende in the ultramafic rocks of the Blashke Islands and Kane Peak bodies, and the generally low esseneite component of clinopyroxene in these bodies, suggest that the magmas that crystallized these two bodies were probably less hydrous and less oxidizing than the magmas that crystallized the other bodies. The calcium-tschermakite component (CaTs) remains relatively low through the differentiation sequence (table 6).

The hornblendes in the Alaska-type ultramafic rocks and gabbros are mainly pargasite but also include pargasitic hornblende and tschermakitic hornblende (table 7; fig. 17). Experimental studies indicate that the upper stability limit of pargasite is 1,050°C between 8 and 16 kbar (Jenkins, 1983), which is higher than that of other amphiboles. The most Mg-rich hornblendes (Mg # 0.970, 0.981) occur as a postcumulus phase in the olivine-rich peridotite at Kane Peak. A gap between the Mg # of hornblende in olivine-rich peridotite and that of clinopyroxenite and hornblendite, where the range is from 0.893 to 0.602, implies no systematic relation between Mg # and modal mineralogy. The Mg # of hornblende in gabbro ranges from 0.777 to 0.594.

Phlogopite biotite is relatively common in the ultramafic rocks (table 8). The Mg # is 0.918 and 0.914 in wehrlite and olivine-rich peridotite at Dall Island and Kane Peak, respectively, and decreases systematically through clinopyroxenite to 0.572 in hornblendite. The most iron-rich biotite (Mg # 0.469) occurs in biotite gabbronorite at Union Bay.

Chromian spinel is common as an accessory mineral in dunite, wehrlite, and some olivine clinopyroxenites. Its general absence in clinopyroxenites, however, probably reflects a reaction between chromian spinel and clinopyroxene as suggested by Irvine (1967b). The major chemical variation of chromian spinel is a Cr # range that increases as the Fe^{2+} # increases (table 9, fig. 18). Excluding the Red Bluff Bay complex, the Fe^{3+} # ranges from 0.133 to 0.398, which is markedly higher than that for chromian spinels in ultramafic rocks

Table 6. Analyses of clinopyroxene in Alaskan-type ultramafic and mafic rocks, southeastern Alaska.

[Electron microprobe analyses (in weight percent) by G.R. Himmelberg. Blashke Islands and Salt Chuck analyses from Himmelberg and others (1986b) and Loney and Himmelberg (1992). Abbreviations given in table 2. $Mg/(Mg+Fe^{2+})$, atomic ratio of normative silicates. -, not detected; n.d., not determined]

	Blashke Islands										
Sample No.----	80BI48	80BI43	80BI10	80BI13	80BI47	80BI14	80BI28	80BI17	80BI15	80BI49	80BI29
Rock type-----	Ol Cpxite	Du	Du	Ol Cpxite	Whr	Ol Cpxite	Ol Hbl Gbn	Hbl Gb	Gb	Gbn	Hbl Px Gb
SiO_2----------	53.80	54.80	53.40	54.30	53.20	52.30	53.20	53.80	52.20	52.10	53.00
TiO_2----------	.17	.06	.03	.13	.25	.26	.24	.24	.30	.50	.25
Al_2O_3----------	1.91	.91	1.49	1.61	2.87	2.87	2.12	1.86	2.24	2.35	1.98
Cr_2O_3----------	.32	.09	.05	.30	n.d.	.23	n.d.	.30	n.d.	n.d.	n.d.
FeO*----------	2.95	2.43	2.64	3.45	3.72	4.41	4.58	5.79	7.96	8.47	7.76
MnO----------	.11	.06	.05	.09	.09	.13	.12	.43	.48	.41	.56
MgO----------	17.50	17.40	17.90	17.40	16.70	16.00	16.30	14.70	14.50	15.20	14.20
CaO----------	23.70	24.80	24.80	23.60	23.40	23.70	23.40	23.40	22.40	21.20	22.30
Na_2O----------	.17	.03	.06	.17	.22	.18	.16	.36	.35	.37	.48
Total----------	100.63	100.58	100.42	101.05	100.45	100.08	100.12	100.88	100.43	100.60	100.53
	Formula per 4 cations										
Si----------	1.941	1.980	1.926	1.955	1.927	1.910	1.943	1.968	1.925	1.915	1.953
Al^{IV}----------	.059	.020	.064	.045	.073	.090	.057	.032	.075	.085	.047
Al^{VI}----------	.023	.019	.000	.023	.050	.034	.034	.048	.022	.017	.039
Ti----------	.005	.002	.001	.004	.007	.007	.007	.007	.008	.014	.007
Cr----------	.009	.003	.001	.009	n.d.	.007	n.d.	.009	n.d.	n.d.	n.d.
Fe^{3+}----------	.030	.000	.000	.018	.024	.047	.022	.000	.061	.067	.028
Fe^{2+}----------	.059	.073	.080	.086	.088	.087	.118	.177	.184	.194	.212
Mn----------	.003	.002	.002	.003	.003	.004	.004	.013	.015	.013	.017
Mg----------	.942	.938	.963	.934	.903	.872	.888	.802	.798	.833	.781
Ca----------	.917	.961	.960	.912	.910	.929	.917	.918	.886	.836	.882
Na----------	.012	.002	.004	.012	.015	.013	.011	.026	.025	.026	.034
$\frac{Mg}{(Mg+Fe^{2+})}$	.941	.927	.923	.916	.911	.909	.882	.819	.812	.811	.787
Wo†----------	.440	.471	.479	.443	.433	.433	.442	.444	.426	.403	.438
En----------	.527	.491	.481	.510	.516	.515	.492	.456	.466	.485	.442
Fs----------	.033	.038	.040	.047	.051	.052	.066	.101	.108	.113	.120
Ac----------	.012	.000	.000	.012	.015	.013	.011	.000	.025	.026	.028
Es----------	.018	.000	.000	.006	.009	.035	.010	.000	.036	.040	.000
CaTs----------	.023	.017	.000	.023	.050	.034	.034	.023	.022	.017	.033

	Dall Island			Douglas Island			Haines			
Sample No.-----	90GH6A	90GH6C	90GH6B	86DB69A	86DB64A	86DB68A	84GH53B	84GH53C	84GH54B	84GH55B
Rock type------	Phl Whr	Bt Hbl Cpxite	Cpxite	Plg Cpxite	Cpxite	Hb Cpxite	Hbl Cpxite	Hbl Cpxite	Bt Cpxite	Hbl Cpxite
SiO_2----------	52.24	51.63	51.05	47.50	49.00	50.60	48.69	50.04	50.45	49.20
TiO_2----------	.20	.30	.39	.92	.91	.68	.82	.62	.47	.90
Al_2O_3----------	2.83	3.42	4.02	6.14	5.64	4.24	5.22	4.36	3.35	5.62
Cr_2O_3----------	.67	.04	-	-	-	-	-	-	-	-
FeO*----------	3.21	5.50	5.30	7.81	7.61	6.62	7.17	6.39	6.61	6.78
MnO----------	.11	.13	.11	.21	.19	.13	.19	.13	.16	.12
MgO----------	16.32	15.32	14.71	12.70	12.60	14.00	13.58	14.58	13.96	13.32
CaO----------	23.47	23.47	24.00	23.40	23.70	23.40	23.51	22.84	23.71	24.13
Na_2O----------	.29	.26	.21	.36	.43	.24	.21	.23	.33	.20
Total----------	99.34	100.05	99.80	99.04	100.08	99.91	99.37	99.19	99.04	100.27
	Formula per 4 cations									
Si----------	1.915	1.892	1.878	1.777	1.816	1.870	1.812	1.857	1.880	1.815
Al^{IV}----------	.085	.108	.122	.223	.184	.130	.188	.143	.120	.185
Al^{VI}----------	.037	.040	.052	.048	.063	.055	.041	.047	.028	.060
Ti----------	.005	.008	.011	.026	.025	.019	.023	.017	.013	.025
Cr----------	.019	.001	.000	.000	.000	.000	.000	.000	.000	.000
Fe^{3+}----------	.038	.069	.063	.148	.101	.054	.117	.078	.090	.089
Fe^{2+}----------	.060	.099	.100	.096	.135	.151	.106	.121	.117	.120
Mn----------	.003	.004	.003	.007	.006	.004	.006	.004	.005	.004
Mg----------	.892	.837	.807	.709	.697	.772	.754	.807	.776	.733
Ca----------	.923	.923	.947	.939	.942	.928	.938	.909	.948	.955
Na----------	.021	.019	.015	.026	.031	.017	.015	.017	.024	.014
$\frac{Mg}{(Mg+Fe^{2+})}$	.937	.894	.890	.881	.838	.837	.876	.870	.869	.860
Wo†----------	.435	.425	.431	.397	.420	.427	.406	.409	.439	.417
En----------	.529	.514	.506	.531	.486	.480	.521	.515	.487	.501
Fs----------	.036	.061	.063	.072	.094	.094	.074	.077	.073	.082
Ac----------	.021	.019	.015	.026	.031	.017	.015	.017	.024	.014
Es----------	.018	.051	.048	.122	.070	.037	.102	.061	.066	.075
CaTs----------	.037	.040	.052	.048	.063	.055	.041	.047	.028	.060

Footnotes at end of table.

Table 6. Analyses of clinopyroxene in Alaskan-type ultramafic and mafic rocks, southeastern Alaska—Continued.

	Haines–Continued		Kane Peak						Klukwan	
Sample No.	84GH54A	84GH55A	81SK043A	81SK046A	81KP22A	81KP23A	81KP15A	81KP14A	84GH52D	84GH52F
Rock type	Bt Cpxite	Hbl Cpxite	Whr	Whr	Cpxite	Ol Cpxite	Cpxite	Cpxite	Mag Cpxite	Hbl Cpxite
SiO_2	49.62	50.23	53.85	53.40	52.92	53.57	52.23	51.01	51.21	48.00
TiO_2	.97	.37	.13	.12	.22	.18	.25	.44	.39	.89
Al_2O_3	4.81	3.16	.93	.87	1.34	1.20	1.80	3.42	2.44	6.10
Cr_2O_3	-	-	.68	.74	.41	0.45	.23	.02	-	.01
FeO*	6.94	8.62	2.55	2.52	3.73	3.22	4.50	7.73	5.87	6.69
MnO	.15	.23	.08	.07	.14	.09	.11	.16	.48	.07
MgO	13.47	12.53	17.56	17.74	17.23	17.23	16.42	14.70	15.50	13.20
CaO	23.97	23.28	23.76	23.45	22.78	23.42	22.94	21.18	23.50	24.00
Na_2O	.29	.41	.19	.17	.26	.24	.29	.60	.17	.21
Total	100.20	98.83	99.74	99.06	99.03	99.59	98.77	99.26	99.55	99.14
			Formula per 4 cations							
Si	1.833	1.894	1.961	1.956	1.944	1.957	1.930	1.893	1.891	1.789
Al^{IV}	.167	.106	.039	.037	.056	.043	.070	.107	.106	.211
Al^{VI}	.042	.034	.001	.000	.002	.008	.008	.042	.000	.057
Ti	.027	.011	.004	.003	.006	.005	.007	.012	.011	.025
Cr	.000	.000	.020	.021	.012	.013	.007	.000	.000	.000
Fe^{3+}	.092	.081	.024	.021	.047	.029	.062	.084	.096	.120
Fe^{2+}	.122	.191	.053	.056	.067	.069	.077	.156	.085	.089
Mn	.005	.007	.002	.002	.004	.003	.003	.005	.015	.002
Mg	.742	.705	.954	.969	.944	.939	.905	.814	.853	.734
Ca	.950	.942	.928	.921	.898	.918	.909	.843	.931	.959
Na	.020	.030	.013	.012	.018	.017	.021	.043	.012	.015
$\frac{Mg}{(Mg+Fe^{2+})}$	.858	.787	.947	.946	.933	.932	.921	.839	.909	.892
Wo†	.428	.443	.455	.451	.437	.450	.437	.402	.429	.406
En	.491	.438	.516	.519	.526	.512	.519	.502	.519	.530
Fs	.081	.119	.029	.030	.038	.038	.044	.096	.052	.064
Ac	.020	.030	.013	.012	.018	.017	.021	.043	.012	.015
Es	.072	.051	.011	.009	.029	.013	.041	.040	.084	.105
CaTs	.042	.034	.001	.000	.002	.008	.008	.042	.000	.057

	Port Snettisham			Red Bluff Bay			Salt Chuck				
Sample No.	87GH18A	87GH19A	87GH17A	90GH18A	90GH15B	90GH16B	86GH23A	86GH34B	86GH20A	86GH25A	86GH1B
Rock type	Cpxite	Cpxite	Cpxite	Whr	Cpxite	Cpxit	Mag Cpxite	Cpxite	Mag Cpxite	Mag Cpxite	Mag Cpxite
SiO_2	49.19	49.21	48.77	54.46	53.82	53.60	48.60	48.82	49.45	48.54	48.88
TiO_2	.89	.90	.98	-	.03	.08	.53	.64	.42	.61	.61
Al_2O_3	4.90	4.84	5.40	.02	1.09	1.46	4.78	4.65	4.16	5.28	4.47
Cr_2O_3	-	-	-	-	.60	.28	-	-	-	-	-
FeO*	6.00	6.04	7.12	.89	2.05	2.96	6.91	7.37	6.69	7.15	7.69
MnO	.13	.13	.16	.06	.10	.15	.16	.35	.14	.22	.34
MgO	14.00	13.81	12.90	18.22	17.72	17.25	14.15	14.16	14.34	13.72	13.75
CaO	23.81	24.15	23.95	25.37	23.87	23.88	23.72	23.00	23.53	23.53	23.22
Na_2O	.23	.20	.28	.00	.14	.09	.23	.35	.27	.30	.42
Total	99.15	99.28	99.57	99.03	99.41	99.76	99.08	99.32	99.00	99.35	99.36
				Formula per 4 cations							
Si	1.828	1.828	1.816	1.986	1.962	1.954	1.808	1.813	1.839	1.803	1.818
Al^{IV}	.172	.172	.184	.001	.038	.046	.192	.187	.161	.197	.182
Al^{VI}	.043	.040	.053	.000	.009	.016	.017	.017	.022	.034	.014
Ti	.025	.025	.028	.000	.001	.002	.015	.018	.012	.017	.017
Cr	.000	.000	.000	.000	.017	.008	.000	.000	.000	.000	.000
e^{3+}	.096	.095	.097	.001	.019	.024	.162	.160	.135	.150	.165
Fe^{2+}	.090	.093	.125	.026	.043	.066	.053	.069	.073	.072	.074
Mn	.004	.004	.005	.002	.003	.005	.005	.011	.004	.007	.011
Mg	.776	.765	.716	.991	.964	.938	.785	.784	.796	.760	.763
Ca	.949	.963	.956	.993	.934	.934	.946	.916	.939	.938	.926
Na	.017	.014	.020	.000	.010	.006	.017	.025	.019	.022	.030
$\frac{Mg}{(Mg+Fe^{2+})}$	.896	.892	.852	.974	.957	.934	.937	.919	.916	.913	.911
Wo†	.422	.428	.424	.496	.454	.449	.400	.395	.411	.398	.404
En	.518	.510	.491	.491	.523	.514	.562	.556	.540	.550	.543
Fs	.060	.062	.086	.013	.023	.036	.038	.049	.050	.052	.053
Ac	.017	.014	.020	.000	.010	.006	.017	.025	.019	.022	.030
Es	.080	.081	.077	.001	.010	.018	.146	.135	.116	.129	.135
CaTs	.043	.040	.053	.000	.009	.016	.017	.017	.022	.034	.014

Footnotes at end of table.

Table 6. Analyses of clinopyroxene in Alaskan-type ultramafic and mafic rocks, southeastern Alaska—Continued.

	Salt Chuck — Continued										
Sample No.	86GH9B	86GH35A	86GH8A	86GH11A	86GH12A	86GH7A	86GH1A	86GH27A	86GH3A	86GH30A	86GH3B
Rock type	Mag Gb	Mag Gb	Mag Cpxite	Mag Cpxite	Mag Gb	Gb	Mag Gb	Mag Gb	Mag Gb	Mag Gb	Gb
SiO_2	49.64	49.96	49.53	48.51	48.29	49.64	49.27	50.09	48.85	50.05	50.02
TiO_2	.59	.44	.62	.59	.60	.50	.67	.55	.65	.55	.58
Al_2O_3	4.10	3.69	4.35	5.07	5.30	3.61	4.66	4.05	4.89	3.46	3.78
Cr_2O_3	-	-	-	.01	-	-	-	.01	-	-	-
FeO*	6.78	7.38	7.23	7.44	8.04	7.27	7.10	7.17	7.49	7.33	8.10
MnO	.37	.41	.34	.24	.24	0.42	.33	0.36	.26	.34	.60
MgO	14.56	13.82	14.11	13.39	12.92	14.15	13.91	14.30	13.44	14.38	13.40
CaO	22.74	22.71	23.25	23.34	23.55	22.96	23.05	22.96	23.16	22.34	22.04
Na_2O	.34	.71	.36	.38	.46	.38	.38	.40	.43	.50	.58
Total	99.12	99.11	99.79	98.98	99.40	98.92	99.38	99.89	99.17	98.95	99.10
	Formula per 4 cations										
Si	1.844	1.859	1.832	1.811	1.799	1.853	1.830	1.850	1.821	1.865	1.871
Al^{IV}	.156	.141	.168	.189	.201	.147	.170	.150	.179	.135	.129
Al^{VI}	.024	.021	.021	.035	.032	.012	.034	.026	.036	.017	.037
Ti	.017	.012	.017	.017	.017	.014	.019	.015	.018	.015	.016
Cr	.000	.000	.000	.000	.000	.000	.000	.000	.000	.000	.000
Fe^{3+}	.124	.147	.138	.147	.168	.135	.127	.123	.138	.124	.102
Fe^{2+}	.087	.082	.085	.085	.083	.092	.094	.099	.095	.105	.152
Mn	.012	.013	.011	.008	.007	.013	.010	.011	.008	.011	.019
Mg	.807	.767	.778	.746	.718	.788	.771	.788	.747	.799	.748
Ca	.906	.907	.923	.935	.941	.919	.918	.910	.926	.893	.884
Na	.025	.051	.026	.027	.033	.027	.028	.029	.031	.036	.042
$\frac{Mg}{(Mg+Fe^{2+})}$	.903	.903	.901	.898	.897	.895	.892	.889	.887	.884	.831
Wo†	.404	.420	.407	.404	.404	.414	.406	.409	.407	.412	.415
En	.538	.523	.534	.535	.535	.525	.529	.525	.526	.519	.486
Fs	.058	.056	.059	.061	.061	.061	.064	.066	.067	.068	.099
Ac	.025	.051	.026	.027	.033	.027	.028	.029	.031	.036	.042
Es	.099	.096	.112	.120	.135	.108	.099	.094	.107	.087	.059
CaTs	.024	.021	.021	.035	.032	.012	.034	.026	.036	.017	.037

	Sukkwan Island	Union Bay								
Sample No.	90GH9A	87GH49A	87GH34A	87GH33A	87GH35A	87GH41A	878GH36A	87GH29A	87GH28A	87GH50A
Rock type	Hbl Cpxite	Ol Cpxite	Whr	Cpxite	Cpxite	Mag Cpxite	Ol Cpxite	Mag Cpxite	Gbn	Bt Gbn
SiO_2	50.36	53.02	52.84	52.70	51.82	49.17	51.40	49.59	50.75	50.87
TiO_2	.51	.11	.13	.15	.22	.64	.34	.39	.56	.24
Al_2O_3	5.05	1.26	1.40	1.54	2.02	4.57	2.68	4.68	3.13	2.05
Cr_2O_3	.28	.63	.62	.53	.46	.00	.14	-	.02	-
FeO*	5.64	1.82	2.21	3.04	4.17	6.22	6.30	7.02	11.40	13.09
MnO	.13	1.00	.07	.08	.16	.15	.16	.21	.36	.54
MgO	14.51	17.54	17.01	16.96	16.32	14.63	15.59	14.51	13.92	11.97
CaO	23.55	23.65	24.67	23.79	23.75	23.45	22.11	22.18	18.98	20.18
Na_2O	.21	.19	.23	.17	.20	.16	.26	.25	.43	.35
Total	100.22	99.21	99.18	98.96	99.12	98.99	98.97	98.83	99.54	99.28
		Formula per 4 cations								
Si	1.847	1.939	1.934	1.937	1.909	1.827	1.907	1.847	1.903	1.937
Al^{IV}	.153	.055	.061	.063	.088	.173	.093	.153	.097	.063
Al^{VI}	.066	.000	.000	.004	.000	.027	.024	.053	.042	.029
Ti	.014	.003	.004	.004	.006	.018	.010	.011	.016	.007
Cr	.008	.018	.018	.015	.013	.000	.004	.000	.001	.000
Fe^{3+}	.065	.044	.052	.047	.077	.121	.064	.097	.054	.046
Fe^{2+}	.108	.012	.015	.046	.052	.072	.132	.122	.304	.371
Mn	.004	.031	.002	.002	.005	.005	.005	.007	.011	.018
Mg	.794	.957	.929	.930	.897	.811	.863	.806	.778	.680
Ca	.927	.928	.969	.938	.939	.935	.880	.887	.763	.824
Na	.015	.013	.016	.012	.014	.011	.018	.018	.031	.025
$\frac{Mg}{(Mg+Fe^{2+})}$	.881	.988	.984	.952	.945	.918	.868	.868	.719	.647
Wo†	.408	.446	.466	.448	.439	.404	.412	.387	.365	.400
En	.521	.547	.526	.526	.531	.547	.510	.532	.457	.388
Fs	.071	.007	.009	.026	.031	.049	.078	.081	.178	.212
Ac	.015	.013	.016	.012	.014	.011	.018	.018	.031	.025
Es	.051	.031	.036	.035	.062	.110	.045	.078	.023	.021
CaTs	.066	.000	.000	.004	.000	.027	.024	.053	.042	.029

* Total iron as FeO; Fe^{3+} and Fe^{2+} in mineral formula calculated from charge balance.
†Pyroxene components calculated according to the procedures of Lindsley and Andersen (1983).

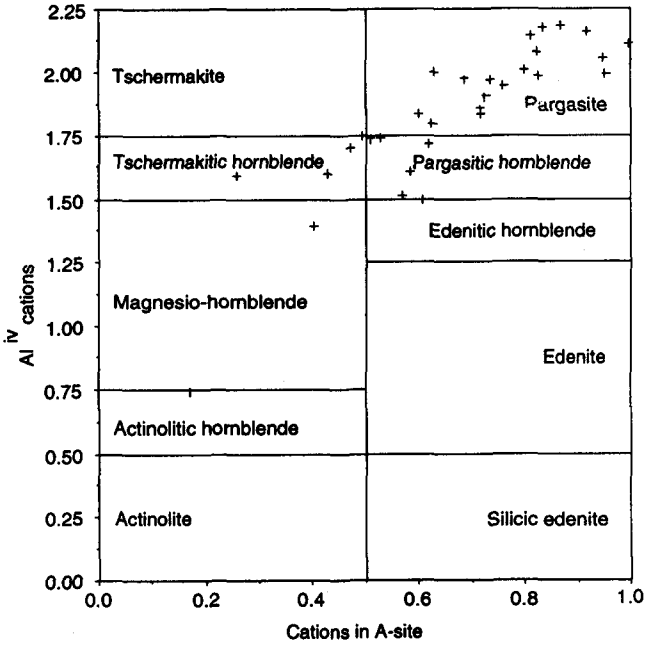

◀ **Figure 17.** Plot of Al^{IV} against cations in A-site for hornblende in ultramafic rocks and gabbro of Alaskan-type intrusions, southeastern Alaska. Nomenclature from Leake (1978).

from other tectonomagmatic environments and is a characteristic originally pointed out by Irvine (1967b). The significantly lower Fe^{3+} # of chromite in clinopyroxenite and dunite at Red Bluff Bay (0.080 and 0.126) supports the interpretation that this body is not an Alaskan-type ultramafic intrusion. Studies on Mg-Fe exchange between olivine and chromian spinel have shown that these minerals reequilibrate at subsolidus temperatures (Irvine, 1965; Evans and Frost, 1975; Fabriès, 1979; Henry and Medaris, 1980; Engi, 1983). Subsolidus exchange of Mg-Fe will modify the $Mg/(Mg+Fe^{2+})$ of both olivine and spinel, but the effect will be small for olivine and large for spinel because of the large difference in modal proportions of these two minerals in the rocks. Temperatures of equilibration calculated for 13 olivine and chromian spinel pairs in the Alaskan-type ultramafic rocks, using the calibration of Fabriès (1979), range from 470 to 820°C, which is consistent with subsolidus reequilibration.

The chromian spinel compositions in the Alaskan-type ultramafic rocks are similar to those reported in arc-related cumulates and lavas (Conrad and Kay, 1984; Dick and Bullen, 1984; DeBari and others, 1987; DeBari and Coleman, 1989).

Plagioclase is confined to the relatively minor gabbroic rocks of the Alaskan-type ultramafic-mafic intrusions. Analyses of plagioclase in representative Alaskan-type gabbros are given in table 10.

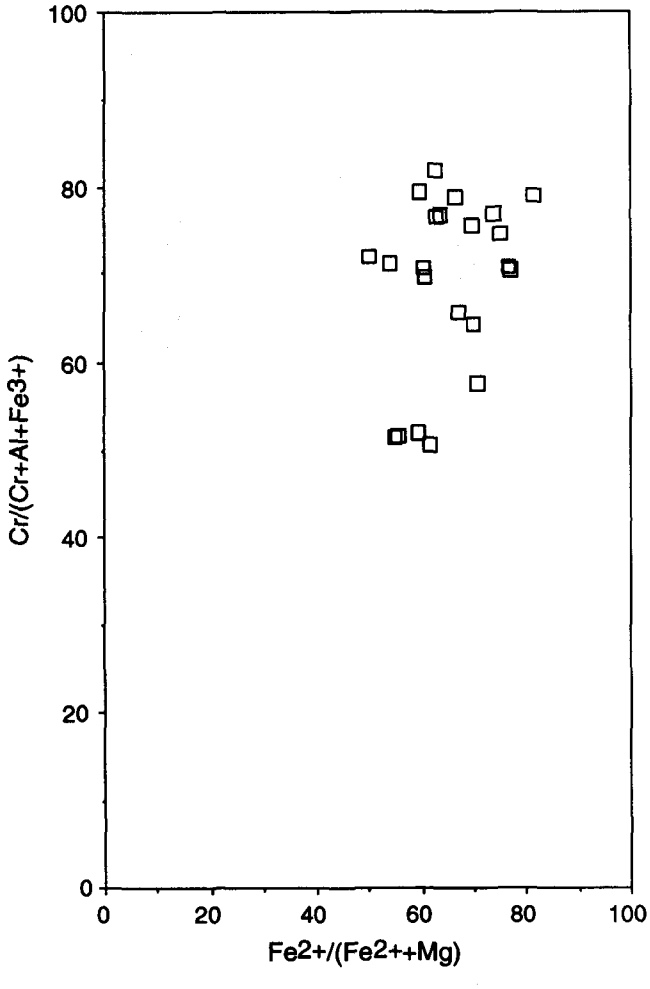

◀ **Figure 18.** Plot of Cr # $[Cr/(Cr+Al+Fe^{3+})]$ against Fe^{2+} # $[Fe^{2+}/(Mg+Fe^{2+})]$ for chromian spinel in ultramafic rocks of Alaskan-type intrusions, southeastern Alaska.

DISCUSSION

CRYSTALLIZATION CONDITIONS OF ULTRAMAFIC-MAFIC ROCKS

Several factors leave no doubt that the Alaskan-type ultramafic-mafic bodies formed from a basaltic magma by crystal fractionation and mineral concentration processes. These factors are (1) the sequence of appearance of primary minerals, (2) the common occurrence of essentially monomineralic and bimineralic rocks having chemistries that do not represent liquid compositions, (3) the rock REE patterns, (4) the mineral chemistry trends, and (5) the cumulus textures. The temperature, pressure, water content, and oxygen fugacity during crystallization of the Alaskan-type intrusions can be qualitatively estimated by comparing the natural

Table 7. Analyses of hornblende in Alaskan-type ultramafic and mafic rocks, southeastern Alaska.

[Electron microprobe analyses (in weight percent) by G.R. Himmelberg. Blashke Islands analyses from Himmelberg and others (1986b); sample 80BI19, g, green rim; b, brown core. Salt Chuck analyses from Loney and Himmelberg (1992). Abbreviations given in table 2. Mg/(Mg+Fe^{2+}+Mn), atomic ratio of normative silicates.]

	Alava Bay	Blashke Islands								Dall Island	
Sample No.----	90GH02	80BI14	80BI49	80BI15	80BI19b	80BI29	80BI19g	80BI28	80BI17	90GH6B	90GH6C
Rock type------	Bt Hblite	Ol Cpxite	Gbn	Gb	Gb	Hbl Px Gb	Gb	Ol HblGbn	Hbl Gbn	Cpxite	Bt Hbl Cpxite
SiO_2----------	41.51	45.10	43.60	43.10	43.40	44.10	50.80	43.10	45.30	42.12	41.72
TiO_2----------	1.75	1.00	2.73	2.67	2.57	2.19	.88	2.16	1.81	1.32	1.24
Al_2O_3----------	13.28	12.20	11.70	13.20	11.80	11.30	5.43	11.60	9.46	14.29	14.24
FeO*----------	15.41	8.46	11.50	11.60	13.60	12.50	13.50	15.60	14.40	8.92	9.76
MnO----------	.18	.10	.23	.30	.42	.38	.52	.26	.40	.09	.13
MgO----------	10.71	16.20	14.20	13.60	12.50	13.30	14.40	12.00	12.70	14.96	14.67
CaO----------	11.72	12.50	12.00	11.90	11.20	11.80	11.80	11.60	11.90	12.24	12.27
Na_2O----------	2.34	1.58	2.35	2.52	2.26	2.29	.99	2.43	1.44	1.80	1.77
K_2O----------	.92	.50	.00	.40	.49	.55	.50	.00	.72	1.72	1.90
Total---------	97.82	97.64	98.31	99.29	98.24	98.41	98.82	98.75	98.13	97.47	97.68
		Formula per 13 cations exclusive of Ca, Na, K									
Si----------	6.166	6.403	6.266	6.162	6.295	6.392	7.251	6.255	6.606	6.096	6.053
Al^{IV}----------	1.834	1.597	1.734	1.838	1.705	1.608	.749	1.745	1.394	1.904	1.947
Al^{VI}----------	.492	.445	.249	.388	.313	.323	.164	.240	.232	.535	.490
Ti----------	.196	.107	.296	.288	.281	.239	.095	.236	.199	.144	.135
Fe^{3+}----------	.367	.604	.537	.451	.618	.391	.416	.736	.499	.455	.517
Fe^{2+}----------	1.548	.401	.846	.936	1.032	1.125	1.196	1.158	1.258	.625	.667
Mn----------	.023	.012	.028	.036	.052	.047	.063	.032	.049	.011	.015
Mg----------	2.374	3.431	3.044	2.901	2.704	2.875	3.066	2.598	2.762	3.229	3.175
Ca----------	1.867	1.904	1.850	1.825	1.743	1.835	1.807	1.806	1.862	1.901	1.909
Na(B)----------	.133	.096	.150	.175	.257	.165	.193	.194	.138	.099	.091
Na(A)----------	.542	.339	.506	.525	.379	.479	.081	.491	.269	.406	.408
K----------	.174	.091	.000	.073	.091	.102	.091	.000	.134	.318	.352
$\frac{Mg}{(Mg+Fe^{2+}+Mn)}$	.602	.893	.777	.749	.714	.711	.709	.686	.679	.835	.823

	Douglas Island			Haines					Kane Peak	
Sample No.----	86DB68A	86DB69A	6DB64A	84GH53C	84GH53B	84GH54B	84GH54A	84GH55A	81KP5A	81KP2A
Rock type------	Hbl Cpxite	Plg Cpxite	Cpxite	Hbl Cpxite	Hbl Cpxite	Bt Cpxite	Bt Cpxite	Hbl Cpxite	Hbl Phl Pd	Hbl Phl Pd
SiO_2----------	39.97	39.77	39.97	42.10	41.11	39.38	39.68	39.23	45.62	46.19
TiO_2----------	2.13	2.60	2.48	1.89	1.90	1.99	2.33	1.52	.92	1.11
Al_2O_3----------	14.92	14.03	13.45	13.84	14.06	13.66	14.25	13.54	11.35	11.37
FeO*----------	10.46	12.79	13.34	8.93	10.45	12.13	11.77	16.44	5.09	4.87
MnO----------	.08	.28	.18	.10	.17	.08	.11	.14	.05	.08
MgO----------	14.00	12.48	11.73	15.68	14.23	13.73	13.35	10.67	18.34	18.58
CaO----------	12.99	12.62	12.36	12.74	12.52	12.28	12.12	11.93	11.73	11.87
Na_2O----------	2.14	2.29	2.23	2.11	2.25	2.31	1.98	1.80	2.33	2.41
K_2O----------	1.92	1.77	1.61	1.04	1.11	1.58	1.73	1.89	.84	.84
Total---------	98.61	98.61	97.33	98.41	97.79	97.14	97.32	97.16	96.27	97.30
				Formula per 13 cations exclusive of Ca, Na, K						
Si----------	5.847	5.887	6.007	6.029	5.989	5.839	5.856	5.921	6.492	6.508
Al^{IV}----------	2.153	2.113	1.993	1.971	2.011	2.161	2.144	2.079	1.508	1.492
Al^{VI}----------	.420	.336	.390	.365	.404	.227	.335	.331	.396	.396
Ti----------	.235	.289	.281	.204	.209	.222	.259	.173	.099	.118
Fe^{3+}----------	.220	.197	.097	.507	.432	.620	.560	.647	.537	.463
Fe^{2+}----------	1.060	1.388	1.581	.562	.842	.885	.893	1.429	.069	.110
Mn----------	.010	.035	.023	.012	.021	.010	.014	.018	.006	.009
Mg----------	3.055	2.755	2.629	3.350	3.092	3.036	2.939	2.402	3.893	3.904
Ca----------	2.039	2.005	1.992	1.957	1.957	1.953	1.919	1.932	1.791	1.794
Na(B)----------	.000	.000	.008	.043	.043	.047	.081	.068	.209	.206
Na(A)----------	.607	.658	.643	.543	.594	.618	.486	.459	.434	.453
K----------	.359	.334	.309	.190	.206	.299	.326	.364	.153	.151
$\frac{Mg}{(Mg+Fe^{2+}+Mn)}$	.741	.652	.621	.854	.782	.772	.764	.624	.981	.970

Footnote at end of table.

Table 7. Analyses of hornblende in Alaskan-type ultramafic and mafic rocks, southeastern Alaska—Continued.

	Kane Peak— Continued		Klukwan		Port Snettisham			Salt Chuck	Sukkwan Island
Sample No.---	81KP1B	81KP1C	84GH52D	84GH52F	87GH18A	87GH19A	87GH17A	86GH9B	90GH9A
Rock type-----	Diorite	Hblite	Mag Cpxite	Hbl Cpxite	Cpxite	Cpxite	Cpxite	Mag Gb	Hbl Cpxite
SiO_2	43.99	42.40	42.86	40.77	40.48	40.32	38.79	40.04	42.82
TiO_2	1.80	1.80	1.43	1.85	2.03	2.08	2.47	2.15	1.88
Al_2O_3	11.79	13.92	13.70	15.09	14.83	14.81	15.05	13.19	12.56
FeO*	13.47	14.14	8.02	11.07	9.84	11.44	14.05	13.00	13.36
MnO	.20	.26	.09	.14	.10	.10	.16	.25	.20
MgO	12.44	11.13	15.95	13.88	15.18	14.10	12.09	12.97	12.44
CaO	10.31	11.72	13.22	12.88	12.72	12.60	12.43	12.31	11.91
Na_2O	1.61	2.07	1.89	1.97	1.97	1.73	1.91	2.56	1.71
K_2O	1.05	1.05	.85	1.42	1.95	2.16	1.84	1.31	.92
Total	96.64	98.46	98.01	99.07	99.10	99.32	98.77	97.79	97.80
	Formula per 13 cations exclusive of Ca, Na, K								
Si	6.409	6.207	6.145	5.887	5.818	5.822	5.711	5.939	6.258
Al^{IV}	1.591	1.793	1.855	2.113	2.182	2.178	2.289	2.061	1.742
Al^{VI}	.434	.609	.461	.455	.331	.344	.323	.245	.422
Ti	.198	.199	.154	.201	.220	.226	.273	.241	.207
Fe^{3+}	.890	.324	.336	.450	.582	.595	.603	.429	.514
Fe^{2+}	.751	1.407	.626	.887	.601	.788	1.128	1.185	1.120
Mn	.024	.032	.011	.017	.012	.012	.019	.031	.025
Mg	2.702	2.429	3.411	2.990	3.254	3.036	2.654	2.869	2.712
Ca	1.612	1.840	2.034	1.996	1.961	1.952	1.963	1.959	1.867
Na(B)	.388	.160	.000	.004	.039	.048	.037	.041	.133
Na(A)	.065	.427	.526	.548	.511	.437	0.508	.697	.352
K	.194	.196	.156	.262	.358	.398	.346	.249	.172
$\frac{Mg}{(Mg+Fe^{2+}+Mn)}$	.777	.628	.843	.768	.841	.792	.698	0.702	.703

	Union Bay			
Sample No.---	87GH29A	87GH47A	87GH40A	87GH44A
Rock type-----	Mag Hbl Cpxit	Cpxite	Hblite	Hbl Gb
SiO_2	41.55	41.46	40.48	42.50
TiO_2	1.73	1.77	1.63	1.53
Al_2O_3	14.42	14.61	14.15	12.32
FeO*	9.90	11.69	13.40	15.99
MnO	.12	.23	.17	.46
MgO	14.36	13.35	11.91	10.71
CaO	12.21	12.28	12.27	12.00
Na_2O	2.07	1.96	2.23	1.63
K_2O	1.10	.94	1.20	1.31
Total	97.44	98.29	97.41	98.43
	Formula per 13 cations exclusive of Ca, Na, K			
Si	6.025	5.995	6.014	6.285
Al^{IV}	1.975	2.005	1.986	1.715
Al^{VI}	.490	.485	.493	.432
Ti	.188	.193	.182	.170
Fe^{3+}	.523	.601	.350	.423
Fe^{2+}	.678	.813	1.316	1.554
Mn	.015	.028	.021	.058
Mg	3.106	2.879	2.639	2.362
Ca	1.900	1.905	1.955	1.903
Na(B)	.100	.095	.045	.097
Na(A)	.482	.455	.597	.370
K	.204	.174	.227	.247
$\frac{Mg}{(Mg+Fe^{2+}+Mn)}$	.818	.774	.664	.594

* Total iron as FeO; Fe^{3+} and Fe^{2+} calculated from charge balance.

mineral assemblages and crystallization sequence to products of hydrous melting and crystallization experiments using natural basaltic compositions. These factors are discussed in detail below.

The sequence of appearance of cumulus phases and the mineral chemical depletion trends indicate the following cumulate sequence for the Alaskan-type ultramafic rocks:

Olivine+chromian spinel (dunite)

Olivine+clinopyroxene±chromian spinel±phlogopite (wehrlite, olivine clinopyroxenite)

Clinopyroxene±magnetite (clinopyroxenite)

Clinopyroxene+hornblende±phlogopite±magnetite (hornblende-biotite clinopyroxenite)

Hornblende±magnetite (hornblendite).

The occurrence of gabbro at the Blashke Islands, Union Bay, and Salt Chuck indicates evolved crystallization of the cumulus assemblage:

Plagioclase+clinopyroxene±orthopyroxene± magnetite.

The crystallization order appropriate to the Alaskan-type cumulate sequence of rocks is therefore olivine + minor chromite, clinopyroxene, magnetite, hornblende, plagioclase ± orthopyroxene. This crystallization sequence, with the exception of orthopyroxene, has been duplicated by experimental studies of water-saturated and -undersaturated basaltic melts at an oxygen fugacity near that of the nickel-nickel oxide (NNO) buffer (Holloway and Burnham 1972;

Table 8. Analyses of biotite in Alaskan-type ultramafic and mafic rocks, southeastern Alaska.

[Electron microprobe analyses (in weight percent) by G.R. Himmelberg. Abbreviations given in table 2. Mg/(Mg+Fe), atomic ratio of normative silicates. -, not detected.]

	Alava Bay	Dall Island		Haines			Kane Peak		
Sample No.----	90GH02	90GH06A	90GH06C	84GH54A	84GH54B	84GH55A	81KP2A†	81KP15A	81KP14A
Rock type------	Bt Hblite	Phl Whr	Bt Hbl Cpxite	Bt Cpxite	Bt Cpxite	Hbl Cpxite	Hbl Phl Pd	Cpxite	Cpxite
SiO_2----------	37.70	39.61	38.38	37.21	37.33	36.16	40.25	39.54	37.44
TiO_2----------	1.38	.74	1.38	2.67	2.49	2.02	.37	1.86	4.21
Al_2O_3----------	15.27	15.81	16.54	17.12	16.91	16.60	14.98	15.22	16.16
FeO*----------	17.73	3.78	9.38	10.07	10.64	16.71	4.30	6.85	11.88
MnO----------	.07	.07	.07	.09	.07	.28	.02	.06	.03
MgO----------	13.31	23.86	20.12	18.96	18.77	14.64	25.68	21.64	16.37
CaO----------	.02	.05	.01	-	-	-	.03	-	-
Na_2O----------	.11	.73	.34	.47	.46	.14	.75	.52	.41
K_2O----------	9.02	8.14	9.22	9.04	9.00	9.16	9.05	9.23	9.69
Total----------	94.61	92.79	95.44	95.62	95.67	95.68	95.43	94.92	96.19
				Cations per 11 oxygens					
Si----------	2.859	2.847	2.774	2.699	2.712	2.712	2.839	2.839	2.733
Al^{IV}----------	1.141	1.153	1.226	1.301	1.288	1.288	1.161	1.161	1.267
Al^{VI}----------	.223	.187	.183	.162	.160	.178	.084	.127	.122
Ti----------	.079	.040	.075	.145	.136	.114	.020	.100	.231
Fe----------	1.124	.227	.567	.611	.646	1.048	.254	.411	.725
Mn----------	.005	.004	.004	.005	.004	.017	.001	.004	.002
Mg----------	1.504	2.557	2.168	2.049	2.032	1.636	2.700	2.316	1.780
Ca----------	.002	.004	.001	.000	.000	.000	.002	.000	.000
Na----------	.017	.102	.047	.067	.065	.020	.103	.072	.058
K----------	.872	.746	.850	.836	.834	.876	.814	.845	.960
$\frac{Mg}{(Mg+Fe)}$	.572	.918	.793	.770	.759	.610	.914	.849	.711

	Kane Peak — Continued		Port Snettisham		Salt Chuck			Union Bay
Sample No.----	81KP1B	81KP1C	87GH18A	87GH19A	86GH8A	86GH9B	86GH12A	87GH50A
Rock type------	Diorite	Hblite	Cpxite	Cpxite	Mag Cpxite	Mag Gb	Mag Gb	Bt Gbn
SiO_2----------	38.31	37.18	37.63	36.95	36.64	35.76	36.26	36.43
TiO_2----------	2.06	1.99	1.87	2.01	4.03	3.70	3.58	4.27
Al_2O_3----------	17.84	17.56	17.75	17.35	16.55	16.93	17.10	15.50
FeO*----------	13.85	16.79	8.34	10.67	10.99	12.06	13.04	20.22
MnO----------	.32	.15	.06	.09	.17	.19	.20	.16
MgO----------	14.04	12.57	21.12	18.94	17.59	17.47	16.00	10.02
CaO----------	-	-	.01	-	.04	.15	.10	.01
Na_2O----------	.36	.19	.47	.17	.62	.39	.27	.08
K_2O----------	9.24	9.76	9.99	10.14	8.56	7.90	7.72	9.60
Total----------	96.03	96.18	97.24	96.32	95.18	94.53	94.26	96.29
				Cations per 11 oxygens				
Si----------	2.804	2.769	2.674	2.684	2.683	2.642	2.689	2.766
Al^{IV}----------	1.196	1.231	1.326	1.316	1.317	1.358	1.311	1.234
Al^{VI}----------	.343	.310	.161	.169	.111	.117	.183	.153
Ti----------	.113	.111	.100	.110	.222	.205	.200	.244
Fe----------	.848	1.046	.496	.648	.673	.745	.809	1.284
Mn----------	.020	.009	.003	.006	.011	.012	.013	.010
Mg----------	1.532	1.395	2.237	2.051	1.919	1.924	1.768	1.134
Ca----------	.000	.000	.001	.000	.003	.012	.008	.001
Na----------	.052	.027	.065	.023	.088	.056	.039	.011
K----------	.862	.927	.906	.939	.799	.744	.730	.930
$\frac{Mg}{(Mg+Fe)}$	.644	.572	.819	.760	.740	.721	.686	.469

† NiO=0.16.
* Total iron as FeO.

Table 9. Analyses of chromian spinel in Alaskan-type ultramafic and mafic rocks, southeastern Alaska.

[Electron microprobe analyses (in weight percent) by G.R. Himmelberg. Blashke Islands analyses from Himmelberg and others (1986b). Abbreviations given in table 2. Cr/(Cr+Al), Mg/(Mg+Fe^{2+}), Fe^{3+}/(Cr+Al+Fe^{3+}), atomic ratios of normative silicates. n.d., not determined.]

	Blashke Islands								Dall Island	Kane Peak	
Sample No.----	80BI37	80BI5	80BI6	80BI43	80BI10	80BI12	80BI44	80BI13	90GH6A	81SK046A	81SK048A
Rock type------	Du	Du	Du	Du	Du	Du	Whr	Ol Cpxite	Whr	Whr	Du
SiO_2----------	n.d.	n.d.	n.d.	n.d.	n.d.	n.d.	n.d.	n.d.	0.03	0.03	0.02
TiO_2----------	0.38	0.44	0.57	0.44	0.60	0.96	0.83	0.58	1.03	.64	.89
Al_2O_3----------	12.00	11.90	11.20	11.40	20.00	18.60	18.70	16.40	10.92	7.35	8.00
Cr_2O_3----------	45.80	43.60	40.20	38.90	31.60	30.10	28.80	33.40	29.02	49.20	46.05
Fe_2O_3----------	13.18	14.91	18.02	19.95	17.82	19.79	20.62	17.25	27.99	11.77	14.63
FeO*----------	17.73	18.97	20.96	21.13	20.35	21.77	22.42	24.66	22.73	22.63	22.34
MnO----------	1.26	1.40	1.29	1.27	1.03	1.23	1.12	1.19	3.30	.48	.48
MgO----------	9.93	9.03	7.71	7.72	9.38	8.38	7.85	5.76	5.52	6.64	7.18
Total--------	100.27	100.25	99.96	100.81	100.78	100.83	100.34	99.24	100.52	98.76	99.59
Formula normalized to 3 cations											
Si----------	n.d.	n.d.	n.d.	n.d.	n.d.	n.d.	n.d.	n.d.	0.00	0.001	0.001
Ti----------	0.009	0.011	0.014	0.011	0.014	0.023	0.020	0.015	.03	.017	.023
Al----------	.465	.465	.444	.449	.750	.706	.716	.649	.44	.301	.324
Cr----------	1.190	1.142	1.070	1.027	.795	.767	.740	.886	.78	1.354	1.250
Fe^{3+}----------	.326	.372	.457	.502	.427	.480	.504	.436	.72	.309	.378
Fe^{2+}----------	.488	.526	.591	.591	.542	.587	.609	.693	.65	.660	.643
Mn----------	.035	.039	.037	.036	.028	.034	.031	.034	.10	.014	.014
Mg----------	.487	.446	.387	.384	.445	.403	.380	.288	.28	.344	.367
$\frac{Cr}{(Cr+Al)}$	.719	.711	.707	.696	.515	.521	.508	.577	.642	.818	.794
$\frac{Mg}{(Mg+Fe^{2+})}$	.499	.459	.396	.394	.451	.407	.384	.294	.309	.343	.363
$\frac{Fe^{3+}}{(Cr+Al+Fe^{3+})}$	.165	.188	.232	.254	.216	.246	.257	.221	.371	.157	.194

	Kane Peak— Continued						Red Bluff Bay		Union Bay		
Sample No.-----	81SK043A	81KP7A	81KP5A	81KP17A	81SK045A	81KP23A	90GH15B	90GH16A	87GH34A	87GH27B	87GH27A
Rock type-------	Whr	Du	Hbl Phl Pd	Whr	Du	Ol Cpxite	Cpxite	Du	Whr	Du	Du
SiO_2----------	0.03	0.03	0.03	0.03	0.01	0.01	0.00	0.00	0.00	0.00	0.00
TiO_2----------	.71	.36	.58	.61	1.54	2.82	.20	.34	.79	.68	1.10
Al_2O_3----------	8.77	9.22	9.24	10.34	10.50	8.01	16.18	22.01	8.73	8.99	8.40
Cr_2O_3----------	48.65	45.83	44.92	47.46	38.02	28.47	46.23	36.65	42.76	43.85	36.89
Fe_2O_3----------	10.64	12.52	11.60	10.13	17.56	28.01	6.41	10.55	18.02	16.23	21.50
FeO*----------	23.53	24.92	27.10	24.68	26.74	28.67	24.05	22.13	22.52	22.06	25.93
MnO----------	.51	.60	.81	.61	.54	.43	.67	.60	.46	.48	.46
MgO----------	6.32	5.03	3.44	5.68	4.92	4.30	6.59	8.66	7.23	7.31	4.82
Total----------	99.15	98.50	97.72	99.54	99.83	100.72	100.33	100.94	100.51	99.60	99.10
Formula normalized to 3 cations											
Si----------	0.001	0.001	0.001	0.001	0.000	0.000	0.000	0.000	0.000	0.000	0.000
Ti----------	.018	.009	.016	.016	.040	.074	.005	.008	.020	.018	.029
Al----------	.356	.380	.388	.418	.427	.329	.628	.819	.350	.362	.348
Cr----------	1.328	1.269	1.267	1.287	1.037	.786	1.204	.915	1.149	1.185	1.025
Fe^{3+}----------	.277	.330	.311	.262	.456	.736	.159	.251	.461	.418	.569
Fe^{2+}----------	.680	.730	.809	.709	.772	.838	.663	.585	.641	.631	.763
Mn----------	.015	.018	.024	.018	.016	.013	.019	.016	.013	.014	.014
Mg----------	.325	.262	.183	.290	.253	.224	.323	.407	.366	.373	.253
$\frac{Cr}{(Cr+Al)}$	.789	.770	.765	.755	.708	.705	.657	.528	.767	.768	.747
$\frac{Mg}{(Mg+Fe^{2+})}$	.323	.264	.184	.291	.247	.211	.328	.411	.364	.371	.249
$\frac{Fe^{3+}}{(Cr+Al+Fe^{3+})}$	.141	.167	.158	.133	.237	.398	.080	.126	.235	.212	.293

* Total iron was determined and FeO and Fe_2O_3 was calculated from stoichiometry.

Table 10. Analyses of plagioclase in Blashke Islands Alaskan-type gabbro, southeastern Alaska.

[Electron microprobe analyses (in weight percent) from Himmelberg and others (1986b).

Sample No.----	80BI49	80BI15	80BI17	80BI28	80BI29	80BI19
Rock type------	Gbn	Gb	Hbl Gb	Ol Hbl Gbn	Hbl Px Gb	Gb
SiO_2----------	48.10	47.10	48.70	50.20	49.40	53.80
Al_2O_3----------	33.60	33.50	32.40	32.60	31.90	29.20
FeO*----------	n.d.	.40	.43	n.d.	.33	.14
MgO----------	n.d.	.06	.06	n.d.	.07	.04
CaO----------	17.20	17.40	16.00	15.10	15.30	11.60
Na_2O----------	2.03	2.10	2.82	3.16	3.26	5.37
K_2O----------	.04	.10	.12	.06	.04	.18
Total---------	100.97	100.66	100.53	101.12	100.30	100.33
			Cations per 8 oxygens			
Si----------	2.186	2.158	2.225	2.265	2.256	2.430
Al----------	1.800	1.809	1.745	1.734	1.717	1.554
Fe----------	n.d.	.015	.016	n.d.	.013	.005
Mg----------	n.d.	.004	.004	n.d.	.005	.003
Ca----------	.838	.854	.783	.730	.749	.561
Na----------	.179	.187	.250	.276	.289	.470
K----------	.002	.006	.007	.003	.002	.010
An----------	82.2	81.6	75.3	72.3	72.0	53.9
Ab----------	17.6	17.8	24.0	27.4	27.8	45.1
Or----------	.2	.6	.7	.3	.2	1.0

* Total iron as FeO

Helz, 1973). The abundance of magnetite and hornblende indicates that the magma from which the ultramafic rocks crystallized was substantially rich in Fe_2O_3 and H_2O, at least by the time magnetite and hornblende crystallized. The occurrence of cumulus magnetite as the oxide phase, crystallizing after clinopyroxene but before hornblende, suggests that the oxidation conditions of the magma at the time of crystallization were at least as high as the NNO buffer (Holloway and Burnham, 1972; Helz, 1973). At lower oxidizing conditions, the fayalite-magnetite-quartz (FMQ) buffer ilmenite is the near-liquidus phase, and its upper stability limit is lower than that of hornblende. At conditions of the hematite-magnetite (HM) buffer, Fe-Ti oxide phases are among the earliest to crystallize, but they include abundant titanohematite (Helz, 1973), which was not observed in the Alaskan-type intrusions. The substantial esseneite component of clinopyroxene in most magnetite clinopyroxenites and hornblende clinopyroxenites also suggests a relatively high oxygen fugacity during crystallization of these rocks. Variation in esseneite component of clinopyroxene and the near absence of magnetite and hornblende in the ultramafic rocks at the Blashke Islands and Kane Peak, however, indicate that the oxygen fugacity and water content probably varied among the different intrusions. Similar oxidizing conditions near the NNO buffer were reported for arc-basalt ultramafic xenoliths that have mineral assemblages similar to Alaskan-type ultramafic rocks (Arculus and Wills, 1980; Conrad and Kay, 1984).

The crystallization sequence of most of the Alaskan-type intrusions suggests that the ultramafic cumulates crystallized under pressures greater than about 3 kbar, but the upper pressure limit is not well constrained. Experimental studies of hydrous basalts at the NNO buffer have shown that at moderate to high pressures hornblende crystallizes at a temperature substantially higher than that at which plagioclase crystallizes; however, at low pressures (2–3 kbar) the upper stability of plagioclase and hornblende are relatively close, and below about 2.5 kbar plagioclase crystallizes before hornblende (Holloway and Burnham, 1972). The crystallization sequence of the Salt Chuck intrusion, where plagioclase follows magnetite, and hornblende is nearly absent, indicates that the Salt Chuck body crystallized under a pressure of 2 kbar or less (Loney and Himmelberg, 1992).

Proposed mineral composition barometers do not further constrain the pressure of crystallization. A steep increase in Al_2O_3 of clinopyroxene with differentiation (a decrease in Mg #) has been argued to indicate a high-pressure origin (Medaris, 1972; Asahina and Komatsu, 1979; Yokoyama, 1980; Ishiwatari, 1985; Ishizuka, 1985; DeBari and Coleman, 1989). Clinopyroxene in the Alaskan-type cumulates shows a moderately steep increase of Al_2O_3 with differentiation (fig. 15); however, in this case, the accommodation of Al in pyroxene is more likely related to crystallization of clinopyroxene from progressively more hydrous melts characteristic of arc magmas (Murray, 1972; Conrad and Kay, 1984; Loucks, 1990). The partitioning of Al between octahedral and

tetrahedral sites in clinopyroxene (Green and Ringwood, 1967; Aoki and Kushiro, 1968) also does not indicate high-pressure crystallization of the Alaskan-type ultramafic clinopyroxenes. Chromian spinel has also been suggested as a geobarometer because the composition becomes more Al-rich as the pressure increases (Green and others, 1971; Jaques and Green, 1980). Allan and others (1988), however, have shown that spinel compositions are also strongly dependent on small variations in host-liquid composition and thus their use as a geobarometer is limited.

The metamorphic grade of the country rock surrounding the Alaskan-type bodies indicates that the magma chambers in which the ultramafic rocks accumulated were at relatively shallow crustal levels. Mineral assemblages indicate the grade of metamorphism to be greenschist or subgreenschist facies (Brew and others, 1992). Irvine (1967a, 1974), Findlay (1969), James (1971), and Himmelberg and others (1986b) attribute the zoned character of the bodies to diapiric reemplacement following crystallization and accumulation in a deeper magma chamber. As discussed below, however, we believe the zoned character developed by flow differentiation rather than by diapiric reemplacement Even if diapiric reemplacement did occur, Irvine (1974) suggests that the upward movement of the dense ultramafic cumulates would have been limited to only a few kilometers at the very most; thus the metamorphic grade of the country rocks would still be a reasonable indicator of depth of crystallization.

On the basis of geobarometry of pelitic schist pendants, emplacement depth of the Baranof Lake pluton, which intrudes the Red Bluff Bay ultramafic body, might have been about 18 to 20 km (Himmelberg, unpub. data). However, Loney and others (1975) interpret the Red Bluff Bay body to have been tectonically emplaced at its present structural level; thus, it may have crystallized at a deeper crustal level. We note again, however, that the Red Bluff Bay body may not be an Alaskan-type complex, and its depth of crystallization may not be appropriate to constrain that of the Alaskan-type intrusions.

The temperature of crystallization of the cumulus assemblages is best estimated by comparison to the hydrous basalt melting and crystallization experiments referred to above. The liquidus temperature is not determined; however, at 5 kbar and the NNO buffer, the upper stability of magnetite is 1,085°C and the upper stability of hornblende is 1,025°C. These conditions suggest that the magnetite and hornblende clinopyroxenites and hornblendites crystallized at about this temperature range (Holloway and Burnham, 1972; Helz, 1973). On the basis of the upper stability of plagioclase, the gabbros would have begun crystallizing at about 925°C, and crystallization would have been complete at about 815°C (Holloway and Burnham, 1972). The presence of pargasite as a postcumulus phase in the olivine-rich peridotite at Kane Peak suggests that the cumulus minerals in these rocks crystallized above about 1,025°C. These temperatures increase with increase of pressure.

We conclude that the Alaskan-type ultramafic rocks crystallized from hydrous basaltic magmas at shallow crustal depths, probably in the range of 6 to 18 km. Water content and oxygen fugacity was somewhat variable among the different bodies, but the latter was probably above the NNO buffer and below the HM buffer. Crystallization temperatures ranged from above 1,025°C to about 815°C.

NATURE OF THE PARENT MAGMA

The Alaskan-type complexes have long been recognized as a distinct class of ultramafic-mafic intrusions (Noble and Taylor, 1960; Taylor and Noble, 1960; Irvine 1974), and the nature of the parental magma has long been debated. No chilled margins representing the parental magma have been found, so the original melt composition can only be inferred from consideration of cumulate sequences and from rock and mineral chemistry relative to experimental and theoretical studies. James (1971), Murray (1972), Himmelberg and others (1986b), and more recently Loucks (1990) and Loney and Himmelberg (1992) have argued that at least some of the Alaskan-type ultramafic rocks were fractionated from subalkaline orthopyroxene-normative island-arc basaltic parental magmas with the resultant production of residual basaltic and andesitic liquids. Subalkaline island-arc basaltic parental magmas for Alaskan-type ultramafic rocks were also implied by Conrad and Kay (1984) and DeBari and others (1987), who equated xenoliths in Aleutian island-arc volcanic rocks with Alaskan-type ultramafic rocks. Irvine (1967a, 1974), on the other hand, argued that the Alaskan-type ultramafic rocks were fractionated from high-calcium, high-magnesium, alkaline ultramafic parental magmas with the resulting production of residual, critically undersaturated, alkali basalts.

Our data and that of others clearly indicate that the magma that crystallized these ultramafic rocks must have been substantially rich in Fe_2O_3 by the time magnetite crystallized and that the abundance of hornblende, and commonly biotite, indicates a substantial H_2O content. Irvine (1974) argued that the parental magma must have been extremely rich in MgO and CaO to crystallize so much olivine and clinopyroxene. He further argued that, in those rocks where postcumulus minerals are abundant, the bulk rock composition should qualitatively reflect the composition of the parent magma. Alaskan-type ultramafic rocks with abundant postcumulus hornblende typically have nepheline in the norm. On the basis of experimentally determined systems, Irvine (1974) then showed that a critically undersaturated (nepheline-normative) magma would crystallize to yield the cumulate sequence of ultramafic rocks and account for the abundance of magnetite typical of Alaskan-type ultramafic rocks. Loucks (1990), however, pointed out that the experimental studies of Bowen (1928), Helz (1973), and Wones (1979) all showed that hornblende precipitated from orthopyroxene- or quartz-normative melts is generally nepheline-normative. Thus hornblende- or biotite-

bearing cumulates that crystallized from saturated hydrous magmas will commonly be feldspathoid-normative, and a nepheline-normative magma is not required.

Our preferred interpretation is that the mineral assemblages, the crystallization sequence, and the rock and mineral chemistry all indicate fractionation from a silica-saturated, hypersthene-normative parental magma similar to those that yield island-arc basalts. Although modal orthopyroxene is not common in many Alaskan-type ultramafic rocks, it does occur in trace amounts in wehrlite and olivine clinopyroxenite at the Blashke Islands and is common as a postcumulus phase along with hornblende and phlogopite in some peridotites at Kane Peak. Most importantly, as discussed above, the ultramafic rock mineral assemblages and crystallization sequence are duplicated by crystallization experiments of hydrous silica-saturated basaltic melts having an oxygen fugacity near that of the NNO buffer (Holloway and Burnham, 1972; Helz, 1973). Hornblende in the hornblende clinopyroxenites is typically feldspathoid normative, as noted in the experimental studies of Helz (1973), and the clinopyroxene compositions change from hypersthene normative to feldspathoid-normative with fractionation. The clinopyroxenes become feldspathoid normative with fractionation, owing to an increase in the esseneite component as a result of the hydrous oxidizing nature of the magma. Loucks (1990) argued that in a hydrous and oxidizing basaltic magma the activity of enstatite component would be depressed and the activities of the aluminous pyroxene components in the melt would be raised, promoting crystallization of olivine and clinopyroxene and yielding wehrlite and olivine clinopyroxenite in place of gabbronorite in early cumulate sequences. This crystallization order has the added consequence of enhancing the alumina and silica content of progressive residual liquids thus leading to crystallization of high-alumina basalts common to an arc crust (Loucks, 1990). The increasing alumina content of clinopyroxene with fractionation, the steep trend of the Al:Ti ratio in clinopyroxene in Alaskan-type bodies (fig. 16) and other rocks from island-arc environments (Loucks, 1990), and the crystallization of hornblende support this interpretation. Fractionation of ultramafic cumulates has been proposed by Conrad and Kay (1984) and by Kay and Kay (1985a, b) as the mechanism of deriving high-alumina basalt magmas.

The more evolved rocks associated with the Tulameen complex in British Columbia range from gabbro to syenitic (Findlay, 1969). In the Sierra Nevada and Klamath Mountains, California, however, James (1971) and Snoke and others (1981, 1982) documented a genetic relation between ultramafic bodies having Alaskan-type characteristics and mafic rocks ranging from olivine gabbro, through gabbronorite, to diorite, tonalite, and granodiorite. Irvine (1974) questioned, however, whether such occurrences are truly Alaskan-type complexes because of their obvious fractionation from saturated magmas and his conviction that the Alaskan-type bodies were derived from undersaturated magmas. Gabbros are also associated with classic Alaskan-type complexes at Duke Island, Blashke Islands, Union Bay, and Salt Chuck. As pointed out above, at Duke Island the gabbros are obviously older than the ultramafic rocks and need not be considered in the petrogenesis of that complex. At Union Bay the mafic rocks are dominantly gabbronorite and form an outermost zone about the ultramafic rocks. Biotite and hornblende from the gabbroic rocks yield K/Ar ages of 101 to 110 Ma (M.A. Lanphere, written commun., 1990), and similar ages of Alaskan-type ultramafic rocks (Lanphere and Eberlein, 1966; M.A. Lanphere, written commun., 1990) suggest that the gabbroic rocks and ultramafic rocks are genetically related and were fractionated from a subalkaline, saturated parental magma. At the Blashke Islands, two-pyroxene gabbros also form an outermost zone of the ultramafic complex. These gabbroic rocks grade from pyroxene gabbro at the contact with olivine clinopyroxenite to hornblende gabbro near the periphery. These gabbroic rocks have not been dated by isotopic methods, but Himmelberg and others (1986b) argued that they are crystallization products of the same magma that had fractionated the ultramafic rocks. At Salt Chuck, magnetite clinopyroxenite and magnetite gabbro represent a continuous sequence, which Loney and Himmelberg (1992) interpreted to have been fractionated from hydrous, saturated basaltic parental magma.

Irvine (1967a,1974), Murray (1972), and Himmelberg and others (1986b) all proposed that the Alaskan-type ultramafic complexes accumulated in subvolcanic magma chambers. Murray (1972) and Irvine (1974) tried to draw correlations between the Alaskan-type ultramafic complexes and associated volcanic rocks as evidence for parental magma type, however these arguments remain inconclusive. In southeastern Alaska the volcanic rocks of the Gravina-Nutzotin belt of Berg and others (1972) form a discontinuous belt nearly coincident with the Klukwan-Duke mafic-ultramafic belt. Berg and others (1972) indicated that these volcanic rocks were dominantly andesite. However, studies by Irvine (1973) and Ford and Brew (1988) indicate that these volcanic rocks, at least in the vicinity of Juneau, Alaska, are basaltic and include high-potassium basalt. The generally accepted age of these volcanic rocks is Jurassic to Cretaceous (Buddington and Chapin, 1929; Lathram and others 1965; Berg and others, 1972), but recent studies by H. Cohen (written commun., 1992) suggest that they are mid-Cretaceous in age. Irvine (1973; 1974) argued that they are possibly related as part of the same petrologic province and could have been derived from the same alkaline parental magma type. Mortimer (1986) and Nixon and Rublee (1988) have suggested that the Tulameen Alaskan-type complex is coeval with the volcanic rocks of the Upper Triassic Nicola Group in British Columbia, Canada. These volcanic rocks are also island-arc related, clinopyroxene-phyric, calc-alkaline to shoshonitic lavas (Mortimer, 1986). Similarly, Alaskan-type complexes in New South Wales are part of a belt of Ordovician shoshonitic volcanic and associated intrusive rocks (Derrick, 1991). Remarkably similar compositions of clinopyroxene phenocrysts in

the Douglas Island Volcanics (Himmelberg, unpub. data) and clinopyroxene in the ultramafic complexes support the argument that these two rock groups may be genetically related. As discussed above, however, these pyroxene compositions are compatible with crystallization from a hydrous basaltic magma. Thus, as mentioned above, arguments about parental magma type based on possible coeval volcanic rock compositions remain inconclusive.

The older 400- to 440-Ma Alaskan-type complexes in southern southeastern Alaska were emplaced into a volcanic-arc environment (Gehrels and Saleeby, 1987). Volcanic rocks of the Descon Formation consist of basalts and andesites and were extruded during the Early Ordovician through the Early Silurian (Gehrels and Saleeby, 1987). The Salt Chuck body is intruded into the Descon Formation (Loney and Himmelberg, 1992) so, as with the younger Alaskan-type complexes and associated volcanics, there is the possibility that the exposed volcanic rocks may be somewhat older than the ultramafic-mafic complex.

Our current preferred interpretation is that all of the Alaskan-type ultramafic complexes are cumulates that fractionated from a hydrous subalkaline island-arc basaltic magma. Himmelberg and others (1986b), in contrast, suggested that all the Alaskan-type complexes may not have been derived from the same parent magma type. Reexamination of all the characteristics of all the bodies, including REE patterns, indicates that they are so similar that a common parent magma composition seems most reasonable. The Mg-rich olivine in Alaskan-type dunite and wehrlite suggests that the parental melt was an unfractionated mantle-derived melt. The high Cr # of the chromian spinel suggests equilibrium of the magma with a mantle peridotite that underwent a high degree of melting (Dick and Bullen, 1984). Although the exact composition of the primary melt is uncertain, we suggest it was possibly similar to the hydrous olivine basalt primary magma proposed for the Aleutian island-arc lavas (Perfit and others, 1980; Kay and others, 1982; Nye and Reid, 1986; Conrad and Kay, 1984; DeBari and others, 1987). This suggestion is based on the similarities of mineralogy, texture, and rock and mineral chemistry of the Alaskan-type ultramafic rocks and gabbros and Aleutian island-arc xenoliths and plutonic gabbros described by Perfit and others (1980), Kay and others (1983), Conrad and Kay (1984), and DeBari and others (1987). The $^{87}Sr/^{86}Sr$ ratio in Alaskan-type ultramafic rocks ranges from 0.702 to 0.705 (Lanphere, 1968), which is within the range for Aleutian island-arc plutonic and volcanic rocks and xenoliths (Kay and others, 1986; 1990). At Salt Chuck the magnetite clinopyroxenite is intruded by a diabase dike that has an appropriate chemical composition, Mg #, and redox state to represent a plausible parental liquid for the Salt Chuck mineral assemblages (Loney and Himmelberg, 1992). The diabase dike is hypersthene-normative and somewhat similar in chemical composition to the 1921 Kilauea olivine tholeiite used in the hydrous experiments of Holloway and Burnham (1972) and Helz (1973).

INTRUSIVE MECHANISM AND ZONAL STRUCTURE

Researchers generally agree that Alaskan-type ultramafic complexes originated by fractional crystallization and accumulation in subvolcanic magma chambers or feeder conduits (Irvine, 1967a, 1974; Murray, 1972; Himmelberg and others (1986b). However, there are differences of opinion on the primary processes responsible for the magmatic differentiation and zonal structure. Murray (1972) proposed that the zoned Alaskan-type ultramafic intrusions originated by crystal fractionation and flow differentiation of basaltic magma in the feeder pipes of volcanoes, whereas Irvine (1974) proposed that in most cases the zonal structure is a result of diapiric reemplacement of stratiform sequences of cumulates.

On the basis of field relations and heat-flow models, Irvine (1974) argued that flow differentiation would not be an effective process for producing the zonal structures in intrusions as large as the Duke Island, Union Bay, and Tulameen bodies. He believed that any effect of flow differentiation would be obliterated by convection and crystal settling. Irvine proposed instead that the sequence of ultramafic rocks in Alaskan-type complexes accumulated in subvolcanic magma chambers by crystal fractionation and crystal settling to form rudely stratiform complexes and that the zonal structure was produced by later diapiric reemplacement caused by tectonic compression. Irvine (1974) explains the absence of widespread deformation to the presence of intercumulus liquid during diapiric emplacement, which is represented by undeformed postcumulus minerals.

The mechanism of flow differentiation is a well-established hydraulic process that has been studied since 1825 for many compound liquids, such as printing ink, coal slurries, and melted chocolate. Flow differentiation was first considered as a magmatic process to explain structures in the Labrador Trough of Canada (Baragar, 1960), the Skye picritic dikes and sills of Scotland (Bhattacharji and Smith, 1964), and the Muskox intrusion of Canada (Simkin 1967). Bhattacharji and Smith (1964) showed experimentally that the type of monomineralic segregation and cryptic zonation found in picritic dikes of Skye, and also in the feeder dike of the Muskox intrusion, could be produced by magmatic flowage differentiation. In the Muskox intrusion only the vertical feeder dike shows zonation; the main part of the body, the subhorizontal central-layered series, is typical of layered cumulates developed largely by fractional crystallization and crystal settling (Smith 1962; Irvine and Smith, 1967).

Murray (1972) attributed the zonal structure of Alaskan-type ultramafic rocks to the flow differentiation model as developed by Bhattacharji and Smith (1964) and Bhattacharji (1967a). According to this model, during flow through a conduit, segregation takes place by particles in liquid moving away from the walls toward the central axis and then parallel to the axis. Thus in a vertical conduit containing

rising mafic magma, early-formed Mg-rich olivine crystals move from the wall toward the center where they form an olivine-rich rock. The olivine is followed by pyroxene, plagioclase, and so on, as crystallization proceeds. Because of fractional crystallization, individual minerals would also show characteristic trends in chemical composition. As upward movement of the magma and core continues, further crystallization and flow differentiation would develop a zonal sequence of rocks similar to that of the Alaskan-type ultramafic complexes. Postintrusion crystal settling is minor because of the high viscosity of the concentration (Bhattacharji and Smith, 1964; Shaw, 1965). Murray (1972) suggested that the gabbros commonly associated with, and in some cases apparently intruded by, the ultramafic rocks could represent solidification of derived magmas that were later intruded by the continually rising and crystallizing ultramafic core. Bhattacharji (1967a, b) also showed, through a carefully scaled experiment, that the zoned configuration created in a feeder conduit can continue into a sill. The resulting zoned geometry is remarkably similar to the interpretation shown in figure 4 for the Union Bay intrusion as constructed by Ruckmick and Noble (1959, pl. 4) and supported by our work.

The extent of flow differentiation in basaltic magma feeder conduits, dikes, and sills is dependent on the velocity of flow and viscosity of the magma. If velocity decreases or viscosity increases to critical values, flow differentiation decreases and other processes such as gravity settling or current modifications may prevail (Simkin, 1967; Bhattacharji, 1967a, b). Texturally, on the basis of the present data, it does not seem possible to distinguish gravity and current-modified gravity cumulates from products of flow differentiation. The main evidence for flow differentiation is on a larger scale, namely the symmetrical arrangement of layering in pipes, dikes, and sills, such as at Blashke Islands, Union Bay (fig. 4), and at Skye (Bhattacharji and Smith, 1964), which cannot be explained by gravity settling.

The Alaskan-type bodies display both gradational and sharp, in some cases intrusive, contacts between the various rock types. Both Murray (1972) and Irvine (1974) argued that these relations can be explained by flow differentiation as the major process and by diapiric reemplacement. Other than at Duke Island, possible large Alaskan-type in situ cumulus bodies are lacking in southeastern Alaska. Although we have no direct evidence to document the exact nature of emplacement and development of zonal structure in the Alaskan-type ultramafic bodies, we prefer the flow differentiation interpretation proposed by Murray (1972). The common symmetrical nature of the distribution of rock types for the size of most of the intrusions is compatible with the flow differentiation model. The olivine petrofabrics of the Union Bay body are attributed to regional tectonic recrystallization. The data suggest that the Kane Peak body was possibly intruded during that regional deformation event, but the olivine microfabric retains an igneous signature. The ultramafic body at the Blashke Islands shows no evidence of being involved in deformation of the western metamorphic belt. Both the Kane Peak and Blashke Islands intrusions appear to be subvertical cylindrical structures that contain subvertical olivine microfabrics suggestive of subvertical magmatic flow. Some of these features could be produced by diapiric emplacement as well as by flow differentiation, but there is little data on the details of magmatic diapiric emplacement and how to distinguish it from flow differentiation intrusion.

In keeping with the flow differentiation proposal, we attribute the variations in character of the various Alaskan-type intrusions to different degrees of interaction of flow, gravity settling, and current activity. The Duke Island body shows little evidence of flow differentiation. Magma was emplaced into a relatively large chamber in which the velocity decreased as the chamber filled, thus, gravity settling along with density-current activity prevailed, as in the main part of the Muskox intrusion. The Union Bay body illustrates a vertical zoned conduit that extends into a moderately sized, zoned, nappe-like sill. Open folding about subvertical northwest-striking axial planes related to regional metamorphism deform the nappe-like structure, but it seems likely that the nappe itself, with its symmetrical intricate zonation, was caused by the flow differentiation discussed above. The Kane Peak body, although disturbed by later granitic intrusion, retains its igneous character. Because of the subvertical macroscopic and microscopic structural orientation in both the Blashke Islands and Kane Peak bodies, we believe they represent sections through zoned subvertical conduits. According to Robertson (1956), the Klukwan intrusion is a subvertical mass and probably represents a zoned conduit or dike, but details are lacking. Most of the other bodies are generally too small and poorly exposed to yield diagnostic information.

Gabbro and ultramafic rock relations also differ somewhat in the different intrusions. At the Blashke Islands the prominent flow banding in the peripheral gabbro indicates that it moved upward with the ultramafic rocks, as part of the flow-differentiation process. At Union Bay, however, the gabbro could represent a derived liquid that crystallized at a level above the ultramafic rocks and was subsequently intruded by the continuing upward-moving ultramafic core, as proposed in the model of Murray (1972). At Salt Chuck the gradational cumulus relations between the ultramafic rocks and the gabbro, and the absence of zonation, suggest crystal settling in a small static magma chamber.

CONCLUSIONS

Our study reaffirms that those bodies referred to as Alaskan-type complexes are a distinct class of ultramafic-mafic intrusions. They are characterized primarily by their tectonic setting, rock types, rock chemistry including REE, and mineral chemistry. The Alaskan-type complexes are cumulates formed from a basaltic magma by crystal-fractionation and mineral-concentration processes. They are characterized by Mg-rich olivine, diopsidic to augitic clinopyroxene, magne-

tite, and hornblende. Clinopyroxene in the later differentiates (magnetite clinopyroxenite and hornblende clinopyroxenite) generally have a substantial esseneite component which is a result of the hydrous, oxidizing nature of the magma. Orthopyroxene and plagioclase are rare in the ultramafic rocks but are locally common in associated gabbros. Some of the larger complexes are crudely zoned, with dunite in the core and wehrlite, olivine clinopyroxenite, magnetite clinopyroxenite, hornblende clinopyroxenite, and in some cases hornblendite and gabbro occurring successively outward. However, zoning is not universal and is not a criterion for recognition of Alaskan-type intrusions. Many of the bodies consist of only hornblende clinopyroxenite or hornblendite. Irvine (1974) implied that the term "Alaskan-type complex" should be restricted to those bodies that fractionated from an alkaline ultrabasic liquid. We disagree strongly because an argument can be made that most bodies recognized as Alaskan-type complexes were fractionated from a hydrous, saturated basaltic magma, and we do not believe the definition of an Alaskan-type complex should be restricted on the basis of parental magma composition at this time.

The Alaskan-type complexes in southeastern Alaska fall into two distinct age groups—about 400 to 440 Ma and 100 to 118 Ma. Both groups occur in island-arc petrologic-tectonic environments, and their distribution suggests an eastward migration of arc-basaltic magmatism. The intrusion of the Alaskan-type complexes is part of a long-lived magmatic, metamorphic, and tectonic evolution of the convergent continental margin of southeastern Alaska and western Canada. The similarity of rock and mineral chemistry, including chondrite-normalized REE patterns for individual rock types from the different bodies, suggests that the parent magmas and conditions of crystallization for all the bodies were similar. The mineral chemistry and phase equilibria of the ultramafic rocks suggest that they crystallized and accumulated in magma chambers at depths ranging from about 6 to 18 km. We found no evidence that suggests deep crustal levels (30–35 km) as proposed for other island-arc ultramafic-mafic bodies and xenoliths associated with island-arc basalts. Although not conclusive, most of the field, petrographic, and chemical characteristics suggest to us that most of the bodies in southeastern Alaska crystallized from hydrous island-arc-basalt primary magmas. Furthermore, the petrographic and chemical similarities of the rocks in the Alaskan-type complexes and the Aleutian island-arc xenoliths and plutonic gabbros suggest that the parental magmas for the Alaskan-type ultramafic-mafic bodies were similar to the parental magmas proposed for island-arc basalts and andesites.

Irvine (1974) proposed that the zonal structure is a result of diapiric reemplacement of stratiform sequences of cumulates. We found no evidence for diapiric reemplacement. Instead, we believe that the zonal structure is a result of crystal fractionation and flow differentiation in subvolcanic conduits and sills, which is consistent with the proposal of Murray (1972). We attribute the variations in character of the various Alaskan-type complexes to the size of the bodies, which affected whether flow differentiation or gravity settling was dominant, and to the level of exposure.

Although the Red Bluff Bay intrusion on Baranof Island has been included by some as an Alaskan-type complex and is discussed in this report, evidence suggests that it should not be classified as an Alaskan-type complex.

REFERENCES CITED

Albee, A.L., and Ray, Lily, 1970, Correction factors for electron probe microanalysis of silicates, oxides, carbonates, phosphates, and sulfates: Analytical Chemistry, v. 42, p. 1408–1414.

Allan, J.F., Sack, R.O., and Batiza, Rodey, 1988, Cr-rich spinels as petrogenetic indicators: MORB-type lavas from the Lamont seamount chain, eastern Pacific: American Mineralogist, v. 73, p. 741–753.

Aoki, Ken-ichiro, and Kushiro, Ikuo, 1968, Some clinopyroxenes from ultramafic inclusions in Dreiser Weiher, Eifel: Contributions to Mineralogy and Petrology, v. 18, p. 326–337.

Arculus, R.J., and Wills, K.J.A., 1980, The petrology of plutonic blocks and inclusions from the Lesser Antilles island arc: Journal of Petrology, v. 21, p. 743–799.

Asahina, T., and Komatsu, M., 1979, The Horokanai ophiolitic complex in the Kamuikotan tectonic belt, Hokkaido, Japan: Geological Society of Japan Journal, v. 85, no. 6, p. 317–330.

Avé Lallemant, H.G., 1975, Mechanisms of preferred orientations of olivine in tectonic peridotite: Geology, v. 3, p. 653–656.

Baragar, W.R.A., 1960, Petrology of basaltic rocks in part of the Labrador trough: Geological Society of America Bulletin, v. 71, p. 1589–1644.

Bence, A.E., and Albee, A.L., 1968, Empirical correction factors for the electron microanalysis of silicates and oxides: Journal of Geology, v.76, p. 382–403.

Berg, H.C., Jones, D.L., and Coney, P.J., 1978, Map showing pre-Cenozoic tectonostratigraphic terranes of southeastern Alaska and adjacent areas: U.S. Geological Survey Open-File Report 78–1085, 2 sheets, scale 1:1,000,000.

Berg, H.C., Jones, D.L., and Richter, D.H., 1972, Gravina-Nutzotin belt—Tectonic significance of an upper Mesozoic sedimentary and volcanic sequence in southern and southeastern Alaska, *in* Geological Survey Research 1972: U.S. Geological Survey Professional Paper 800–D, p. D1–D24.

Bhattacharji, Somdev, 1967a, Mechanics of flow differentiation in ultramafic and mafic sills: Journal of Geology, v. 75, p. 101–112.

Bhattacharji, Somdev, 1967b, Scale model experiments on flowage differentiation in sills, Part 3.IV *in* Wyllie, P.I, ed., Ultramafic and related rocks: New York, John Wiley, p. 69–70 .

Bhattacharji, Somdev, and Smith, C.H., 1964, Flowage differentiation: Science, v. 145, p. 150–153.

Bowen, N.L., 1928, The evolution of the igneous rocks: Princeton, N. J., Princeton University Press, 334 p.

Brew, D.A., 1990, Plate-tectonic setting of Glacier Bay National Park and Preserve and Admiralty Island National Monument, southeastern Alaska, *in* Milner, A.M. ed., Second Glacier Bay Science Symposium Proceedings: U.S. National Park Service Science Publications Office, Atlanta, Ga. p. 1–5.

Brew, D.A., and Ford, A.B., 1984, Tectonostratigraphic terranes in

the Coast plutonic-metamorphic complex, southeastern Alaska, *in* Reed, K.M., and Bartsch-Winkler, Susan, eds., The United States Geological Survey in Alaska: accomplishments during 1982: U.S. Geological Survey Circular 939, p. 90–93.

Brew, D.A., and Ford, A.B., 1985, Southeastern Alaska coincident zone, *in* Bartsch-Winkler, Susan, ed., The United States Geological Survey in Alaska: accomplishments during 1984: U.S. Geological Survey Circular 967, p. 82–86.

Brew, D.A., Ford, A.B., and Himmelberg, G.R., 1989, Evolution of the western part of the Coast plutonic—metamorphic complex, southeastern Alaska, U.S.A.: a summary, *in* Daly, J.S., Cliff, R.A., and Yardley, B.W.D., eds., Evolution of metamorphic belts: London, Geological Society Special Publication 43, p. 447–452.

Brew, D.A., and Grybeck, D.J., 1984, Geology of the Tracy Arm–Fords Terror Wilderness Study Area and vicinity, Alaska, *in* Mineral resources of the Tracy Arm–Fords Terror Wilderness Study Area and vicinity, Alaska: U.S. Geological Survey Bulletin 1525–A, p. 19–52.

Brew, D.A., Himmelberg, G.R., Ford, A.B., and Jachens, R.C., 1987, Ultramafic and mafic sills in the vicinity of the Treadwell gold deposits, Douglas Island, southeastern Alaska, *in* Hamilton, T.D., and Galloway, J.P., eds., Geologic studies in Alaska by the U.S. Geological Survey during 1986: U.S. Geological Survey Circular 998, p. 119–123.

Brew, D.A., Himmelberg, G.R., Loney, R.A., and Ford, A.B., 1992, Distribution and characteristics of metamorphic belts in the south-eastern Alaska part of the North American Cordillera: Journal of Metamorphic Geology, v. 10, p. 465–482.

Brew, D.A., Karl, S.M., Barnes, D.F., Jachens, R.C., Ford, A.B., and Horner, Robert, 1991, A northern Cordilleran ocean-continent transect: Sitka Sound, Alaska, to Atlin Lake, British Columbia: Canadian Journal of Earth Sciences, v. 28, 840–853.

Brew, D.A., and Morrell, R.P., 1983, Intrusive rocks and plutonic belts of southeastern Alaska, U.S.A., *in* Roddick, J.A., ed., Circum-Pacific plutonic terranes: Geological Society of America Memoir 159, p. 171–193.

Brew, D.A., Ovenshine, A.T., Karl, S.M., and Hunt, S.J., 1984, Preliminary reconnaissance geologic map of the Petersburg and parts of the Port Alexander and Sumdum 1:250,000 quadrangles, southeastern Alaska: U.S. Geological Survey Open-File Report 84–405, 43 p.

Brothers, R.N., 1959, Flow orientation of olivine: American Journal of Science, v. 257, p. 574–584.

Brothers, R.N., 1964, Petrofabric analyses of Rhum and Skaergaard layered rocks: Journal of Petrology, v. 5, p. 255–274.

Buddington, A.F., and Chapin, Theodore, 1929, Geology and mineral deposits of southeastern, Alaska: U.S. Geological Survey Bulletin 800, 398 p.

Burns, L.E., 1985, The Border Ranges ultramafic and mafic complex, south-central Alaska: cumulate fractionates and island-arc volcanics: Canadian Journal of Earth Sciences, v. 22, p. 1020–1038.

Burrell, P.D., 1984, Cretaceous plutonic rocks, Mitkof and Kupreanof Islands, Petersburg quadrangle, southeast Alaska, *in* Coonrad, W.L., and Elliot, R.L., eds., The United States Geological Survey in Alaska: accomplishments during 1981: U.S. Geological Survey Circular 868, p. 124–126.

Carter, N.L. , and Ave´ Lallemant, H.G., 1970, High temperature flow of dunite and peridotite: Geological Society of America Bulletin, v. 81, p. 2181–2202.

Clark, Thomas., 1980, Petrology of the Turnagain ultramafic complex, northwestern British Columbia: Canadian Journal of Earth Sciences, v.17, p. 744–757.

Coleman, R.G., 1977, Ophiolites; ancient oceanic lithosphere?; Vol. 12 *of* Minerals and rocks: New York, Springer-Verlag, 229 p.

Coleman, R.G., and Keith, T.E., 1971, A chemical study of serpentinization—Burro Mountain, California: Journal of Petrology, v. 12, p. 311–328.

Conrad, W.K., and Kay, R.W., 1984, Ultramafic and mafic inclusions from Adak Island: crystallization history, and implications for the nature of primary magmas and crustal evolution in the Aleutian arc: Journal of Petrology, v. 25, p. 88–125.

DeBari, S.M., and Coleman, R.G., 1989, Examination of the deep levels of an island arc: evidence from the Tonsina ultramafic-mafic assemblage, Tonsina, Alaska: Journal of Geophysical Research, v. 94-B, p. 4373–4391.

DeBari, S.M., Kay, S.M., and Kay, R.W., 1987, Ultramafic xenoliths from Adagdak volcano, Adak, Aleutian Islands, Alaska: deformed igneous cumulates from the Moho of an island arc: Journal of Geology, v. 95, p. 329–341.

Den Tex, E. ,1969, Origin of ultramafic rocks, their tectonic setting and history: a contribution to the discussion of the paper "The origin of ultramafic and ultrabasic rocks" by P.J. Wyllie: Tectonophysics, v. 7, p. 457–488.

Derrick, G.M., 1991, Geology and economic potential of the Tout Complex, NSW, *in* Elliott, S.J., and Martin, A.R., eds., Geology and mineralization of the Fifield platinum province, New South Wales—Sixth International Platinum Symposium, Perth, Western Australia, Guidebook for the pre-symposium field excursion: Perth, Western Australia, Geological Society of Australia, p. 24–34.

Dick, H.J.B., and Bullen, Thomas, 1984, Chromian spinel as a petrogenetic indicator in abyssal and alpine-type peridotites and spatially associated lavas: Contributions to Mineralogy and Petrology, v. 86, p. 54–76.

Douglass, S.L., and Brew, D.A., 1985, Polymetamorphism in the eastern Petersburg quadrangle, southeastern Alaska, *in* Bartsch-Winkler, Susan, ed., The United States Geological Survey in Alaska: accomplishments during 1984: U.S. Geological Survey Circular 967, p. 89–92.

Elliott, S.J., and Martin, A.R., 1991, Geology and mineralization of the Fifield platinum province, New South Wales—Sixth International Platinum Symposium, Perth, Western Australia, Guidebook for the pre-symposium field excursion: Perth, Western Australia, Geological Society of Australia, 42 p.

Elthon, Don., Casey, J.F., and Komor, S., 1982, Mineral chemistry of ultramafic cumulates from the North Arm Mountain massif of the Bay of Islands ophiolite: evidence from high-pressure crystal fractionation of oceanic basalts: Journal of Geophysical Research, v. 87-B, p. 8717–8734.

Engi, Martin, 1983, Equilibria involving Al-Cr spinel: Mg-Fe exchange with olivine. Experiments, thermodynamic analysis, and consequences for geothermometry: American Journal of Science, v. 283-A, p. 29–71.

Evans, B.W., and Frost, B.R., 1975, Chrome-spinel in progressive metamorphism—A preliminary analysis: Geochimica et Cosmochimica Acta, v. 39, p. 959–972.

Fabriès, Jacques, 1979, Spinel-olivine geothermometry in peridotites from ultramafic complexes: Contributions to Mineralogy and Petrology, v. 69, p. 329–336.

Findlay, D.C., 1969, Origin of the Tulameen ultramafic-gabbro complex, southern British Columbia: Canadian Journal of Earth Sciences, v. 6, p. 399–425.

Floss, Christine, and Crozaz, Ghislaine, 1991, Ce anomalies in the LEW85300 eucrite: evidence for REE mobilization during Antarctic weathering: Earth and Planetary Science Letters, v. 107, p. 13–24.

Ford, A.B., and Brew, D.A., 1988, Major-element geochemistry of metabasalts of the Juneau-Haines region, southeastern Alaska, *in* Galloway, J.P., and Hamilton, T.P, eds., Geological studies in Alaska by the U.S. Geological Survey during 1987: U.S. Geological Survey Circular 1016, p. 150–155.

Ford, A.B., and Brew, D.A., 1993, Geochemical character of upper Paleozoic and Triassic greenstone and related metavolcanic rocks of the Wrangellia terrane in northern southeastern Alaska, *in* Dusel-Bacon, Cynthia, and Till, A.B., eds., Geologic studies in Alaska by the U.S. Geological Survey, 1992: U.S. Geological Survey Bulletin 2068, p. 197–217.

Gehrels, G.E., McClelland, W.C., Samson, S.D., Patchett, P.J., and Jackson, J.L., 1990, Ancient continental margin assemblage in the northern Coast Mountains, southeast Alaska and northwest Canada: Geology, v. 18, p. 208–211.

Gehrels, G.E., and Saleeby, J.B., 1987, Geologic framework, tectonic evolution, and displacement history of the Alexander terrane: Tectonics, v. 6, p. 151–173.

Gehrels, G.E., Saleeby, J.B., and Berg, H.C., 1987, Geology of Annette, Gravina, and Duke Islands, southeastern Alaska: Canadian Journal of Earth Sciences, v. 24, p. 866–881.

Gray, Floyd, Page, N. J, Carlson, C.A., Wilson, S.A., and Carlson, R.R., 1986, Platinum-group element geochemistry of zoned ultramafic intrusive suites, Klamath Mountains, California and Oregon: Economic Geology, v. 81, p. 1252–1260.

Green, D.H., and Ringwood, A.E., 1967, The stability fields of aluminous pyroxene peridotite and garnet peridotite and their relevance in upper mantle structure: Earth and Planetary Science Letters, v. 3, p. 151–160.

Green, D.H., Ringwood, A.E., Ware, N.G., Hibberson, W.O., Major, A., and Kiss, E., 1971, Experimental petrology and petrogenesis of Apollo 12 basalts, *in* Levinson, A.A., ed., Proceedings of the Second Lunar Science Conference, Houston, Texas: Geochimica et Cosmochimica Acta, Supp. 2, v. 1, p. 601–615.

Guild, P.W., and Balsley, J.R., Jr., 1942, Chromite deposits of Red Bluff Bay and vicinity, Baranof Island, Alaska: U.S. Geological Survey Bulletin 936–G, p. 171–187.

Hammack, J.L., Nixon, G.T., Wong, R.H., and Paterson, W.P.E., 1990, Geology and noble metal geochemistry of the Wrede Creek ultramafic complex, north-central British Columbia, *in* Geologic fieldwork 1989: British Columbia Ministry of Energy, Mines, and Petroleum Resources, Paper 1990-1, p. 405–415.

Hanson, G.N., 1980, Rare earth elements in petrogenetic studies of igneous systems: Annual Review of Earth and Planetary Sciences, v. 8, p. 371–406.

Harnois, Luc, and Morency, Maurice, 1989, Geochemistry of Mount Orford ophiolite complex, northern Appalachians, Canada: Chemical Geology, v. 77, p. 133–147.

Harnois, Luc, Trottier, Jacques, and Morency, Maurice, 1990, Rare earth element geochemistry of Thetford Mines ophiolite complex, northern Appalachians, Canada: Contributions to Mineralogy and Petrology, v. 105, p. 433–445.

Helz, R.T., 1973, Phase relations of basalts in the melting range at P_{H_2O}=5 kb as a function of oxygen fugacity: Journal of Petrology, v. 14, p. 249–302.

Henry, D.J., and Medaris, L.G., Jr., 1980, Application of pyroxene and olivine-spinel geothermometers to spinel peridotites in southwestern Oregon: American Journal of Science, v. 280-A, p. 211–231.

Himmelberg, G.R., Brew, D.A., and Ford, A.B., 1986a, Chemical composition of olivine and orthopyroxene in peridotite of the Coast plutonic-metamorphic complex near Skagway, *in* Bartsch-Winkler, Susan, and Reed, K.M., eds., Geologic studies in Alaska by the U.S. Geological Survey during 1985: U.S. Geological Survey Circular 978, p. 95–98.

Himmelberg, G.R., and Loney, R.A., 1980, Petrology of ultramafic and gabbroic rocks of the Canyon Mountain ophiolite, Oregon: American Journal of Science, v. 280-A, p. 232–268.

Himmelberg, G.R., and Loney, R.A., 1981, Petrology of the ultramafic and gabbroic rocks of the Brady Glacier nickel-copper deposit, Fairweather Range, southeastern Alaska: U.S. Geological Survey Professional Paper 1195, 26 p.

Himmelberg, G.R., Loney, R.A., and Craig, J.T., 1986b, Petrogenesis of the ultramafic complex at the Blashke Islands, southeastern Alaska: U.S. Geological Survey Bulletin 1662, 14 p.

Himmelberg, G.R., Loney, R.A., and Nabelek, P.I., 1987, Petrogenesis of gabbronorite at Yakobi and northwest Chichagof Islands, Alaska: Geological Society of America Bulletin, v. 98, p. 265–279.

Holloway, J.R., and Burnham, C.W., 1972, Melting relations of basalt with equilibrium water pressure less than total pressure: Journal of Petrology, v. 13, p. 1–29.

Irvine, T.N., 1965, Chromian spinel as a petrogenetic indicator; part 1, Theory: Canadian Journal of Earth Sciences, v. 2, p. 648–672.

Irvine, T.N., 1967a, The Duke Island ultramafic complexes, southeastern Alaska, Part 4.II *in* Wyllie, P.J., ed., Ultramafic and related rocks: New York, John Wiley, p. 84–97.

Irvine, T.N., 1967b, Chromian spinel as a petrogenetic indicator; part 2, Petrologic applications: Canadian Journal of Earth Sciences, v. 4, p. 71–103.

Irvine, T.N., 1973, Bridget Cove volcanics, Juneau area, Alaska: possible parental magma of Alaskan-type ultramafic complexes: Carnegie Institution Washington Yearbook, 72, 1972–1973, p. 478–491.

Irvine, T.N., 1974, Petrology of the Duke Island ultramafic complex, southeastern Alaska: Geological Society of America Memoir 138, 240 p.

Irvine, T.N., 1976, Alaskan-type ultramafic-gabbroic bodies in the Aiken Lake, McConnel Creek, and Toodoggone map areas, *in* Report of activities, part A: Geological Survey Canada Paper 76-1A, p. 76–81.

Irvine, T.N., 1982, Terminology for layered intrusions: Journal of Petrology, v. 23, 127–162.

Irvine, T.H. , and Smith, C.H., 1967, The ultramafic rocks of the Muskox intrusion, Northwest Territories, Canada, Part 2.III *in* Wyllie, P.J., ed., Ultramafic and related rocks: New York, John Wiley, p. 38–49.

Ishiwatari, Akira, 1985, Granulite-facies metacumulates of the Yakuno ophiolite, Japan: evidence for unusually thick oceanic crust: Journal of Petrology, v. 26, p. 1–30.

Ishizuka, Hideo, 1985, Prograde metamorphism of the Horokanai ophiolite in the Kamuikotan Zone, Hokkaido, Japan: Journal of Petrology, v. 26, p. 391–417.

IUGS Subcommission on the Systematics of Igneous Rocks, 1974, Classification and nomenclature of plutonic rocks, recommendations: Neues Jahrbuch für Mineralogie Monatschefte, 1973, v. 4, p. 149–164.

Jackson, E.D., and Thayer, T.P., 1972, Some criteria for distinguish-

ing between stratiform, concentric, and alpine peridotite-gabbro complexes: International Geological Congress, 24th, Montreal, 1972, Proceedings, Section 2, p. 289–296.

James, O.B., 1971, Origin and emplacement of the ultramafic rocks of the Emigrant Gap area, California: Journal of Petrology, v. 12, p. 523–560.

Jaques, A.L., and Green, D.H., 1980, Anhydrous melting of peridotite at 0–15 kb pressure and the genesis of tholeiitic basalts: Contributions to Mineralogy and Petrology, v. 73, p. 287–310.

Jenkins, D.M., 1983, Stability and composition relations of calcic amphiboles in ultramafic rocks: Contributions to Mineralogy and Petrology, v. 83, p. 375–384.

Karl, S.M., Brew, D.A., and Wardlaw, B.R., 1990, Significance of Triassic marble from Nakwasina Sound, southeastern Alaska, *in* Dover, J.H., and Galloway, J.P., eds., Geologic studies in Alaska by the U.S. Geological Survey, 1989: U.S. Geological Survey Bulletin 1946, p. 21–28.

Kay, S.M., and Kay, R.W., 1985a, Role of crystal cumulates and the oceanic crust in the formation of the lower crust of the Aleutian arc: Geology, v. 13, p. 461–464.

Kay, S.M., and Kay, R.W., 1985b, Aleutian tholeiitic and calc-alkaline magma series, I: the mafic phenocrysts: Contributions to Mineralogy and Petrology, v. 90, p. 276–290.

Kay, S.M., Kay, R.W., Brueckner, H.K., and Rubenstone, J.L., 1983, Tholeiitic Aleutian arc plutonism: the Finger Bay pluton, Adak, Alaska: Contributions to Mineralogy and Petrology, v. 82, p. 99–116.

Kay, S.M., Kay, R.W., and Citron, G.P., 1982, Tectonic controls on tholeiitic and calc-alkaline magmatism in the Aleutian arc: Journal of Geophysical Research, v. 87-B, p. 4051–4072.

Kay, S.M., Kay, R.W., Citron, G.P., and Perfit, M.R., 1990, Calc-alkaline plutonism in the intra-oceanic Aleutian arc, Alaska, *in* Kay, S.M., and Rapela, C.W., eds., Plutonism from Antarctica to Alaska: Geological Society of America Special Paper 241, p. 233–255.

Kay, R.W., Rubenstone, J.L., and Kay, S.M., 1986, Aleutian terranes from Nd isotopes: Nature, v. 322, p. 605–609.

Kennedy, G.C., and Walton, M.S., Jr., 1947, Geology and associated mineral deposits of some ultrabasic rock bodies in southeastern Alaska: U.S. Geological Survey Bulletin 947–D, p. 65–84.

Komor, S.C., Elthon, Don, and Casey, J.F., 1985, Mineralogic variation in a layered ultramafic cumulate sequence at the North Arm Mountain massif, Bay of Islands ophiolite, Newfoundland: Journal of Geophysical Research, v. 90-B, p. 7705–7736.

Kretz, Ralph, 1983, Symbols for rock-forming minerals: The American Mineralogist, v. 68, p. 277–279.

Lanphere, M.A., 1968, Sr-Rb-K and Sr isotopic relationships in ultramafic rocks, southeastern Alaska: Earth and Planetary Science Letters, v. 4, p. 185–190.

Lanphere, M.A., and Eberlein, G.D., 1966, Potassium-argon ages of magnetite-bearing ultramafic complexes in southeastern Alaska [abs.]: Geological Society of America Special Paper 87, p. 94.

Lathram, E.H., Pomeroy, J.S., Berg, H.C., and Loney, R.A., 1965, Reconnaissance geology of Admiralty Island, Alaska: U.S. Geological Survey Bulletin 1181–R, 48 p.

Leake, B.E., 1978, Nomenclature of amphiboles: Canadian Mineralogist, v. 16, p. 501–520.

LeBas, M.J., 1962, The role of aluminum in igneous clinopyroxenes with relation to their parentage: American Journal of Science, v. 260, p. 267–288.

Lindsley, D.H., and Andersen, D.J., 1983, A two-pyroxene thermometer; proceedings of the Thirteenth Lunar and Planetary Science Conference, part 2: Journal of Geophysical Research, v. 88 Supp. A, p. A887–A906.

Loney, R.A., and Brew, D.A., 1987, Regional thermal metamorphism and deformation of the Sitka Graywacke, southern Baranof Island, southeastern Alaska: U.S. Geological Survey Bulletin 1779, 17 p.

Loney, R.A., Brew, D.A., Muffler, L.J.P., and Pomeroy, J.S., 1975, Reconnaissance geology of Chichagof, Baranof, and Kruzof Islands, southeastern Alaska: U.S. Geological Survey Professional Paper 792, 105 p.

Loney, R.A., and Himmelberg, G.R., 1983, Structure and petrology of the La Perouse gabbro intrusion, Fairweather Range, southeastern Alaska: Journal of Petrology, v. 24, p. 377–423.

Loney, R.A., and Himmelberg, G.R., 1989, The Kanuti ophiolite, Alaska: Journal of Geophysical Research, v. 94-B, p. 15,869–15,900.

Loney, R.A., and Himmelberg, G.R., 1992, Petrogenesis of the Pd-rich intrusion at Salt Chuck, Prince of Wales Island: an early Paleozoic Alaskan-type ultramafic body: Canadian Mineralogist , v. 30 p. 1005–1022.

Loney, R.A., Himmelberg, G.R., and Shew, Nora, 1987, Salt Chuck palladium-bearing ultramafic body, Prince of Wales Island, *in* Hamilton, T.D., and Galloway, J.P., eds., Geologic studies in Alaska by the U.S. Geological Survey during 1986: U.S. Geological Survey Circular 998, p. 126–127.

Loucks, R.R., 1990, Discrimination of ophiolitic from nonophiolitic ultramafic-mafic allochthons in orogenic belts by the Al/Ti ratio in clinopyroxene: Geology, v. 18, p. 346–349.

McDonough, W.F., and Frey, F.A., 1989, Rare earth elements in the upper mantle rocks, *in* Lipin, B.R., and McKay, G.A., eds., Geochemistry and mineralogy of rare earth elements: Reviews in Mineralogy, v. 21, p. 99–145.

Medaris, L.G., Jr., 1972, High-pressure peridotites in southwestern Oregon: Geological Society of America Bulletin, v. 83, p. 41–58.

Meen, J.K., Ross, D.K., and Elthon, Don., 1991, Gross isotopic heterogeneity in layered ultramafic cumulates [abs.]: EOS, Transactions of the American Geophysical Union, v. 72, p. 521.

Monger, J.W.H., Price, R.A., and Tempelman-Kluit, D.J., 1982, Tectonic accretion and the origin of the two major metamorphic and plutonic welts in the Canadian Cordillera: Geology, v. 10, p. 70–75.

Morimoto, N., Fabriès, J., Ferguson, A.K., Ginzburg, I.V., Ross, M., Seifert, F.A., Zussman, J., Aoki, K., and Gottardi, G., 1988, Nomenclature of pyroxenes: American Mineralogist, v. 73, p. 1123–1133.

Mortimer, N., 1986, Late Triassic, arc-related, potassic igneous rocks in the North American Cordillera: Geology, v. 14, p. 1035–1038.

Murray, C.G., 1972, Zoned ultramafic complexes of the Alaskan type: feeder pipes of andesitic volcanoes, *in* Shagam, R., and others, eds., Studies in earth and space sciences: Geological Society of America Memoir 132, p. 313–335.

Nicolas, A., 1992, Kinematics in magmatic rocks with special reference to gabbros: Journal of Petrology, v. 33, no. 4, p. 891–915.

Nixon, G.T., and Hammack, J.L., 1991, Metallogeny of ultramafic-mafic rocks in British Columbia with emphasis on the platinum-group elements, *in* Ore deposits, tectonics and metallogeny in the Canadian Cordillera: British Columbia Ministry of Energy, Mines, and Petroleum Resources, Paper

1991-4, p. 125–161.

Nixon, G.T., Hammack, J.L., Connelly, J.N., Case, G., and Paterson, W.P.E., 1990, Geology and noble metal geochemistry of the Polaris ultramafic complex, north-central British Columbia, *in* Geological fieldwork 1989: British Columbia Ministry of Energy, Mines, and Petroleum Resources, Paper 1990-1, p. 387–404.

Nixon, G.T., and Rublee, V.J., 1988, Alaskan-type ultramafic rocks in British Columbia: new concepts of the structure of the Tulameen complex, *in* Geologic fieldwork 1987: British Columbia Ministry of Energy, Mines, and Petroleum Resources, Paper 1988-1, p. 281–294.

Noble, J.A., and Taylor, H.P., Jr., 1960, Correlation of the ultramafic complexes of southeastern Alaska with those of other parts of North America and the world: International Geological Congress, 21st, Copenhagen, 1960, Report, part 13, p. 188–197.

Nye, C.J., and Reid, M.R., 1986, Geochemistry of primary and least-fractionated lavas from Okmok volcano, central Aleutians: implications for arc magmagenesis: Journal of Geophysical Research, v. 91-B, p. 10,271–10,287.

Pallister, J.S., and Hopson, C.A., 1981, Samail ophiolite plutonic suite: field relations, phase variation, cryptic variation and layering, and a model of a spreading ridge magma chamber: Journal of Geophysical Research, v. 86-B, p. 2593–2644.

Pallister, J.S., and Knight, R.J., 1981, Rare-earth element geochemistry of the Samail ophiolite near Ibra, Oman: Journal of Geophysical Research, v. 86-B, p. 2673–2697.

Perfit, M.R., Brueckner, Hannes, Lawrence, J.R., and Kay, R.W., 1980, Trace element and isotopic variations in a zoned pluton and associated volcanic rocks, Unalaska Island, Alaska: a model for fractionation in Aleutian calcalkaline suite: Contributions to Mineralogy and Petrology, v. 73, p. 69–87.

Prinzhofer, Alain, and Allègre, C.J., 1985, Residual peridotites and the mechanisms of partial melting: Earth and Planetary Science Letters, v. 74, p. 251–265.

Robertson, E.C., 1956, Magnetite deposits near Klukwan and Haines, southeastern Alaska: U.S. Geological Survey Open-File Report, 37 p.

Roeder, P.L., and Emslie, R.F., 1970, Olivine-liquid equilibrium: Contributions to Mineralogy and Petrology, v. 29, p. 275–289.

Rubin, C.M., and Saleeby, J.B., 1991, Tectonic framework of the upper Paleozoic and lower Mesozoic Alava sequence: a revised view of the polygenetic Taku terrane in southern southeast Alaska: Canadian Journal of Earth Sciences, v. 28, p. 881–893.

Rubin, C.M., and Saleeby, J.B., 1992, Tectonic history of the eastern edge of the Alexander terrane, southeast Alaska: Tectonics, v. 11, p. 586–602.

Ruckmick, J.C., and Noble, J.A., 1959, Origin of the ultramafic complex at Union Bay, southeastern Alaska: Geological Society of America Bulletin, v. 70, p. 981–1018.

Saleeby, J.B., 1991, Age and tectonic setting of the Duke Island ultramafic intrusion, southeast Alaska [abs.]: EOS, Transactions of the American Geophysical Union, v. 72, p. 521.

Samson, S.D., McClelland, W.C., Patchett, P.J., Gehrels, G.E., and Anderson, R.G., 1989, Evidence from neodymium isotopes for mantle contributions to Phanerozoic crustal genesis in the Canadian Cordillera: Nature, v. 337, p. 705–709.

Shaw, H.R., 1965, Comments on viscosity, crystal settling, and convection in granitic magmas: American Journal of Science, v. 263, p. 120–152.

Simkin, Tom, 1967, Flow differentiation in the picritic sills of North Skye, Part 3.III *in* Wyllie, P.J. ed., Ultramafic and related rocks: New York, John Wiley, p. 64–70.

Smith, C.H., 1962,. Notes on the Muskox intrusion, Coppermine River area, District of Mackenzie: Geological Survey of Canada Paper 61-25, 16 p.

Snoke, A.W., Quick, J.E., and Bowman, H.R., 1981, Bear Mountain igneous complex, Klamath Mountains, California: an ultrabasic to silicic calc-alkaline suite: Journal of Petrology, v. 22, p. 501–552.

Snoke, A.W., Sharp, W.D., Wright, J.E., and Saleeby, J.B., 1982, Significance of mid-Mesozoic peridotitic to dioritic intrusive complexes, Klamath Mountains–western Sierra Nevada, California: Geology, v. 10, p. 160–166.

Stebbins, R.H., 1957, Field description of the Percy Islands ultramafic complex, southeastern Alaska: New York, Columbia University, M.A. thesis.

Taylor, H.P., Jr., 1967, The zoned ultramafic complexes of southeastern Alaska, Part 4.III *in* Wyllie, P.J., ed., Ultramafic and related rocks: New York, John Wiley, p. 96–118.

Taylor, H.P., Jr., and Noble, J.A., 1960, Origin of the ultramafic complexes in southeastern Alaska: International Geological Congress, 21st, Copenhagen, 1960, Report, Part 13, p. 175–187.

Thorne, R.L., and Wells, R.R., 1956, Studies of the Snettisham magnetite deposit, southeastern Alaska: U.S. Bureau of Mines Report of Investigations 5195, 41 p.

Turner, F.J., 1942, Preferred orientation of olivine crystals in peridotites, with special reference to New Zealand examples: Royal Society of New Zealand Transactions, v. 72, p. 280–300.

Ulmer, Peter, 1989, The dependence of the Fe^{2+}-Mg cation-partitioning between olivine and basaltic liquid on pressure, temperature and composition, an experimental study to 30 kbars: Contributions to Mineralogy and Petrology, v. 101, p. 261–273.

Wager, L.R., Brown, G.M., and Wadsworth, W.J., 1960, Types of igneous cumulates: Journal of Petrology, v. 1, p. 73–85.

Walton, M.S., Jr., 1951, The Blashke Island ultrabasic complex, with notes on related areas in southeastern Alaska: U.S. Geological Survey Open-File Report [1586], 266 p.

Watkinson, D.H., and Melling, D.R., 1992, Hydrothermal origin of platinum-group mineralization in low-temperature copper sulfide-rich assemblages, Salt Chuck intrusion, Alaska: Economic Geology, v. 87, p. 175–184.

Wheatley, Michael, and Rock, N.M.S., 1988, SPIDER: a Macintosh program to generate normalized multi-element "spidergrams": American Mineralogist, v. 73, p. 919–921.

Wilson, A.H., 1992, The geology of the Great Dyke, Zimbabwe: crystallization, layering, and cumulate formation in the P1 pyroxenite of Cyclic Unit 1 of the Darwendale Subchamber: Journal of Petrology, v. 33, p. 611–663.

Wones, D.R., 1979, The fractional resorption of complex minerals and the formation of strongly femic alkaline rocks, *in* Yoder, H.S. Jr., ed., The evolution of the igneous rocks; fiftieth anniversary perspectives: Princeton, N.J., Princeton University Press, p. 413–422.

Wyllie, P.J., ed., 1967, Ultramafic and related rocks: New York, John Wiley, 464 p.

Yokoyama, Kazumi, 1980, Nikubuchi peridotite body in the Sanbagawa metamorphic belt; thermal history of the 'Al-pyroxene-rich suite' peridotite body in high pressure metamorphic terrain: Contributions to Mineralogy and Petrology, v. 73, p. 1–13.

GPO 683-048/20002